Energy & Environmental Science

ROYAL SOCIETY OF CHEMISTRY

REVIEW

View Article Online
View Journal | View Issue

Open Access Article. Published on 02 November 2022. Downloaded on 10/16/2025 7:02:22 PM.
This article is licensed under a Creative Commons Attribution 3.0 Unported Licence.

Check for updates

Cite this: *Energy Environ. Sci.*, 2022, **15**, 4982

Recent advances in triplet–triplet annihilation upconversion and singlet fission, towards solar energy applications

Andrew J. Carrod,[a] Victor Gray *[b] and Karl Börjesson *[a]

Solar energy is an ample renewable energy resource, with photovoltaic (PV) technology enabling a direct route from light to electricity. Currently, PVs are limited in photon conversion efficiency, due in major part to spectral losses. Mitigation of these losses is therefore important, economically and environmentally. Two processes that aim to increase solar light utilisation are described herein. The first is triplet–triplet annihilation upconversion (TTA-UC), through which two incoherent photons of low energy can produce one of higher energy, reducing below bandgap losses. Secondly, singlet fission (SF), through which two triplet states may be obtained from one initial singlet excited state, in theory allowing two electrons per photon in a PV, reducing thermalisation losses. These fields are often covered seperately, despite being the reverse processes of one another. This work aims to consolidate research in the two fields and highlight their similarities and common challenges, specifically those relevant to PV applications. Herein, we cover systems primarily based on organic small molecules (anthracene, rubrene, tetracene, pentacene), and detail the fabrication of functional materials containing them (MOFs, gels, SAMs on TiO_2, thin evaporated and solution cast films, and cavities). We further offer our recommendations for the focus of future work in both the TTA and SF fields, and discuss the need to address current limitations such as poor triplet diffusion, limited charge injection to PVs, and material stability. Specifically, one could do this by cherry picking ideas from other research fields, for example photosensitisers for photodynamic therapy could be used as TTA sensitisers, and molecules having a considerable excited state aromaticity could be considered as SF materials. We hope this review may aid development towards the end goal of an efficient PV, incorporating either, or both, SF and TTA-UC materials.

Received 17th May 2022,
Accepted 1st November 2022

DOI: 10.1039/d2ee01600a

rsc.li/ees

Broader context

Renewable energy is positioned to take centre-stage in future decarbonisation efforts, such as those agreed at the Paris and COP26 summits. One renewable energy source, solar light, holds the potential to mitigate the growing energy and environmental crisis. Researchers have continuously tried to increase the efficiency of solar harvesting devices, yet limitations have been unavoidable since some of the energy from the solar spectrum is inaccessible. If solar cells were more efficient, the cost per unit of electricity produced in PVs would drastically decrease, leading to an increased uptake of this technology. Subsequently, a reduction in fossil fuel reliance will be observed. To reduce spectral losses, and therefore increase efficiencies in PVs, one could imagine the monochromation of solar light. Two of the most relevant candidates for this are triplet–triplet annihilation upconversion (TTA-UC) and singlet fission (SF) materials. We here provide a detailed overview of both techniques, critically assessing progress and state of the art in the development of TTA-UC and SF materials. This will guide the future development of new TTA-UC and SF materials that may be incorporated into PVs, and is further of interest to other optoelectronic devices such as OLEDs.

Introduction

Sunlight is a near infinite source of energy, and assuming ideal conditions, sunlight reaches the Earth's surface with an irradiance of 1000 W m^{-2}.[1] To put the number in perspective, if all sunlight could be turned into electricity with no losses, an area of around 7 m^2 would provide the same energy per hour as

[a] *University of Gothenburg, Department of Chemistry and Molecular Biology, Kemivägen 10, 41296, Gothenburg, Sweden. E-mail: karl.borjesson@gu.se*
[b] *Department of Chemistry - Ångström Laboratory, Uppsala University, Box 523, 751 20, Uppsala, Sweden. E-mail: victor.gray@kemi.uu.se*

This journal is © The Royal Society of Chemistry 2022

Open Access Article. Published on 02 November 2022. Downloaded on 10/16/2025 7:02:22 PM.
This article is licensed under a Creative Commons Attribution 3.0 Unported Licence.

combusting 1 kg of coal.[2] With the global call for decarbonisation,[3] and renewed commitment from the world's leading energy consumers to an increased use of renewable energy,[4–6] it is important to create solar energy harvesting technologies with the highest possible efficiency.

Energy production through photovoltaic (PV) devices has grown nearly exponentially in the previous 10 years,[7] as a result of a radical decrease in the levelised cost of electricity (LCOE) from solar cells. One large factor in this decrease is the decline in production costs with increasing manufacturing scale, to a point at which production cost is only a small factor in PV price.[8] Further increases to the efficiency of these devices, which are currently limited in maximum theoretical efficiency, can drive the LCOE even lower and would be of great scientific interest, with large economic and environmental impact.[9] Furthermore, an increase in PV module efficiency leads not only to cheaper prices for energy consumers but also to a decrease in the space needed to provide a similar energy output. In turn efficiency increases will allow the integration of PV devices into increasingly innovative locations, as in urban design with building integrated photovoltaics, reducing the need for land space sacrifice in energy production from PV's.[10]

In this review we describe the existing limitations of single junction photovoltaics and describe the loss mechanisms inherent to these PV devices. We further detail two distinct yet complimentary photophysical processes; triplet–triplet annihilation upconversion (TTA-UC) and singlet fission (SF), as well as assessing their practical use as strategies for the enhancement of solar cell efficiency. Currently TTA-UC and singlet fission are seen as viable chemical approaches to PV efficiency enhancement. They achieve this through monochromation of the solar spectrum. It is therefore prudent to consolidate this research, detailing the recent progress in the field and its future perspectives.

Andrew J. Carrod

Andrew J. Carrod graduated from the University of Hull, earning a degree in chemistry with honors in 2016. He later earned a PhD degree in chemistry from the University of Birmingham in 2021, with a thesis on the subject of photoactive iridium(III) complexes, under the supervision of Professor Zoe Pikramenou. After working as a postdoctoral researcher for Professor Karl Börjesson at the University of Gothenburg, he has been awarded a MSCA postdoctoral fellowship to remain at the same institution. His current research interests focus on chemical synthesis of photoactive molecules, and further studying their utility in triplet–triplet annihilation upconversion systems.

Limitations in current photovoltaic devices

The limit of theoretical efficiency for single junction non-concentrated solar cells has been determined as 33.16% reached at a bandgap of 1.34 eV. Known as the Shockley–Queisser (SQ) limit, this value was calculated using some fundamental assumptions and approximations.[11,12] Assumptions made were that all photons with energies above the bandgap (E_g) create free electrons and holes, which will yield one electron per photon. Furthermore, that re-emission of light would occur upon each hole–electron recombination. As it is a maximum theoretical limit, the SQ value was also calculated based on perfect materials containing no defects, and the end of the absorption window is estimated as a step function.

Victor Gray

Victor Gray is a researcher at Uppsala University, Department of Chemistry – Ångström in Sweden. He obtained his PhD from Chalmers University of Technology in Sweden with Kasper Moth Poulsen (2017). He spent 3 years at the Cavendish Laboratory, University of Cambridge (UK), as a postdoctoral researcher with Akshay Rao working on organic–inorganic hybrid systems for photon conversion. In 2022 he joined Uppsala University as an independent researcher studying photophysical processes in solar energy harvesting materials.

Karl Börjesson

Karl Börjesson is Professor in physical chemistry at the University of Gothenburg. He obtained his PhD from Chalmers University of Technology in Sweden under the supervision of Bo Albinsson in 2011, and where after that a postdoctoral fellow at the University of Strasbourg with Paolo Samori and at Chalmers University of Technology with Kasper Moth-Poulsen. He started his independent career in 2015 at the University of Gothenburg and has been there since. His research is focused on photochemistry and photophysics, strong light-matter interactions, and materials chemistry. His prime methodologies include optical spectroscopy and physical organic chemistry.

Open Access Article. Published on 02 November 2022. Downloaded on 10/16/2025 7:02:22 PM.
This article is licensed under a Creative Commons Attribution 3.0 Unported Licence.

These assumptions do not hold true in real-world conditions; however it is possible to assess real-world cells under true laboratory conditions and contrast them to the SQ value, assessing their energy loss channels so as to elucidate methods to improve their efficiency.

A detailed look at energy loss in solar cells

In this section we will aim to detail the major energy loss channels in PV cells. Energy loss processes in solar cells are broadly classified into two terms, intrinsic[13] and extrinsic losses.[14] These umbrella terms are used to denote processes which can be eliminated (extrinsic) or that are fundamental limitations (intrinsic). As we will later consider energy enhancement assuming perfect cells, we will not describe in detail extrinsic losses, as these can in theory be eliminated. We will consider each of the intrinsic factors in turn then, and briefly describe their physical mechanism and magnitude.

Firstly, some energy loss in any solar cell can be attributed to the deliberate tuning of the solar cell E_g to a sizeable value. The E_g value must be large enough to produce a reasonable voltage, however this does not allow for the capture of the whole range of the solar spectrum. A sizeable proportion of the solar irradiation at ground level appears in the near infrared region (Fig. 1a).[1] Many of the solar cell materials have E_g larger than

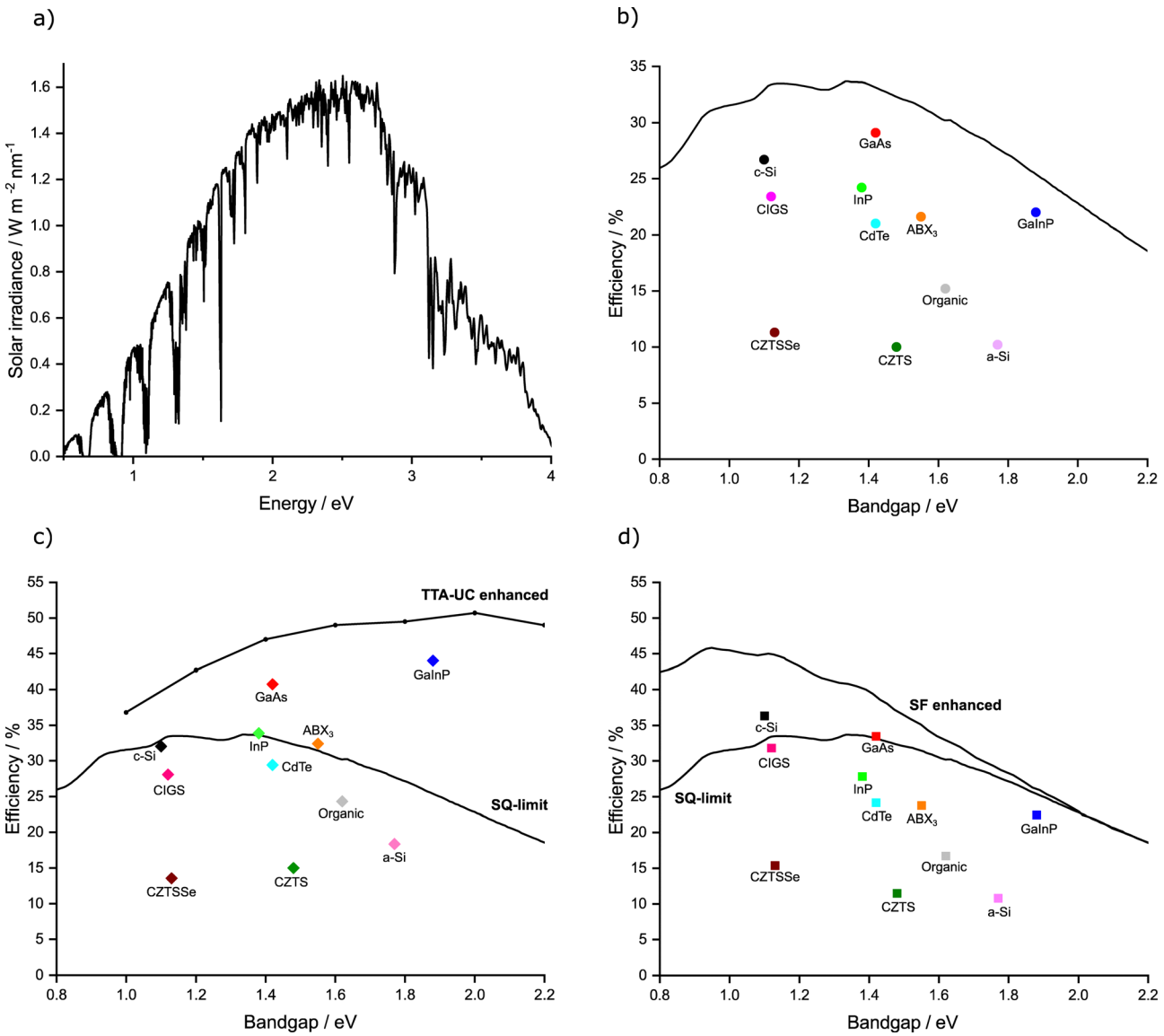

Fig. 1 Graphical representation of (a) the AM 1.5 solar spectrum. (b) Shockley–Queisser limit of efficiency (black line) plotted alongside the cells of highest confirmed efficiency in each major class of solar cell. Where c-Si = crystalline silicon, GaAs = gallium arsenide, and GaInP = gallium indium phosphide, InP = indium phosphide, CIGS = copper indium gallium selenide, CdTe = cadmium telluride, ABX_3 = perovskite, CZTS = Copper zinc tin sulphide, CZTSSe = Copper zinc tin sulphide selenide, a-Si = amorphous silicon. (c and d) SQ and TTA-UC/SF enhanced efficiency limits (black lines) plotted alongside current highest maximum efficiency possible in each major class of solar cell assuming ideal TTA-UC/SF enhancement. We use the data from Fig. 1b and increases are calculated as per ref. 46 and 52, for TTA-UC and SF respectively.

Open Access Article. Published on 02 November 2022. Downloaded on 10/16/2025 7:02:22 PM.
This article is licensed under a Creative Commons Attribution 3.0 Unported Licence.

1.1 eV (1130 nm), in which case the loss of energy through an inability to absorb infrared light is significant.[15] Thermalisation is the second major loss of energy; due to the absorption of photons with energy larger than E_g. Relaxation to the bandgap energy is realised through a release of heat.[16] Other less substantial but still measurable energy loss pathways are emission losses, Carnot losses and Boltzmann losses. Emission losses are due to the radiative electron–hole recombination events occurring within the single bandgap PV's.[17] Some energy loss is inherent upon the transfer of heat energy to electrical work, the voltage drop due to this exchange in photovoltaic device is known as the Carnot factor.[18] Entropy is increased due to an angular discrepancy between absorption and emission. This in turn leads to a voltage decrease known as the Boltzmann loss.[15] This review focuses on strategies to mitigate the first two loss processes; reducing sub-bandgap losses and thermalisation, through utilisation of known photophysical processes. The next section will discuss these methods, and how they operate to enable the improvement of the efficiency of known solar cells.

Overcoming the SQ limit: mitigating losses through photon conversion

Overcoming the SQ limit for solar cells can be achieved in a seemingly facile manner, by eliminating some or all of the losses described above. One way to do this would be to extend the optical window in which a PV device may operate without compromise on the bandgap of the material. This is possible in multi-junction photovoltaics where current efficiencies have been experimentally measured at 47% in six junction concentrator systems.[19] These are theorised to give a possible maximum efficiency of around 87% at an infinite number of junctions.[20] Multi-junction solar cells are however not widely used in terrestrial energy production, due to the complexity of fabrication and scarcity of raw materials required in multi junction PVs.[21,22]

To improve single junction photovoltaics, one could consider monochromation of all or part of the solar spectrum. Two methods for doing so are upconversion and singlet fission (SF). Sub-bandgap photons may be converted to a photon with energy above that of E_g in a process known as upconversion. This process has been observed in a variety of molecules *e.g.* those containing lanthanide ions,[23,24] and organic chromophores,[25] albeit through differing mechanisms. Lanthanide based upconversion has been covered in depth by other reviews,[26–29] and readers are referred to this literature for a full overview of the mechanism and properties. In terms of use in solar harvesting the main challenge for lanthanide-based UC is the requirement of high intensity excitation light, due to narrow and weak absorption bands. Strategies are being developed to counter these drawbacks, mainly focussed on imaging applications.[30] In this review we will focus on systems using small organic molecules as annihilators, in which the most described upconversion process relevant to solar cells is triplet–triplet annihilation photon upconversion (TTA-UC). The benefit of the TTA-UC process is that high conversion efficiencies can be reached using a low-intensity and non-coherent excitation light source.

To mitigate the loss of energy through thermalisation, multiexciton generation (MEG) has been proposed. Through this method, two excitons are generated from one excitation event. It has been observed in a variety of materials, such as semiconducting quantum dots,[31,32] lanthanide ions[33] and organic molecules.[34] For inorganic materials (QDs and lanthanide nanoparticles) the topic has been extensively covered by others.[32,35–37] We will not discuss these materials in depth, but recognise that the challenges in QD based MEG are related to modest yield, as well as how to efficiently extract the multiple excited states due to their often ultrashort lifetimes.[38–40] Instead, we will focus on singlet fission (SF), a multiexciton generation process in organic molecules. SF is a spin-allowed process, in which the production of two triplet excited states occurs from one initial excited singlet state. It thus offers the possibility of creating two electron–hole pairs from one high-energy photon when in conjunction to a solar cell. This process is widely observed in polycyclic aromatic hydrocarbons, either on the same chromophore (homofission) or on different chromophores (heterofission).[34] SF has been observed with efficiencies of unity,[41] and has seen implementation in PV devices to raise their external quantum efficiency.[42,43] To summarise, by including SF and/or TTA-UC capabilities into PV devices, thermalisation and below bandgap energy losses can be mitigated.

Prospect of photon conversion in different classes of PV devices

The maximum measured efficiency as of this review using each kind of PV material (in single junction, non-concentrated cells) is given in Fig. 1b.[44] It can be observed that many cells are nearly reaching the theoretical limit, with crystalline silicon (c-Si), gallium arsenide (GaAs), and gallium indium phosphide (GaInP) all reaching above 80% of their theoretical maximum value. The champion cell remains GaAs,[44,45] but concerns have been raised about the toxicity of the material.

The relative benefits of TTA-UC to solar cell technology depends on the E_g of the solar cell in question. Trupke *et al.* have calculated a solar cell efficiency limit based on the theoretical increases provided by an upconversion process.[46] Fig. 1c displays this TTA-UC enhanced limit alongside the traditional SQ limit, both under AM 1.5 irradiation. Assumptions were made by the original authors, such as a near constant refractive index over the range of bandgaps, which was used to be representative of several types of PVs (Si and GaAs).[47] The values were based on ideal upconversion systems for each E_g. Nonetheless, it gives an estimation of maximum efficiency when applying upconversion to PVs. We have also predicted and plotted in this figure the maximum efficiency value that would be possible for the record device in each class of PV if an ideal TTA-UC system were applied. We do this by taking the ratio between the traditional SQ limit and the TTA enhanced limit, then multiplying by the current record percentage efficiency.

Open Access Article. Published on 02 November 2022. Downloaded on 10/16/2025 7:02:22 PM.
This article is licensed under a Creative Commons Attribution 3.0 Unported Licence.

The map of solar cell potential is redrawn by using TTA-UC. Now, the potential of large E_g systems is considerably increased, while small E_g systems are only marginally increased. By measure of efficiency increase, GaAs, InP or GaInP, and ABX_3 show high performance potential when utilising TTA-UC. GaAs, InP and GaInP cells are all expensive technologies that see little use in commercial PV's today.[48] Perovskite solar cells have seen a remarkable amount of progress in recent years and whilst stability issues remain, the rapid progress is encouraging.[49] The high E_g of perovskite materials make this a noteworthy material to investigate for TTA-UC enhancement. Whilst slightly lower in potential efficiency than the aforementioned perovskites, the next best predicted material would be CdTe. This PV class already possesses a sizeable market share, with fast and cheap manufacturing processes. Moreover, studies have concluded that this system has negligible environmental toxicity as the technology is resistant to normal environmental conditions.[50]

Similar to the case of TTA-UC, the benefit of SF applied to a solar cell depends on the E_g. The revised solar cell efficiency limit of a SF solar cell was calculated by Lee *et al.* and Tayebjee *et al.*[51,52] As can be seen in Fig. 1d, the benefit of SF contrasts that of TTA-UC with the largest benefit for low E_g solar cells, such as c-Si and CIGS solar cells, approaching theoretical efficiencies of roughly 45%. Furthermore, a combined TTA-UC and SF solar cell would have the potential to reach high power conversion efficiencies across the entire range of E_g relevant to known photovoltaic materials.[53]

The triplet pair, the commonality of triplet–triplet annihilation and singlet fission

In essence, TTA and SF are reverse equilibrium processes, where the common denominator is the so-called triplet pair. It is therefore constructive to discuss the triplet pair from both a TTA and SF point of view. A simplistic way of viewing these processes is through the Johnson–Merrifield model (eqn (1)) that describe TTA and SF as a two-step process,[54] with an intermediate correlated triplet pair state (^{1}(TT)):

$$S_1S_0 \rightleftarrows {}^1(TT) \rightleftarrows T_1 + T_2 \qquad (1)$$

This model states that SF and TTA are spin conserving process, as the formed triplet pair state, ^{1}(TT), has an overall spin of singlet character. As such, they can proceed extremely fast, even on sub picosecond timescales in certain materials.[55,56] Our understanding of processes involving the triplet pair comes mostly from the SF literature and has improved greatly over the last decade. It is now generally accepted that SF is more correctly described by a 3-step process (eqn (2)),[57] introduced by Scholes:

$$S_1S_0 \rightleftarrows {}^1(TT) \rightleftarrows [T_1\cdots T_1] \rightleftarrows T_1 + T_1 \qquad (2)$$

Here the first step of SF is the formation of a bound triplet pair state, with similarities to the $2A_g$ state in polyenes.[58,59] The ^{1}(TT) state has both electronic and spin coherence. Over time the triplets move apart, through a triplet energy transfer mechanism.[57,60] The electronic coherence is lost, and a weakly bound triplet pair state $[T_1\cdots T_1]$ is formed.[57,61] Eventually spin coherence is also lost, and two free triplet states are formed ($T_1 + T_1$).[57,61] Here, the backwards reaction is TTA.

The nature of triplet pair states from a SF point of view has been extensively discussed in recent reviews.[59,61–63] Although the triplet pair states in eqn (2) are considered intermediates, it should be noted that in the literature it is not always clear which of the steps are referred to as SF. *I.e.* is rapid and efficient formation of ^{1}(TT) enough to label a system efficient for SF, even if no further separation of ^{1}(TT) occurs? Zhu and co-workers argue that the better and most relevant definition of SF in terms of yield and rates should be the formation of $[T_1\cdots T_1]$.[61] However, it is often difficult to experimentally distinguish between each of the ^{1}(TT), $[T_1\cdots T_1]$ and $T_1 + T_1$ states. For TTA the definition is more clear-cut, as measurable emission is what is typically used to observe TTA. On the other hand, the intermediate states are more challenging to study, due to their fleeting lifetime compared to their often diffusion limited formation time.

In the TTA literature, the widely accepted mechanism is based on a coupling between two triplet states with strong exchange coupling (a parameter describing the strength of the electronic and magnetic interactions between triplets).[64,65] If we consider the two initial triplets in TTA ($T_1 + T_1$), and not taking the weakly bound triplet pair state into account, triplet pair formation with nine possible outcomes is possible (Fig. 2).[66–69] Where one is singlet ^{1}(TT), three are triplets ^{3}(TT) and five are quintets ^{5}(TT). The lack of possibility for quintet formation on a single chromophore (for energetic reasons) would mean that ^{5}(TT) dissociation is the only fate possible and therefore four recombination outcomes are possible and not nine. Moreover, TTA to a higher excited triplet state is plausible, with the consequence of the formation of one ground state and an excited state that will relax and reform T_1,

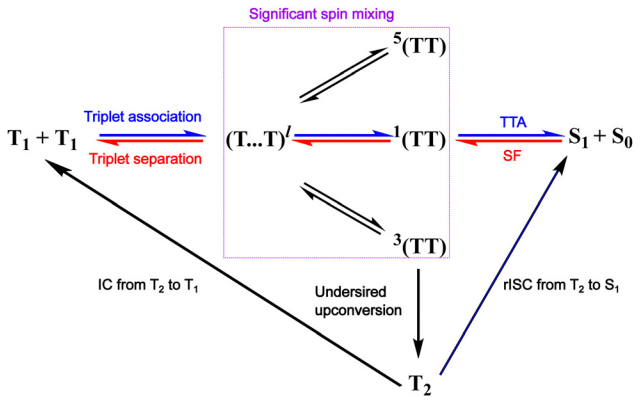

Fig. 2 Model of the TTA and SF processes in accordance with eqn (2), we consider triplet pairs of pure spin states as coupled to one another through the intermediate $(T\cdots T)^l$. If the molecules forming the triplet pair are only weakly exchange coupled, then are triplet states no longer considered as eigenstates and significant spin mixing occurs. Processes directly leading to TTA-UC and SF are marked with blue and red colour, respectively.

Open Access Article. Published on 02 November 2022. Downloaded on 10/16/2025 7:02:22 PM.
This article is licensed under a Creative Commons Attribution 3.0 Unported Licence.

following Kashas rule.[66] Only, TTA of ^{1}(TT) leads to S_1 formation and the spin statistical limit for the process is therefore 40%.

However in recent literature it was proposed that it is more appropriate in some cases to consider the triplet pair as weakly exchange coupled.[69] For such cases, spin is not a good quantum number and states having contributions of different spins form. Now, the quintet states from the strong exchange coupled model gets a fraction of singlet spin state character, enabling TTA to some degree. This changes the theoretical spin statistical limit to 67%.[69] It should be noted that these investigations were done for rubrene in the solid-state, and to date it is unclear if these results are translatable to other materials and conditions. One particular example, annihilation of perylene tolerates bulky substituents, indicating that annihilation does not require a very close contact pair.[70,71]

Theoretical calculations have also played an important role to deepen our understanding of the triplet pair state and their formation, in particular in terms of SF. For theoretical calculations it is most common to consider the coupling between the initial S_1S_0 state and the ^{1}(TT) state when estimating the SF rate.[72] However, the coupling mechanism between chromophores involved in SF has been a topic of recent debate.[73–84] The different coupling mechanisms are presented in Fig. 3. Using first order perturbation theory, coupling occurs directly between S_1S_0 and ^{1}(TT), analogously to internal conversion (direct mechanism, Fig. 3).[72,74] This coupling is, however, often quite small. Using higher order perturbation theory, the coupling of S_1S_0 and ^{1}(TT) to charge transfer (CT) states can be considered, often resulting in a larger coupling.[72,74,77,82,85–87] If the CT states are higher in energy than S_1S_0, they only participate 'virtually' in a super exchange mechanism, and are never populated (mediated mechanism, Fig. 3).[72,77,79,82,83,85,86,88–96] However, in some materials the CT state can be energetically accessible from S_1S_0 and might then be populated as an intermediate in the transition to ^{1}(TT) (two step mechanism, Fig. 3).[97–99] The coupling, and hence the rate of ^{1}(TT) formation, in SF materials varies greatly depending on for example the molecular structure,[81] molecular packing in the solid-state,[75,81,100–106] and solvent for solution phase chromophores.[83,93,94,96,98,99,107–113] If the electronic coupling is weak, SF is often described within a non-adiabatic picture (Fig. 4a), treating the localised region where the diabatic potential curves cross as non-adiabatic. Here the rate increases with increasing coupling as described by conventional Marcus theory for electron transfer.[81,114] With sufficiently large coupling, the non-adiabatic picture is no longer appropriate, instead an adiabatic picture where S_1S_0 continuously evolves to ^{1}(TT) is more suitable (Fig. 4b). It has been shown that in the adiabatic regime the rate of singlet fission becomes independent of electronic coupling.[81,87,92] However, debate is still ongoing as to the exact nature of the coupling responsible for ultrafast SF. For example, in contrast to super-exchange mediated coupling, vibronic coherence between S_1 and ^{1}(TT), along with entropic effects have recently been suggested to drive ^{1}(TT) formation.[99,115–121] The required coupling between chromophores in terms of TTA is a much less explored aspect that likely will become more important as more solid-state TTA systems are developed.

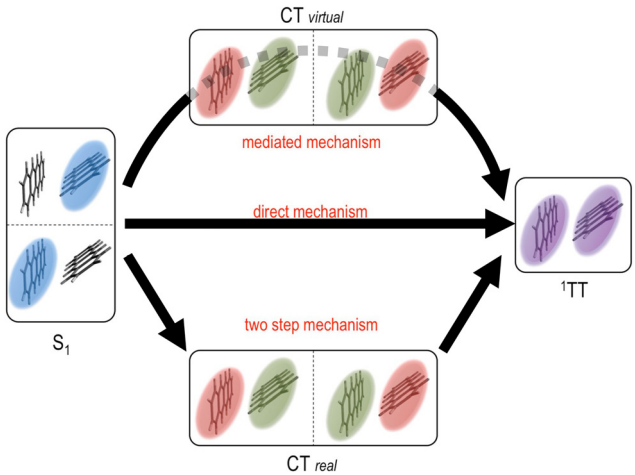

Fig. 3 Possible mechanisms for the S_1S_0 to ^{1}(TT) transition in singlet fission. Top path: The mediated super exchange mechanism where S_1S_0 and/or ^{1}(TT) couple *via* virtual CT states. Middle path: The direct mechanism where S_1S_0 couples directly to ^{1}(TT). Bottom path: The two-step mechanism where an intermediate CT state is formed prior to ^{1}(TT) formation. Figure adapted from ref. 72, with permission from the American Chemical Society. Copyright 2018.

Energetic and entropic requirements

In TTA, the energy of ^{1}(TT) (or by first approximation twice T_1) must be larger or equal to that of S_1 to allow TTA to occur efficiently ($2 \times E_{T_1} \geq E_{S_1}$). The opposite is true for SF, where the initially formed singlet excited state must be higher or equal in energy to the energy of the two formed triplets ($E_{S_1} \geq 2 \times E_{T_1}$). It is noteworthy that some materials can show both SF and TTA, as the energetic barriers are overcome by k_BT.

For SF, this requirement can be further relaxed in some systems. For example, thermally activated triplet dissociation has been observed in systems having a rapid and exothermic relaxation from the S_1 state to ^{1}(TT).[121–124] Another important consideration that relaxes the energetic requirement is the role of entropy in SF. As has been discussed extensively recently, entropy can play a determining role in the efficiency of endothermic SF.[61,73,125,126] Both the step from S_1 to the triplet pair state ^{1}(TT), as well as the step from the triplet pair state to the weakly bound pair state [$T_1 \cdots T_1$] are associated with a gain in entropy as described by the equations below.

$$\Delta S_{S_1 \rightarrow TT} = k_B \ln\left(\frac{\Omega_{TT}}{\Omega_{S_1}}\right) \quad (3)$$

$$\Delta S_{TT \rightarrow T\cdots T} = k_B \ln\left(\frac{\Omega_{T\cdots T}}{\Omega_{TT}}\right) \quad (4)$$

where Ω_i is the number of microstates the ith state can sample.[41,61] As the molecular packing and structure can influence the number of available states, it influences both the electronic coupling and the entropic contributions.[126,127] It is therefore a non-trivial task to design and develop suitable SF materials. Contextualising all these findings to photon

Open Access Article. Published on 02 November 2022. Downloaded on 10/16/2025 7:02:22 PM.
This article is licensed under a Creative Commons Attribution 3.0 Unported Licence.

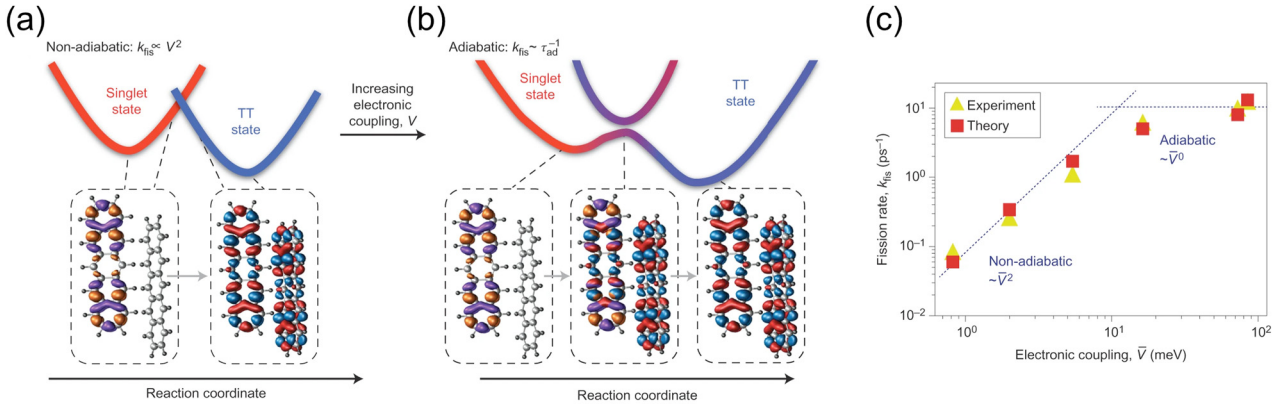

Fig. 4 (a) Non-adiabatic picture of SF for weakly coupled SF chromophores. (b) Adiabatic picture of SF for strongly coupled chromophores. (c) The rate of SF as a function of electronic coupling. Figures reprinted from ref. 81 with permission. Copyright 2014 Nature Springer.

conversion in PV applications, especially considering solid-state systems, we must take special care to appreciate the effect disorder may have on the triplet diffusivity and hence the overall limit of TTA-UC and SF.[75,81,98,100–106,128–130]

It is important to also consider the energy of the second triplet (T_2) state when studying new SF or TTA chromophores.[76,131,132] Ideally T_2 lies higher in energy than the combined energy of the two T_1 states ($E_{T_2} > 2 \times E_{T_1}$), to minimise undesired triplet–triplet annihilation to T_2 (Fig. 2).[34] It is known that reverse intersystem crossing from T_2 to S_1 is possible, which in theory allows for zero wastage of photons if rapid.[133] However, relying on reverse intersystem crossing to kinetically outcompete T_2 to T_1 internal conversion is not a general advisable strategy when designing new materials. Whether considering a model based on a weakly or strongly exchange coupled triplet pair, the energetics of annihilator molecules play a crucial role in limiting TTA yields. Thus, energetics can turn off loss mechanisms from the ^{3}(TT) state, allowing in principle for unity efficiency.[134,135]

Key existing challenges and limitations in TTA-UC and SF

We have discussed fundamental mechanisms and limitations in both the TTA and SF regimes including spin state-coupling dynamics. We will briefly discuss here some of the current material challenges in maximising both yield and/or functionality of TTA or SF in PV applications. We will later reference these challenges in the relevant sections, and how current progress has helped or failed to address them.

Energetic matching to PVs

When designing TTA and SF systems, particular attention must be paid to the absorption energy *vs.* PV absorption edges. We refer to Fig. 1, which highlights the issue. To achieve meaningful solar cell efficiency improvements, it is important that the photon converting system operates far enough below or above the absorption edge. For example, A TTA-UC system that operates with sensitiser absorption at 1.12 eV could improve ABX_3 but not c-Si solar cells due to energetic matching. We will therefore discuss some strategies that are being developed to address energetic requirements and their advantages and drawbacks.

Energy and charge injection

To use the created excited states from TTA or SF, PVs need to extract them in one way or another. It is therefore important to consider the organic–inorganic interface between the photon converting material and PV material. Charge injection kinetics have been studied for both SF and TTA materials on metal oxide surfaces with various degrees of success. Excitonic energy transfer across the organic–inorganic interface is another aspect that either enables the use of nanocrystals as spin-mixers in TTA and SF systems or allows for direct use of the excitons in a PV. This review will cover strategies that are being used to overcome hurdles unique to the organic–inorganic interfaces in TTA and SF.

Material stability

Relevant to both SF and TTA, is the photostability of acenes, which are commonly used in both processes.[136,137] These compounds degrade under photoirradiation, most commonly by reacting with singlet oxygen.[138,139] Oftentimes, acenes are used in SF due to their favourable energetics and planar stacking, making the fabrication of crystalline solids facile. Whilst some groups have modified the acene core to make more photostable derivatives, it is observed that the morphology changes influence the SF efficiency to a significant extent.[140,141] Whilst some strategies such as polymer encapsulation and oxygen scavenging have been used with varied levels of success in TTA-UC,[142–145] these are not always relevant to the solid-state. We will therefore discuss some of the methods being used to negate oxygen quenching in solid-state SF and TTA-UC. We also consider the viability of these strategies in light of morphological requirements.

Triplet diffusion

One of the largest difficulties in solid-state photon conversion is the transport of triplets: either to an interface for charge/energy

Open Access Article. Published on 02 November 2022. Downloaded on 10/16/2025 7:02:22 PM.
This article is licensed under a Creative Commons Attribution 3.0 Unported Licence.

injection in the case of SF; or for TTA, from two sensitisers to the point of annihilation. Molecular diffusion drives the latter process in solution, however in the solid-state this must be achieved by exciton diffusion. It is well known that the orientation, crystallinity and packing of molecules play a large role in the triplet exciton diffusivity of solid materials for SF and OLEDs.[76,146–150] This means that there are two interlinked hurdles common to TTA and SF related to triplet diffusion. One is the reversibility of both processes leading to inherent losses if the energies of excited states are not properly tuned to favour one direction.[132] The other is that molecular structure is highly important to the stacking and packing morphology.[149–151] We will highlight in this review strategies that are being used to overcome morphological hurdles, and equally those that are used to aid exciton diffusion.

Triplet–triplet annihilation based photon upconversion (TTA-UC)

The TTA-UC field started fairly modestly with an initial description of the process given by Parker and Hatchard in the early 1960s.[152] The field faced a renewal of interest in the 2000s,[46,153–155] porphyrin and coordination complexes extend the observed anti-Stokes shift and have led to huge TTA-UC efficiency enhancement over early examples. The field has seemingly progressed to a point that the focus is no longer on understanding of the process, but on the efficiency optimisation and application of TTA-UC systems to functional materials. It can be argued that it has been a pre-mature turn of focus, as there are still many fundamental aspects of TTA that are not well understood (*e.g.* spin selection). In the following sections we will first describe the component photophysical processes governing TTA and the efficiency thereof. We will further detail the figures of merit generally applied in the TTA field, and discuss these in the context of PVs and their efficiency.

Forming annihilator triplets in TTA-UC

We have so far considered the nature of the TTA event, focussing on the interaction of the triplet states. Now we will describe the typical processes used to generate these triplet states. In sensitised TTA, the type focussed on in this work, the overall event is a bimolecular process requiring a sensitiser and annihilator to function. The presence of a sensitiser with a high intersystem crossing yield is necessary, due to the extremely low oscillator strength of direct singlet to triplet transitions for annihilators.[156] The overall photophysical process is described schematically in Fig. 5 together with example spectra and a typical visual observation.[134] The idealised TTA-UC process forms one high energy photon from two low energy photons, and the process can be broken down into stages based on independent processes having their own requirements.

Stage 1. The first stage relies on exciting a population of sensitiser molecules to the triplet state. Most commonly, this occurs *via* excitation to the singlet excited state, before intersystem crossing occurs to reach the sensitiser triplet excited state. These steps can be considered together as a single stage.

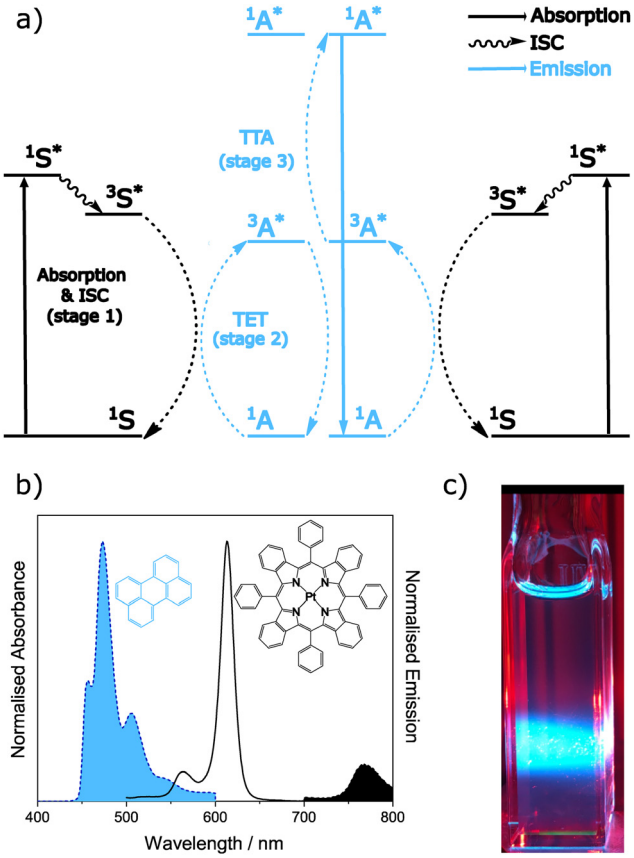

Fig. 5 (a) Energy level diagram for the TTA-UC process. The triplet energy transfer (TET) occurs from the triplet excited state of the sensitiser to the triplet excited state of the annihilator. Two annihilators in their triplet excited states then meet, allowing triplet–triplet annihilation (TTA) to occur, and the subsequent emission from the singlet excited state to be seen. Colours are used to denote the species involved in each process. (b) Representative absorption (black unfilled) and emission (filled blue for annihilator component and filled black for sensitiser component) spectra collected from a solution containing 3 μM of sensitiser (black) and 1 mM of annihilator (blue) excited at 627 nm. (c) Optical camera image taken of the aforementioned solution under excitation from a 617 nm LED source. Data is adapted from ref. 134.

Some ideal characteristics of the sensitiser would be high molar extinction coefficients at low energies but transparent at wavelength of the upconverted emission, a small singlet–triplet energy splitting, efficient inter-system crossing (ISC), and long excited triplet state lifetime. Commonly, metalloporphyrins,[157–159] coordination complexes,[160,161] or nanocrystals[162,163] are used as sensitiser species. Although, methods for sensitisation exist that differ from that described in Fig. 5. Notably, charge transfer state formation at an interface following singlet diffusion,[164] and triplet excited state formation in molecular dyads.[165–167] We will cover specific examples where appropriate.

Stage 2. The next stage is triplet energy transfer (TET) from a sensitiser to an annihilator. At this stage there are two ideal characteristics, close proximity of the sensitiser and annihilator and an isoenergetic or a small downhill energy in the sensitiser to annihilator triplet energy transfer. In solution close proximity is achieved by high diffusivity of the annihilator. In solid-state it requires optimization of the film morphology.

Open Access Article. Published on 02 November 2022. Downloaded on 10/16/2025 7:02:22 PM.
This article is licensed under a Creative Commons Attribution 3.0 Unported Licence.

Stage 3. The final stage is the annihilation event (TTA), where two triplet excited states will recombine resulting in one relaxing back to its ground state and the other being promoted to the singlet excited state, from where photon emission will occur. In solution, the encounter event is realised by molecular diffusion, and in the solid-state the excitons need to diffuse. Annihilators ideally should have long lived triplet states, large TTA rate constants, and high fluorescence quantum yields.

The TTA-UC quantum yield

The upconversion efficiency (Φ_{uc}) in TTA-UC systems is based on the IUPAC definition of the quantum yield (Φ; eqn (5)).[168] In the case where emission is desired, each count of an emitted photon is used to define an event. The maximal Φ_{uc} is therefore 50%, because two absorbed photons generate one emitted photon.

$$\Phi = \frac{\#\text{events}}{\#\text{photons absorbed}} \tag{5}$$

Difficulties arise when making comparisons of Φ_{uc} within the TTA-UC literature. Normalisation based on the photon stoichiometry has been routinely used to inflate upconversion yields.[25] To avoid any confusion,[68,169] we will note quantum yields in accordance with the IUPAC definition (*i.e.* not normalised) and will modify values found in the literature to remain consistent, despite their original presentation.

The upconversion efficiency is a function of the individual efficiencies of each step in the process. Eqn (6) defines the yield of the annihilator singlet states theoretically produced (Φ_{max}). This relies on the efficiency of intersystem crossing (Φ_{ISC}), the sensitiser to annihilator triplet energy transfer efficiency (Φ_{TET}), and efficiency of the triplet–triplet annihilation process (Φ_{TTA}). In eqn (6) the value of Φ_{TTA} incorporates the spin statistical factor, and by definition then has a maximum quantum efficiency of 50%.

$$\Phi_{max} = \Phi_{ISC}\Phi_{TET}\Phi_{TTA} \tag{6}$$

Eqn (7) introduces the concept of back energy transfer, between the annihilator and sensitiser species in either the singlet or the triplet states. This loss channel is accounted for with a second term ($1 - \Phi_{BET}$). It further accounts for the non-radiative losses of the annihilator species, by introducing its inherent fluorescence quantum yield (Φ_f). This gives the yield of generated emitted photons (Φ_{sing}).

$$\Phi_{sing} = \Phi_{smax}\Phi_f(1 - \Phi_{BET}) \tag{7}$$

Finally, eqn (8) defines the observed value of Φ_{uc} by further accounting for procedural losses with an outcoupling term (Φ_{exp}). Losses such as inner filter effects and scattering *etc.* are accounted for here.

$$\Phi_{UC} = \Phi_{sing}\Phi_{exp} \tag{8}$$

For a detailed description of good practices when taking quantum yield measurements, we direct the reader to the articles of Brouwer and Rurack *et al.*[170,171]

The threshold intensity

In the context of PV devices, upconversion is driven by sunlight. It is therefore important that the maximum quantum yield of the upconversion process is reached at equal to or sub-solar photon flux (Fig. 1). The excitation density at which the resultant upconversion intensity is described by equal contribution of first and second order processes is called the threshold intensity (I_{th}).

To mathematically define this term, we separate first order and a second order processes. The first-order decay is a combination of phosphorescence, non-radiative decay and *quasi* first-order quenching processes related to oxygen (this effect should be eliminated in ideal systems). The second-order decay solely originates from triplet–triplet annihilation. We can express the time-based decay of annihilator triplet concentration, $[^3A^*]$, as a function of the rates of first (k_T) and second order (k_{TTA}) decay. Eqn (9) details the overall equation.[71,172]

$$\frac{d[^3A^*]}{dt} = -k_T[^3A^*] - k_{TTA}[^3A^*]^2 \tag{9}$$

From eqn (9) it is evident that at low $[^3A^*]$ values the dominant process will be pushed towards the intrinsic quenching. Only when a sufficient $[^3A^*]$ is reached will the TTA-UC process be dominant.[173] This then means that at low excitation powers, a quadratic relationship with upconverted emission intensity is observed. Therefore, Φ_{uc} will increase with increasing excitation power. At higher excitation powers the relationship of emission intensity with excitation density becomes linear, thus Φ_{uc} remains constant. Often researchers perform an excitation power dependent study of the upconverted emission intensity. From a log–log plot of the excitation and emission intensities, regions of quadratic and linear regimes can be identified (Fig. 6). The crossing point, defined as I_{th}, is the excitation density where the first and second order processes have equal rate. Eqn (10) describes the influence of the integrated sensitiser absorption and first and second order rate constants on I_{th}. As a caveat, it should be mentioned that it is not always possible to identify quadratic and linear sections in a log–log plot. Effectively, in these situations I_{th} cannot be identified. This is often the case if TET is inefficient, or non-radiative

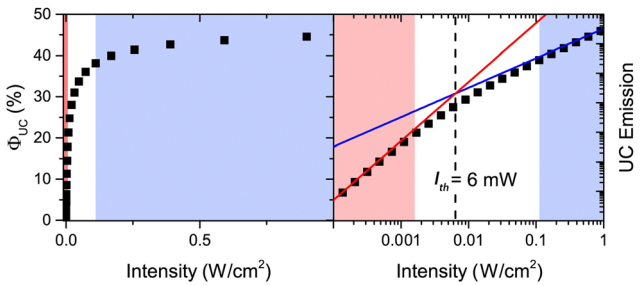

Fig. 6 (left) Typical plot of Φ_{uc}, as a function of excitation intensity. (right) log–log plot of UC emission intensity against excitation intensity. Areas where the weak and strong annihilation limits are valid are shaded in red and blue respectively. The threshold intensity is identified, I_{th}, where the lines with slope 1 (blue) and slope 2 (red) cross. Reproduced with permission from ref. 68. Copyright 2018 Elsevier B.V.

Open Access Article. Published on 02 November 2022. Downloaded on 10/16/2025 7:02:22 PM. This article is licensed under a Creative Commons Attribution 3.0 Unported Licence.

decay and/or oxygen quenching are high in the TTA-UC system.[153]

$$I_{th} = \frac{k_T^2}{2k_{TTA}\alpha[S]} \quad (10)$$

For a detailed discussion on best practice in determining key photophysical parameters in triplet–triplet annihilation photon upconversion, including I_{th}, we direct the reader to Edhborg *et al.*[174]

Red/near infrared to visible TTA-UC systems

It is the energy of the sensitiser that governs which type of PV device that the UC system can be linked to. In general, TTA-UC systems have suffered from a poor match between the sensitiser absorption and the PV E_g. We will, therefore, here discuss TTA-UC, with a focus on the sensitiser species. The absorption wavelengths are considered in the context of differing PV materials and a summary of all the molecular sensitisers covered in this section is given in Fig. 7, in which we detail their structure and properties.

Coordination complexes in NIR to visible TTA-UC

Coordination complexes are a useful class of chemical compounds, allowing low energy transitions due to metal to ligand (or ligand to metal) transitions.[175,176] Even if the metals are not directly involved in the transition, a more efficient ISC can still be observed.[177] The earliest examples of near infrared to visible TTA-UC utilise metalloporphyrin complexes,[155] having a high triplet yield.[178–181] Indeed many groups continue using porphyrin complexes as sensitisers (**1**, **2**),[182–186] although due to the breadth of literature concerning porphyrins we will not specifically cover them in this section. Instead, we will address here recent works related to other classes of organometallic and coordination complexes.

Platinum-group elements has been seen ubiquitously in TTA-UC. However, the scarcity of such metals prompted investigation into alternative photosensitisers based on earth abundant metal centres. Wenger *et al.* presented an example of a Mo(0) complex that shows potential as a sensitiser for upconversion with excitation in the visible red region (**3**).[187] The synthesised Mo(0) complex offers an earth abundant core that possesses high photostability under 500 mW irradiation at 532 nm. Red to blue upconversion using the Mo(0) complex in tandem with 9,10-diphenylanthracene (DPA), was achieved using 635 nm (1.95 eV) excitation light. Castellano *et al.* later used a similar strategy to avoid precious metals, using the ligand-to-metal charge transfer of a Zr(IV) complex (**4**) to sensitise DPA.[188] Importantly, the I_{th} value (0.115 mW cm^{-2}) lies below that of the integrated solar flux through the Zr(IV) photosensitiser's absorption band (26.7 mW cm^{-2}). Both complexes unfortunately suffer from high singlet energies (1.94 eV and 2.13 eV respectively) rendering these complexes less than ideal for PV applications. Referring to Fig. 1C, to be a relevant sensitiser for upconversion assisted energy conversion in the majority of PV cell types, the singlet excited state energy would ideally be somewhere around 1.3–1.7 eV or below. Significant synthetic modifications of their ligands would be necessary to tune the energy levels of these complexes to be favourable in PV applications, however this might be achieved in a similar manner to other coordination complexes.[189,190]

To circumvent the energy loss when sensitisers relax from the initially excited singlet state to the triplet state, direct singlet to triplet excitation can be performed. Such transitions facilitate a gain in the observed anti-Stokes shift of the TTA-UC system. The first example of this phenomena used in TTA-UC was demonstrated by Kimizuka *et al.* wherein an Os(II) complex (**5**) was used as a triplet sensitiser for rubrene.[191] NIR to visible upconversion was observed with an excitation at 938 nm and upconverted emission around 570 nm. Complex **5** has a suitable triplet excitation energy to capture solar light at lower energies than the majority of PV types (Fig. 7). However, the system shows an extremely poor Φ_{UC} of 0.0007% in deaerated dichloromethane. Many further derivatisations have been carried out in order to improve efficiency, or increase the anti-Stokes shift (**6**, **7**, **8**).[192–194] The leading Os(II) complex (**7**) was reported together with anthracene based annihilators, with Φ_{UC} of 5.5% and an anti-Stokes shift of 1.28 eV. One caveat of direct S_0 to T_1 transitions are their small ε values and fast relaxation. It therefore seems unlikely that this type of material will achieve high enough molar absorptivities to get an I_{th} in the solar spectral range. Also, since the absorptivity is fundamentally linked to the rate of emission, mitigation strategies would need to be developed.

Nanocrystal and nanoparticle assisted TTA-UC

Addressing both energetic matching with PV bandgaps and triplet exciton diffusion, lead and cadmium-based nanocrystals (NCs) have been shown to be effective in sensitised upconversion from low intensity and low energy light. Baldo *et al.* reported NIR to visible upconversion sensitised by colloidal NC's with excitation wavelengths above 1 μm (**9**), sparking an interest in NC sensitised TTA-UC.[195] The I_{th} values for this system were higher than the solar photon flux however, due to inefficient TET. To address this issue the group of Tang *et al.* introduced a mediator ligand.[196–198] The role of the mediator was to facilitate TET. This was achieved by covalently attaching a molecule having the appropriate triplet energy, forming a link between the PbS-Cd NC (**10**) and the rubrene annihilator (Fig. 8). This system allowed for the first example of a TTA-UC system based on nanocrystals to operate below the solar photon flux.[196–198]

Lian *et al.* later set out to study the factors governing the overall Φ_{UC} in tetracene mediated UC using NC's.[199] They used a PbS NC (**11**) which was coated with one of three mediators, having different lengths of linker unit. The results showed that the effect of the overall upconversion quantum yield can be broken down into its reliance on two processes, the first and second TET (NC to mediator as TET1, then mediator to annihilator as TET2) such that $\Phi_{UC} \propto \Phi_{TET1}\Phi_{TET2}$. There were two

Open Access Article. Published on 02 November 2022. Downloaded on 10/16/2025 7:02:22 PM.
This article is licensed under a Creative Commons Attribution 3.0 Unported Licence.

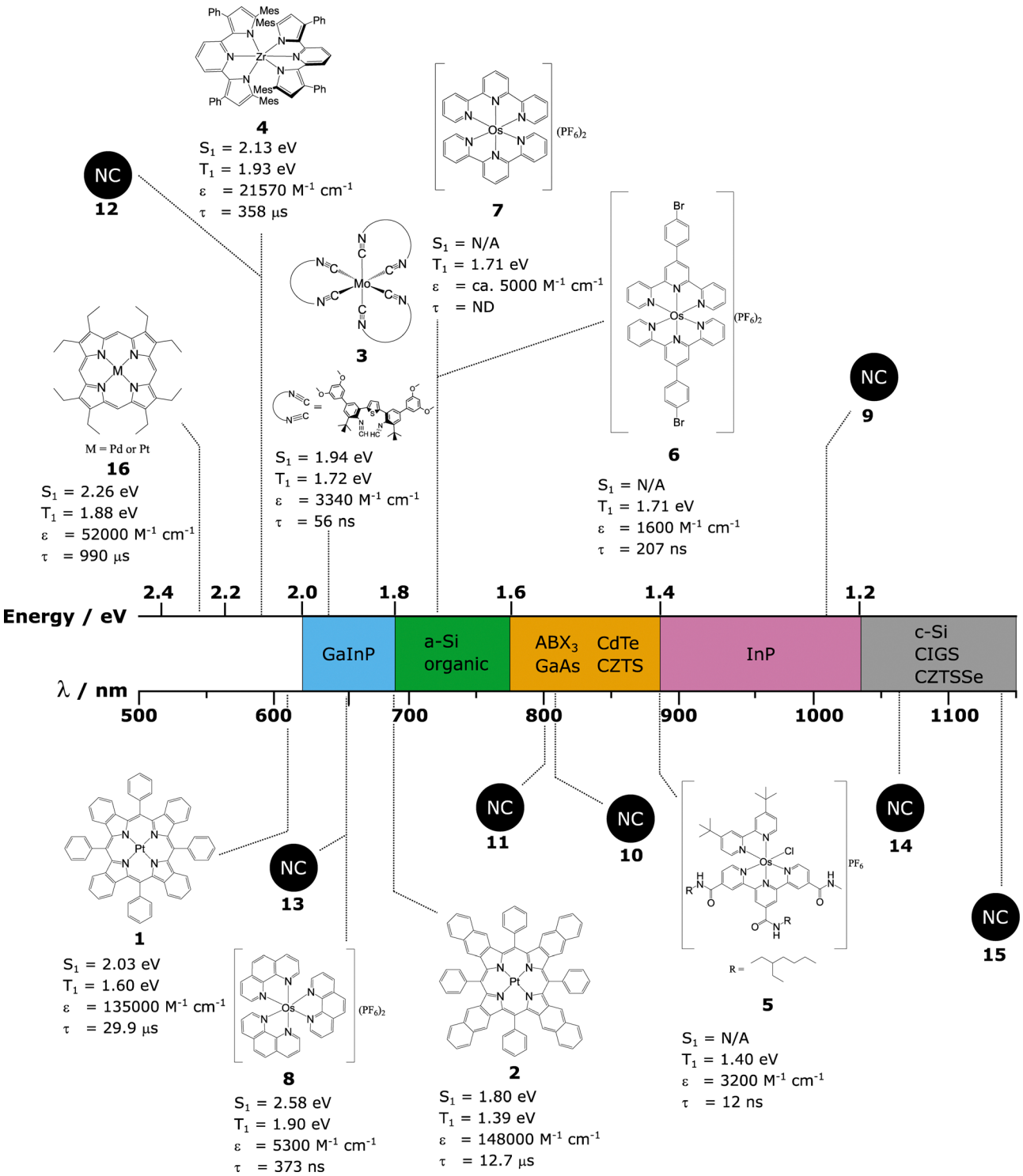

Fig. 7 Structures of the molecular sensitisers discussed in this work, also shown are the excitonic peaks of nanocrystal sensitisers used in TTA-UC discussed in this work. The types of PV material to which the sensitisers could be applied to in order to monochromise sufficient amounts of the solar spectrum to increase device efficiency are roughly split up into coloured areas, white areas inside the central bar indicates energies that are not relevant to any type of current PV material. The S_1 and T_1 energies given are estimates from absorption and emission spectral maxima where no other data is presented in the original works. Lifetimes are the phosphorescence lifetimes of the molecules shown.

key findings in this work. Firstly, the energy transfer rate from NC to tetracene decreases rapidly with increasing spacer length. Secondly, the energy transfer rate from tetracene to annihilator increases with increasing spacer length. Taken as an overall effect, the longer spacer lengths were found to have a detrimental impact on the Φ_{UC} due to the hugely reduced Φ_{TET1}.[199]

Open Access Article. Published on 02 November 2022. Downloaded on 10/16/2025 7:02:22 PM.
This article is licensed under a Creative Commons Attribution 3.0 Unported Licence.

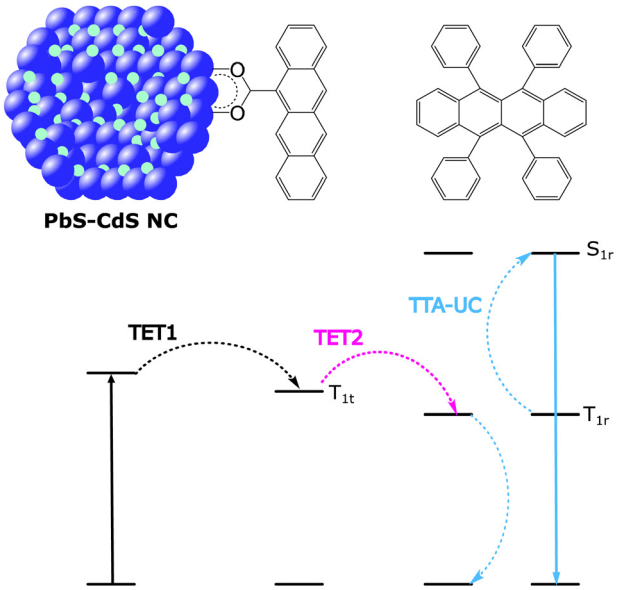

Fig. 8 Working principle of the energy transfer process in acene capped nanocrystals. Here, an excitonic state of a PbS–CdS nanocrystal is excited with long wavelength light (black solid arrow) transfers energy to the triplet state T_{1t} of a bound tetracene-5-carboxylic acid (TET1, black dashed arrow), which in turn will transfer energy to the triplet state T_{1r} of rubrene (TET2, pink dashed arrow). Finally, the triplet states of two diffusing rubrene molecules will recombine (TTA-UC, blue dashed arrows) to produce an upconverted photon (blue solid line).

These results demonstrate the importance of rational mediator design to drive the desired energy transfer process.

The toxicity of nanocrystals fabricated from Cd and Pb has been highlighted as a potential risk. Just as for PV materials containing these elements, there is a drive to demonstrate NC sensitised upconversion with more benign elements.[162,200–202] Wu *et al.* recently proposed InP-based nanocrystals as sensitisers for solution based TTA-UC using anthracene as a mediator and DPA as an annihilator.[203] InP NCs are well known to possess trap states,[204] limiting their use as sensitisers. However, in this work creating a 0.6 nm shell of ZnSe/ZnS (**12**) was sufficient to eliminate the trap states.[203] The highly emissive zinc coated NCs were subsequently coated with 9-anthracene carboxylic acid, and displayed an anti-Stokes shift of 0.98 eV, and a Φ_{UC} of 5%. The non-toxic NCs in this work provide a route for elimination of toxicity in TTA-UC.[203]

Whilst all NC examples discussed above are zero dimensional structures, Nienhaus *et al.* have presented the first example of a 1-dimensional nanorod sensitiser for TTA-UC, *i.e.* where quantum-confinement is present in two dimensions.[163] The study aimed to increase not only the breadth of quantum-confined materials used in TTA-UC but also improve the anti-Stokes shifts shown by nanocrystals. The work used the mediator/annihilator couple of 9-anthracene carboxylic acid (ACA)/DPA sensitised by cadmium telluride nanorods (**13**). The authors demonstrate TTA-UC using a material with well-defined facets and unique anisotropic shape that allows self-assembly into macrostructures. As discussed above, control over macroscopic structure is a key determinant in triplet energy transfer, crucial in TTA-UC and SF.

To be relevant to c-Si solar cells the absorption energy of the sensitiser must lie below 1.12 eV (Fig. 1). In 2020 a PbS nanocrystal (**15**) based TTA-UC system that operates below the bandgap of c-Si was proposed by Schmidt *et al.*,[205] PbS NC's were used as sensitisers, violanthrone derivative (V79) as annihilator and singlet oxygen as mediator. Oxygen's use as a triplet mediator for V79 was previously documented,[206] and relied on the triplet state of the annihilator lying lower in energy than the singlet state of oxygen (0.98 eV). This is the case for V79 where the triplet level was estimated around 0.94 eV. PbS NC's were excited at 1140 nm, and upconversion was observed. Although this occurs at low efficiency due to inefficient TET to oxygen.[206] Rao *et al.* also presented an example of an upconversion system that could operate below the 1.12 eV bandgap of crystalline silicon.[207] The system combined the mediator and annihilator functions into one molecule, 5,11-bis(triethylsilylethynyl)anthradithiophene (TES-ADT). This was achieved by forming a reversible bond to the NP on the timescale of the triplet excited state.[207,208] The material has a triplet level of 1.08 eV and when coupled to a nanocrystal (**14**), displayed upconverted emission after excited at 1125 nm. Whilst the Φ_{UC} is small ($\sim$0.047%), the work avoided the triplet mediator energy limitation of tetracene and allowed an anti-Stokes shift of 0.86 eV.[207] The same TES-ADT system was recently used in a binary solid-state system, using higher energy PbS NCs.[209] The Φ_{UC} determined to 0.2% with 975 nm excitation. One limiting factor is likely the propensity of TES-ADT chromophores to undergo SF in the solid-state.[124,210,211] Both Rao and Schmidt argued that these systems are a step towards relevance of TTA-UC in c-Si solar cells. While this is true, we refer to Fig. 1 to critically assess the importance of upconversion on c-Si solar cells. In c-Si the potential efficiency gain from upconversion is around 5%. This may therefore not be an ideal pairing of UC system to a PV type, we ask would it not be better to use the UC system with a GaAs solar cell for instance? We therefore regard these works as a significant intellectual achievement, stretching the sensitiser absorption edge as well as the annihilator triplet energy towards lower energies. In principle achieving quite optimal annihilator triplet energies for pairing with a high bandgap solar cell.

This section has broadly discussed sensitisers for TTA-UC, which remains an active field of research. We have described above the strategies being developed to address key loss factors. Some of these include singlet–triplet direct energy transfer, and mediated energy transfer from metal nanostructures to TTA annihilators. Both of which simultaneously address low energy absorption and can show efficient TET, and today the structure to function relationship is understood.[199,212] Furthermore, works have addressed wide ranging limitations, from toxicity to earth abundance of the metal centre. For upconversion to be relevant to a majority of PVs, the annihilator emission should be at around 1.7–2.0 eV (the annihilator emission should be slightly lower than the PV bandgap). This translates to a lowest possible annihilator triplet energy

Open Access Article. Published on 02 November 2022. Downloaded on 10/16/2025 7:02:22 PM.
This article is licensed under a Creative Commons Attribution 3.0 Unported Licence.

of 0.85–1 eV (for exothermic TTA). It is an interesting observation, that when being around these triplet energies, singlet oxygen becomes irrelevant as a quencher. Thus, removing the need of encapsulating upconversion systems within PV applications.

Solid-state TTA-UC

Incompatibilities between safety or stability when utilising solution TTA-UC can be difficult to overcome. The solvents used are often flammable, toxic, or volatile. Solid-state TTA-UC offers an alternative that is easier to apply to rigid photovoltaics, and indeed any application where a solid phase is desirable, such as heterogenous catalysis.[213] Triplet exciton diffusion has fundamentally limited development of high efficiency solid-state TTA-UC. In principle, molecular diffusion must be replaced with exciton diffusion when going from solution to solid-state.[214,215] Further major loss factors include back energy transfer and aggregation of sensitisers and/or annihilators, especially tied to the stacking and packing morphology.[68,216] In this section we categorise efforts to reduce losses by material type and detail their outlook in photovoltaics.

Soft-matrix based solid-state TTA-UC

In soft systems, such as gels, the inside of micelles, and in polymers below their glass transition temperature, molecular diffusion is allowed in an otherwise apparent solid-state system.[154,217] The quasi-solid nature of these materials is an intermediate between solution based and fully rigid systems, and therefore they have upconversion efficiencies approaching those in solution.[218]

Gels are liquid in solid emulsions. These materials have been used as a matrix for upconversion systems,[219–221] and temperature responsive systems have further been developed.[222–224] To investigate the existence of a structure-upconversion relationship in gel systems, a low molecular weight gelator was covalently attached to the annihilator DPA with different attachment positions.[225] They were combined with sensitiser **16** (Fig. 7). The $I_{th} \approx$ 400–1000 mW cm^{-2} and Φ_{UC} were found to be attachment position dependent. Morphological effects on upconversion efficiency are however currently unclear in gel systems.

TTA-UC system's working in liquid conditions can be compartmentalised inside micelles. The micelle provides molecular diffusion, and oxygen exclusion. They can further be incorporated into a solid polymer host for a variety of practical applications.[226] A general structure of a solid polymer host incorporating upconversion micelles is given in Fig. 9a. Protein matrices encapsulating micelles formed from SDS were synthesised by Kumar *et al.*[227] Particularly efficient TTA-UC with a Φ_{UC} of 10% was observed from **16** and DPA. However, I_{th} values were in the range of 400–700 mW cm^{-2}. TTA-UC in biopolymeric materials has been further demonstrated by Kimizuka *et al.*, using Triton X-100 micelles containing the

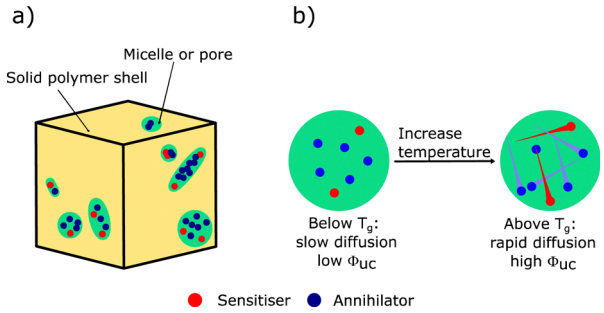

Fig. 9 Graphical representation of the working principle of (a) micelle or pore encapsulated solid gel for TTA-UC, and (b) rubbery polymer matrices with T_g below room temperature.

16-DPA sensitiser–annihilator couple.[228] By changing to a biopolymer, the I_{th} value was lowered to 14 mW cm^{-2}. Furthermore, samples showed stability over 2 years of storage in ambient conditions. Another recent example,[229] uses crosslinked hydrophilic polymers to encapsulate organic hydrophobic solvent containing sensitiser **16** and DPA. Upconversion efficiency (Φ_{UC} = 23%) and stability of the system is high. Whilst the Φ_{UC} is high, so is the I_{th} value (500 mW cm^{-2}). All systems described above have used **16** as a sensitiser and from a UC in PV perspective this is problematic. This is because sensitiser **16** has a singlet energy higher than the absorption edge of all PVs (Fig. 1). We appreciate however that high stabilities were observed, that upconversion efficiencies close to that of dilute solutions were observed and that the concept could be transferred to more PV relevant materials.

Soft polymers with glass transition temperatures below room temperature have also been used as a matrix for TTA-UC. The working principle is graphically demonstrated in Fig. 9b and is based on a relatively high diffusion of dopants in a polymer above T_g. Initial investigations by Castellano *et al.*,[230] sparked many future studies.[231–234] In a more recent example, PVA was used as an oxygen blocking barrier for a thin layer of a soft polymer containing **1** and perylene. This dual polymeric structure was then backed with glass to provide rigidity and an I_{th} of 70 mW cm^{-2} and a Φ_{UC} of 7% was recorded in oxygenated conditions.[235] Following early work with WO_3 photocatalysts,[236,237] a soft polymer matrix containing **1** and perylene was applied to the photocatalyst $BiVO_4$. This aided in the capture of photons below the bandgap of the catalyst, increasing the H_2 and O_2 evolution by around 17% against bare $BiVO_4$.[238] Non-heavy metal based upconversion has also been demonstrated in soft polymers, with thiosquaraine and rubrene doped into a polymer matrix. The formed film was excited at 685 nm under aerated conditions, and upconverted emission was observed. The authors however did not report a Φ_{UC}.[239] Soft polymer matrices can be regarded as a transition from the solution-based gels and micelles to a truly solid-state system. Efficient systems exist, but questions could be raised as to the appropriateness of incorporating rubbery materials within PV technology.

MOF based TTA-UC

Metal–organic-frameworks (MOFs) are porous rigid structures, which are organised based on coordination bonding of the

Open Access Article. Published on 02 November 2022. Downloaded on 10/16/2025 7:02:22 PM.
This article is licensed under a Creative Commons Attribution 3.0 Unported Licence.

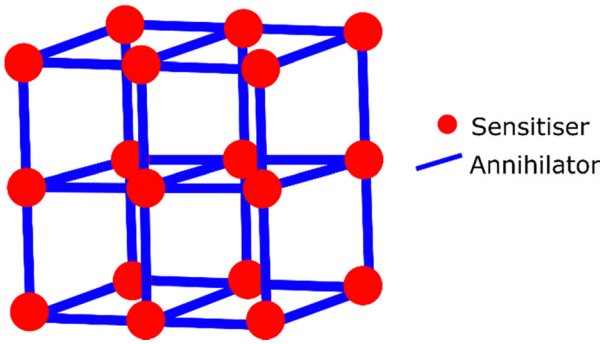

Fig. 10 General structure of a MOF with coordination bonded annihilators and sensitisers in an ordered network.

constituent molecules (Fig. 10). This gives them a much higher order than gel based systems, and can be considered entirely solid-state as they do not require any solvent to be present in the pores.[240] MOFs avoid aggregation of the molecular components, and allow for some level of oxygen exclusion. MOFs have been demonstrated to function as upconverters when dispersed in solution.[241–245] Although they have also been investigated in entirely solid-state systems. A highly crystalline zirconium MOF was synthesised containing linkers of both sensitiser and annihilator in a controlled ratio.[246] The osmium sensitiser is a carboxylic acid derivative of 7 and the annihilator is based on anthracene. MOFs synthesised with a sensitiser : annihilator ratio of 1 : 94 were encapsulated inside a polymer blend and I_{th} and Φ_{UC} values were measured at $\sim$10 W cm^{-2} and 0.006% respectively. The low upconversion quantum yield was reasoned to be due to trap sites from locally disordered structures within the framework. We would argue that MOFs for upconversion applications may benefit when made using a templated surface reactions in a continuous flow approach. This method produces frameworks with lower numbers of defects and a high surface smoothness, which should benefit optical investigations.[247,248]

It was recently shown that by tuning the geometry between chromophores in MOFs the triplet exchange coupling could be controlled to direct the spin-mixing of singlet and quintet triplet pair states.[249] If controlled correctly this could result in improved upconversion yields compared to random oriented materials.

Matrix free solid-state upconversion

We define matrix free TTA-UC as sensitiser and annihilator materials being in their solid-state and no molecular diffusion being present. This may be seen as the most facile processing method for solid films, and easiest to apply to PVs. However, neat conditions can give a multitude of problems such as aggregation-induced energy loss, FRET back to the sensitiser, non-radiative triplet decay, and annihilator quenching such as excimer formation.[71,250–252] In this section we describe recent literature that attempts to understand and find fabrication methods to avoid these losses.

Within bulk solid-state upconversion materials, Kazlauskas *et al.* investigated a method to reduce detrimental aggregation

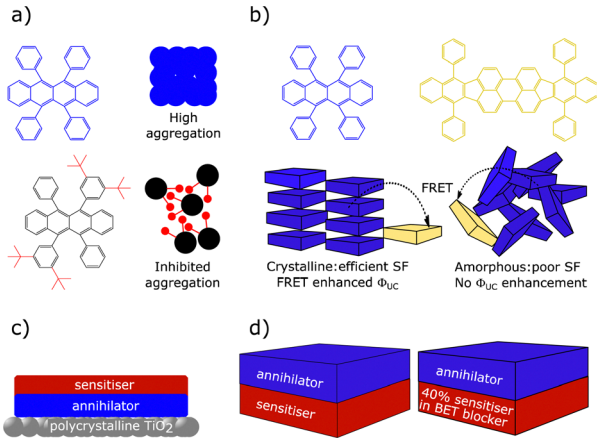

Fig. 11 (a) Structures of the rubrene and *t*-butyl substituted analogue, along with a cartoon depiction of the mechanism behind SF inhibition. (b) Structures of the rubrene annihilator and DBP dopant used to investigate the effect of dopant in crystalline and amorphous films. (c) Sensitiser annihilator bilayer structure for increasing photocurrent in TiO_2. (d) Unmodified bilayer and back energy transfer (BET) preventing DMPPP doped bilayer structures.

of the annihilator.[253] Two analogues, rubrene and *t*-butyl-substituted rubrene, were doped into polystyrene (Fig. 11a). It was shown that *t*-butyl-substitution greatly increased Φ_f, as the substituted rubrene exhibited reduced SF. To raise upconversion yields, tetraphenyldibenzoperiflanthene (DBP) was used at 0.5% weight in the polystyrene film. A study by Nienhaus *et al.* further highlighted the importance of annihilator aggregation in rubrene containing systems.[254] In spin coated disordered films, SF is negligible and DBP doping at any concentration did not lead to increased upconversion yields (Fig. 11b). Later work by Clark *et al.* suggested that the initial singlet fission event from S_1 to ^{1}(TT) actually happens with equal efficiency regardless of the presence of DBP. However, the DBP inhibits further triplet dissociation and leads to the higher yields.[255] The described studies indicate the importance of material design in matrix free systems, with annihilator aggregation and structural order observed to be highly influential on solid-state upconversion efficiency.

Grozema *et al.* described a trilayer TTA-UC system for increasing photocurrent generation. The layers consist of a crystalline zinc phthalocyanine sensitiser layer, and a crystalline perylenetetracarboxylic acid diimide annihilator layer. The layers were made on a polycrystalline TiO_2 support (Fig. 11c).[256] Excitation of the sensitiser at 700 nm resulted in a photoconductance signal. The maximum photon to electron injection quantum yield was 0.92%. Baldo *et al.* later investigated whether sensitiser–annihilator bilayer or blended structures are the most efficient.[257] Several materials based upon **16** and an anthracene based annihilator were made. Spatial separation of sensitiser and annihilator was tested, to observe the effects of reducing back energy transfer (Fig. 11d). The Φ_{UC} for the blocker-doped device (2.5%) was around an order of magnitude higher than for the worst performing bilayer device. Similarly positive results were observed in the value of I_{th}, where the

Open Access Article. Published on 02 November 2022. Downloaded on 10/16/2025 7:02:22 PM.
This article is licensed under a Creative Commons Attribution 3.0 Unported Licence.

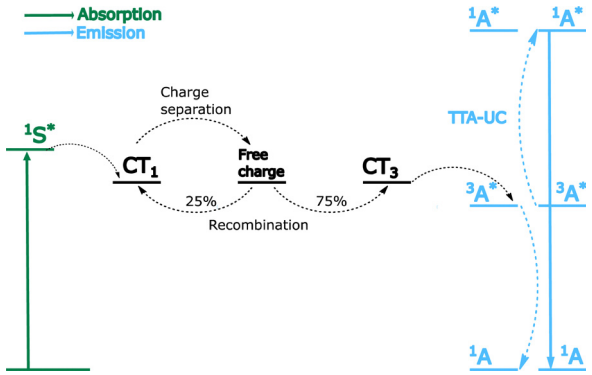

Fig. 12 Energy diagram for the mechanisms of TTA-UC at an organic semiconductor interface, green represents processes happening in the sensitiser layer, black represents processes happening at the interface and blue represents processes happening in the annihilator layer.

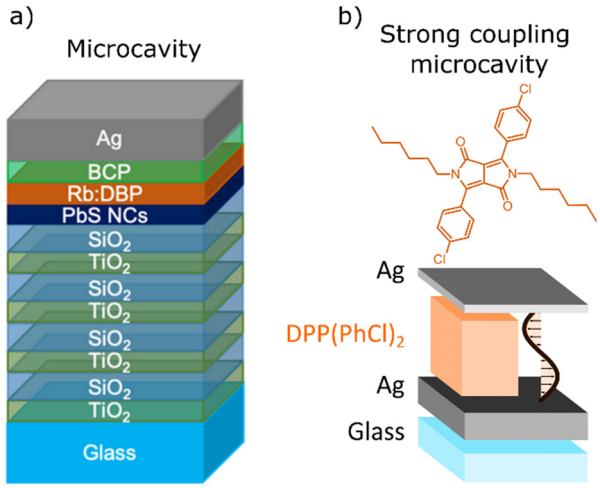

Fig. 13 (a) Microcavity fabricated by Baldo *et al.* to vastly increase absorption through Bragg diffraction, (b) strong coupling microcavity fabricated by Börjesson *et al.* to enable turn-on TTA-UC. Images are adapted from (a) ref. 262, and (b) ref. 265, with permission from the American Chemical Society.

spatially separated blocker-doped, and bilayer devices display values of 238 and 1404 mW cm^{-2}, respectively. This study shows that overcoming back energy transfer to the sensitiser and aggregation, by means of selective doping, provide a pathway to achieving higher performance solid-state TTA upconversion devices. More recently the group of Hiramoto *et al.* have used the concept of charge recombination at a semiconductor interface to facilitate TTA-UC.[258,259] The group used non-fullerene acceptors as bilayers with rubrene, which was used as the annihilator. This energy transfer mechanism does not rely on ISC and therefore differs significantly from the traditional mechanism in Fig. 5. Fig. 12 graphically displays triplet formation at a semiconductor interface in the context of TTA-UC. The first step relies on diffusion of singlet excitons to the sensitiser/annihilator interface, where the energy is relaxed to charge transfer states of singlet character. Triplet annihilators are then created through dynamics between free charges and charge transfer states. Finally, two annihilator triplets form a singlet through TTA, leading to UC emission from the emitter layer.

The work of Hiramoto *et al.* was the first to utilise singlet diffusion followed by charge recombination at an interface to produce efficient TTA-UC. As it was a novel route to realise TTA in the solid-state it is worth significant discussion. Firstly, the influence of the sensitiser ISC on the UC yield is eliminated as CT states are efficiently formed at the interface. Secondly, diffusion in the sensitiser layer is realised by singlet excitons, with triplets formed only near the interface. This prevents non-radiative triplet recombination, which is a major loss process in conventional sensitiser-annihilator bilayer upconverters. Another advantage of this system is that it can be modified to work under both electrical and light stimulus. We would argue that research in this direction should take inspiration from lessons drawn in the field of organic photovoltaics.[260,261] Specifically, it is difficult to make a planar layer absorb all incoming light and at the same time have an efficient exciton diffusion to the interface. Therefore, the use of these materials in bulk heterojunctions should be considered.

Nanophotonic resonators are a lesser explored approach to increase Φ_{UC} and reduce I_{th} in solid-state TTA-UC. In an attempt to reduce I_{th} for NIR to visible upconversion, Baldo *et al.* constructed a Fabry–Pérot microcavity (Fig. 13a).[262] PbS nanocrystals with an excitonic peak tuned to 980 nm were used as the sensitiser and rubrene was used as the annihilator doped with DBP at 1%. For previous solid-state systems using PbS nanocrystals, Φ_{UC} was unmeasurable due to the low absorbance of PbS monolayers.[195,263] Using a Fabry–Pérot cavity, a 74 fold increase of excitons in the PbS monolayer was achieved. The emission intensity of the microcavity is increased by a factor of 227, with a Φ_{UC} of 0.06%.[262] This small value of Φ_{UC} can be ascribed to inefficient TET in the solid-state, high back energy transfer from rubrene to the NCs, and singlet and triplet trap states in the material. The I_{th} value for the microcavity is 13 mW cm^{-2}. The low I_{th} and far increased Φ_{UC} clearly demonstrate the advantages of applying Fabry–Pérot cavities to solid-state TTA-UC. When the coupling between the electromagnetic field in the Fabry–Pérot cavity and the molecular transition dipole moment gets sufficiently large, the system enters the strong coupling regime.[264] Börjesson *et al.* used Fabry–Pérot cavities strongly coupled to $DPP(PhCl)_2$ to "turn-on" TTA-UC (Fig. 13b).[265] Whilst $DPP(PhCl)_2$ shows poor TTA-UC in solution, owing to $E_{S_1} - 2E_{T_1} > 0$, the triplet pair from two triplet excitons could directly convert into exciton–polaritons by TTA inside the microcavity. This is due to a lowered polariton energy compared to the E_{S_1} facilitating the rate of TTA. The most efficient cavities show a small anti-Stokes shift of <0.1 eV (613 nm to 590 nm), therefore this system is currently lacking applicability to PVs. The work however demonstrates the ability to utilise optical cavities rather than chemical modifications to influence TTA-UC parameters. One particular challenge this may address could be the combination of UC and strong-coupling in solar NIR driven catalysis.[266–268]

This section has covered solid-state systems, from encapsulation of liquids to neat solid films. Encapsulated systems

 This journal is © The Royal Society of Chemistry 2022

Open Access Article. Published on 02 November 2022. Downloaded on 10/16/2025 7:02:22 PM.
This article is licensed under a Creative Commons Attribution 3.0 Unported Licence.

provide high upconversion efficiencies and have already found applications.[226] However, they contain solvent, limiting applicability in PV technology. Neat solid-state film upconversion has higher applicability in PV technology, but has so far not reached high enough upconversion efficiencies. Particularly, limiting factors in solid-state upconversion include aggregation induced processes and low triplet diffusion. We encourage continued structure optimisation of annihilator molecules with regards to packing and energy transfer. This has been somewhat less explored than sensitiser modification. Equally, new methods of exciton diffusion must be sought, and we particularly envisage interest in the semiconductor type setup introduced by Hiramoto *et al.* Further to this, new classes of functional materials are being explored, such as MOFs and strong-coupling materials.

Singlet fission based energy conversion

In 1965 Singh *et al.* reported SF for the first time when studying the laser excitation of anthracene crystals.[269] A few years later Swenberg and Stacy explained the temperature dependent fluorescence quenching of tetracene by invoking this newly rationalised photophysical process.[270] About a decade later, in 1979, Dexter proposed that SF in tetracene could be used to improve the efficiency of solar cells.[271] However, it wasn't until the early 2000's that interest in SF for solar energy harvesting really started to grow.[34,74] Since then, the focus has been on understanding the SF process in detail, often through the help of ultrafast optical spectroscopy and magnetic field dependent measurements.[59,61–63,76,80,272–274] Another related research focus has been the design of new SF chromophores.[34,41,74,275] Above we introduced the details of the SF process and its relation to TTA. Here we will start by discussing the efficiency of the SF process followed by a brief overview of SF active materials and their relevance for PV applications. The following section will then summarise and discuss the many examples and approaches towards incorporating photon conversion with PVs.

The singlet fission quantum yield

As with TTA-UC, the reporting of quantum yields is not always consistent across the literature, with the discrepancy arising from how the authors choose to define SF.[61] As briefly mentioned above, it is often unclear if SF refers to the overall process of forming two free triplets from the initial singlet state, or if SF is complete when one of the intermediate triplet pair states is formed (^{1}(TT) or [$T_1\cdots T_1$]). The quantum yield of free triplet formation can reach a maximum of 200% using the IUPAC definition of quantum yields (eqn (1)), as two triplets can be formed for every absorbed photon. However, if the strongly bound correlated triplet pair state ^{1}(TT) is considered as one state (*e.g.* similar the optically dark A_g state in polyenes),[62] then the maximum quantum yield of ^{1}(TT) formation should be reported with a maximum of 100%, which is not always the case. We therefore agree with the discussion of Zhu and co-workers that the most relevant definition of SF is the formation of [$T_1\cdots T_1$].[61]

Measuring the quantum yield of SF can be difficult, first one has to decide how to define SF, and secondly, one has to be able to distinguish between the triplet pair states and free triplet states, as well as measure these states quantitatively. As triplet states are non-emissive, one typically has to rely on transient absorption to follow the SF dynamics. The SF quantum yield can be estimated in a number of ways. It can be determined from the rate of singlet quenching and triplet formation.[276] Singlet quenching can be measured using time-resolved fluorescence measurements. However, this method determines the yield of the state of which S_1 decays into, *i.e.*, ^{1}(TT) and not necessarily free triplet yields. Further, depending on how the singlet quenching is determined this method might overlook other deactivation pathways and overestimate the yield. Hence one should ensure that the singlet quenching rate matches the triplet rise time.

Alternatively, one could use transient absorption spectroscopy. If the ground state bleach is not significantly overlapped the quantum yield can be obtained from the ratio of the ground state bleach at initial excitation to those at longer delay times. The ground state bleach at these times correspond to S_1 and S_1 + T_1 populations, respectively.[107,277] Unfortunately, many molecules have singlet and/or triplet spectra that significantly overlap the ground state bleach, complicating the analysis. Another popular approach requiring transient absorption spectroscopy, is to quantify the triplets generated using the triplet state molar absorptivity.[127,277–281]

In solution, a lower limit of the SF triplet yield can be determined from singlet oxygen emission.[282] The SF yield can also be inferred by measuring the external or internal quantum efficiency of optoelectronic devices such as photovoltaics or photodetectors incorporating SF active materials.[42,81,283,284] Another more recent method is to measure the photoluminescence enhancement of a NC-SF mixture.[285–289] By measuring the triplet transfer efficiency to the NC, the SF yield can be determined. This method has been used in both solution and solid-state, and the yields correspond well with those determined by other means.[285–289]

Which method is better can depend on the actual system and rate of SF. Ultrafast SF might be difficult to resolve accurately using transient absorption spectroscopy setups with a large pulse width. Furthermore, often free triplet states are only fully resolvable on the ns–ms time scale, whereas the initial S_1 population must be determined after initial excitation on the fs timescale. Hence separate setups might be required, complicating the comparison of the population of these states. It is therefore better to estimate the QY in multiple ways, *e.g.* from transient absorption measurements, and if applicable a device/photon enhancement to ensure these values align reasonably.

Singlet fission materials

To fulfil the energetic requirements discussed above, a SF material should have a large S_1–T_1 splitting. There are different

Open Access Article. Published on 02 November 2022. Downloaded on 10/16/2025 7:02:22 PM.
This article is licensed under a Creative Commons Attribution 3.0 Unported Licence.

ways to guarantee a large singlet–triplet splitting in molecular materials and it has been an ongoing debate on how to best design SF chromophores to fulfil this requirement.[34,74,290,291] Below we cover some of the most common materials that have been studied for SF.

Initially, the only types of chromophores that were studied for SF were even-carbon alternant hydrocarbons, such as anthracene, tetracene, pentacene, and polyenes *etc.* (Fig. 14).[34] In these types of structures the HOMO and LUMO overlap significantly, resulting in a large exchange integral $K_{exchange}$ and hence a large S_1–T_1 splitting ($\Delta(S_1\text{–}T_1) \approx 2K_{exchange}$).[34,74] Pentacene and tetracene, and their derivatives, are probably the most studied SF materials to date.[34,41,74,274,275]

In 2006 Michl and co-workers introduced another class of molecules that tend to have large S_1–T_1 separations, biradicals and biradicaloids.[292] With two singly occupied degenerate orbitals, biradicals can have triplet ground states, and by tuning the biradical character of the molecule, the singlet–triplet gap can be tuned (Fig. 15). Michl and co-workers later also demonstrated efficient SF in the biradicaloid 1,3-diphenylisobenzofuran with 200 ± 30% triplet yield (Fig. 14).[277] Nakano and co-workers later refined the biradical approach, by correlating the multiple biradical characters y_0 and y_1 with the energetic requirements for SF (where y_0 and y_1 corresponds to the occupation number of the lowest unoccupied natural orbital LUNO and LUNO + 1, respectively).[293–296] They concluded that materials with a small y_1 and a non-zero y_0 can all fulfil the energy matching criteria for SF, and that molecules with a $y_1/y_0 < 0.2$, are a good starting point for new SF capable materials.[296] Smith and Michl's reviews on SF offers an extensive summary of the even-carbon alternant hydrocarbon and biradicaloid materials that had been investigated up until their publication in 2010 and 2013.[34,74] Since, the quest for more SF materials has continued. Michl and co-workers investigated a series of small molecule biradicaloids, using quantum chemical calculations.[297,298] In 2017, Lukman *et al.* reported SF in the biradicaloid family of zethrene compounds.[123]

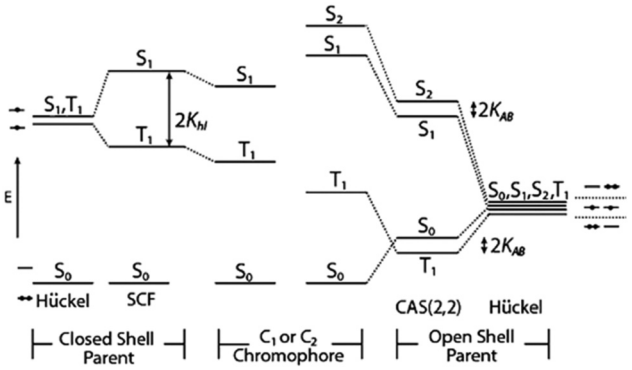

Fig. 15 Energy levels of closed shell (left) and open shell (right). By tuning the biradical character the singlet and triplet gap can be tuned (center). Reprinted from ref. 292 with permission from American Chemical Society, copyright 2006.

Another family of materials similar to the acenes that has large S_1–T_1 separation is rylenes and their diimide derivatives (Fig. 14). Rylene-diimides have been widely studied for optoelectronic applications thanks to their highly versatile and tunable properties.[299–303] SF has also been observed in rylene-diimide crystalline films,[97,101,140,278,304–310] self-assembled nanocrystals and aggregates,[311,312] as well as in some dimer structures.[83,96,127,313,314] Triplet yields have been observed to approach 200% in solid films.

Diketopyrrolopyrroles (DPP, Fig. 14) are another class of molecules that have been investigated extensively for optoelectronic applications, including SF. Since the S_1 energy of DPPs can be tuned without significantly altering the T_1 energy, the energetics can be tuned to fulfil the requirements for SF and/or

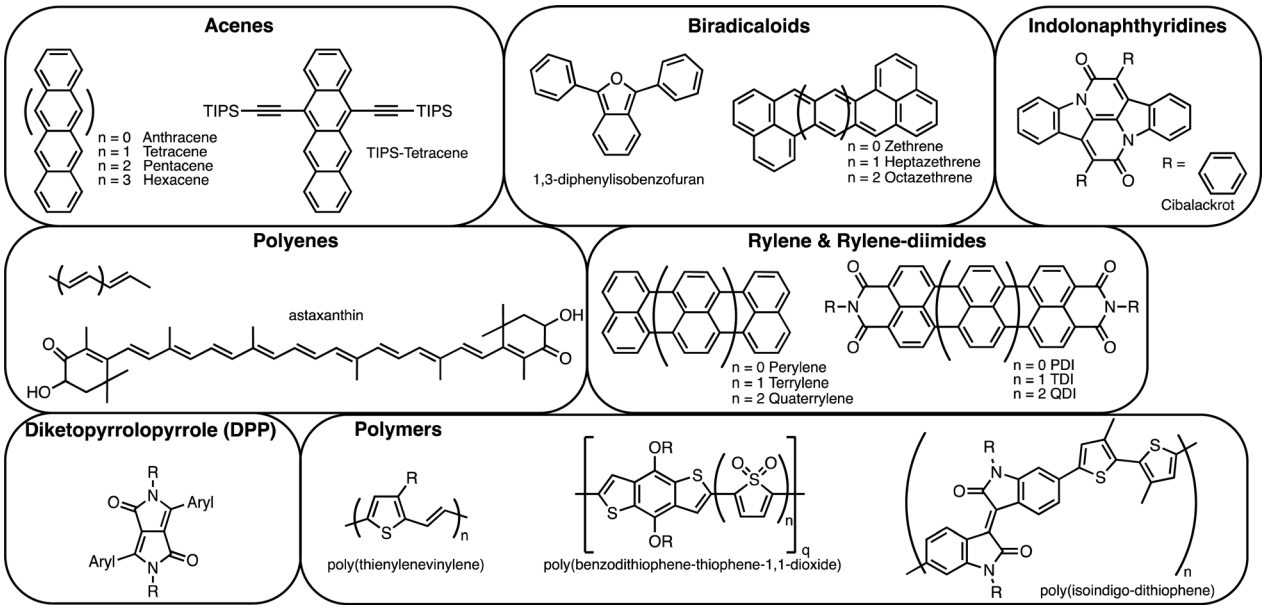

Fig. 14 Molecular structures of chromophore families shown to undergo SF.

Open Access Article. Published on 02 November 2022. Downloaded on 10/16/2025 7:02:22 PM. This article is licensed under a Creative Commons Attribution 3.0 Unported Licence.

TTA.[315] SF has been observed in some DPP materials including films, dimers and nanoparticles, with triplet yields exceeding 150%.[104,109,316–320] Guldi and co-workers summarised the many works on SF chromophores in two recent reviews.[41,275]

Besides intermolecular SF, as observed in the materials discussed above, intramolecular SF has been observed in dimer versions of the same materials.[76,83,94–96,98,99,105,109–111,132,274,276,279,313,314,321–331] Dimers are an interesting class of SF materials as the coupling between the monomers can be systematically engineered. Hence, dimers are useful when probing and addressing fundamental questions of SF. Furthermore, dimers can possibly have an advantage also in devices, where an optimized chromophore coupling could be designed into the structure, removing morphology and packing dependent issues. Although, in many dimers the question remains if complete SF is actually observed as the ^{1}(TT) state does not separate further, contrasting the definition of SF in eqn (2).[63,276] As the triplet excited states are forced to maintain close proximity in the dimers, it is not surprising that free triplets are seldom observed. To overcome this issue, Campos and co-workers developed structures where triplet separation was energetically downhill.[56] Another approach is to extend the dimers to oligomers or polymers to allow the individual triplets to physically separate.[127,331,332] However, it is not always enough to extend the dimers to oligomers to obtain free triplets, for example Sanders *et al.* reported that in polypentacene the triplet pair never separated into free triplets.[326] Other polymers that have been reported to undergo SF are poly(thienylenevinylene),[333] benzodithiophene-thiophene-1,1-dioxide donor–acceptor polymers,[108,334] and isoindigo based donor–acceptor polymers.[335] Understandably, most work on SF dimers has been performed in solution, as it allows for a cleaner system to study and address specific questions related to *e.g. inter*molecular coupling. However, it is highly relevant from a device perspective to also study dimers in the solid-state. For example, it is unclear if some of the limits observed in dimer solutions (*i.e.* poor dissociation of ^{1}(TT)) can be overcome in solid-state.

Recently new design strategies to develop new SF materials have emerged. Tuning of the S_1 and T_1 energies in materials can be achieved by altering the degree of aromatic/antiaromatic character in the ground and excited states, as explored by Fallon *et al.* and El Bakouri *et al.*[290,291,336] Fallon *et al.* and Zeng *et al.* showed that Cibalackrot and other indolonaphthyridines can be suitable SF chromophores (Fig. 14).[290,291] Wang *et al.* also used the tuning of aromaticity and developed a fused dipyrrolonaphthyridinedione chromophore with a triplet energy around 1.2 eV and triplet yield of 173%.[337] Another approach to tuning the singlet–triplet gap is introducing strain to the molecular structure.[305] Furthermore, Padula *et al.* searched through the Cambridge Structural Database and evaluated over 40 000 structures to find around 200 possible SF chromophores, many not previously considered.[338] The development of SF materials is in its infancy, many more will undoubtedly be experimentally demonstrated in the future. As will be evident from the next section, the development of new SF chromophores has a huge potential impact on photovoltaic applications, as today the proof-of-principle devices have all used the same three types of molecules (or derivatives thereof): pentacene, tetracene and 1,3-diphenylisobenzofuran.

Incorporation of TTA and SF with photovoltaics

In recent years the progress in overcoming the fundamental limitations of TTA and SF has further allowed progress in applying the systems to photovoltaics and other devices. In this section we will discuss the incorporation of photon conversion materials to functional devices. We will first detail the work carried out and then finish with a critical overview of continuing challenges and limitations to commercial uptake.

TTA-UC in solar cells

TTA-UC has cemented its place in many research fields related to photochemistry.[216,339–347] Although, none is as prevalent as photovoltaics.[67,348–356] In the following section, we will discuss the incorporation of TTA-UC into photovoltaics. Even though initially most examples of TTA-UC enhanced devices relied on solution phase systems,[340,350,351,357–362] we will limit our discussion to the more recent and practically relevant solid-state systems.

We have discussed above (see discussion around Fig. 1) the theoretical improvements that can be made to the efficiencies of PVs when utilising TTA-UC. In practicality these improvements are harder to realise. Device architecture, dye sensitisation and the upconversion process all play a role in the improvements to short circuit current densities (J_{SC}) seen.[363] An earlier perspective by Schmidt *et al.* remarked that to be relevant to PV use, a significant increase in short circuit current density when using upconversion must be observed over a suitable reference material. *I.e.* ($\Delta J_{uc} > 0.1$ mA cm^{-2} under one sun excitation density).[364] In this section we will highlight recent examples of solar cells assisted by upconversion, and where possible assess them against the ΔJ_{uc} figure of merit.

Much effort has been made in applying upconverting layers to TiO_2 dye sensitised solar cells. In 2018 Nagata *et al.* immobilised both a platinum sensitiser complex (PtTPO), and a DPA carboxylic acid derivative onto TiO_2 nanoparticles at an FTO electrode (Fig. 16a).[158] Immobilisation of the DPA or platinum complex alone led to no significant current density increases. On immobilisation of the two dyes concurrently (10 : 1, annihilator : sensitiser), a small ΔJ_{uc} of 3.6×10^{-2} mA cm^{-2} was observed under 1 sun irradiation. This led to a 0.72% power conversion efficiency for the upconverting device compared to 0.60% with annihilator immobilised alone. Immobilised molecular layers were again used by Hanson *et al.* in 2019.[365] Supramolecular assemblies were constructed, consisting of a singlet sensitiser, a triplet sensitiser and an annihilator (Fig. 16b). The addition of the singlet sensitiser broadened the absorption envelope of the upconversion layer and allowed the filling of a so-called transparency window in the triplet

Open Access Article. Published on 02 November 2022. Downloaded on 10/16/2025 7:02:22 PM.
This article is licensed under a Creative Commons Attribution 3.0 Unported Licence.

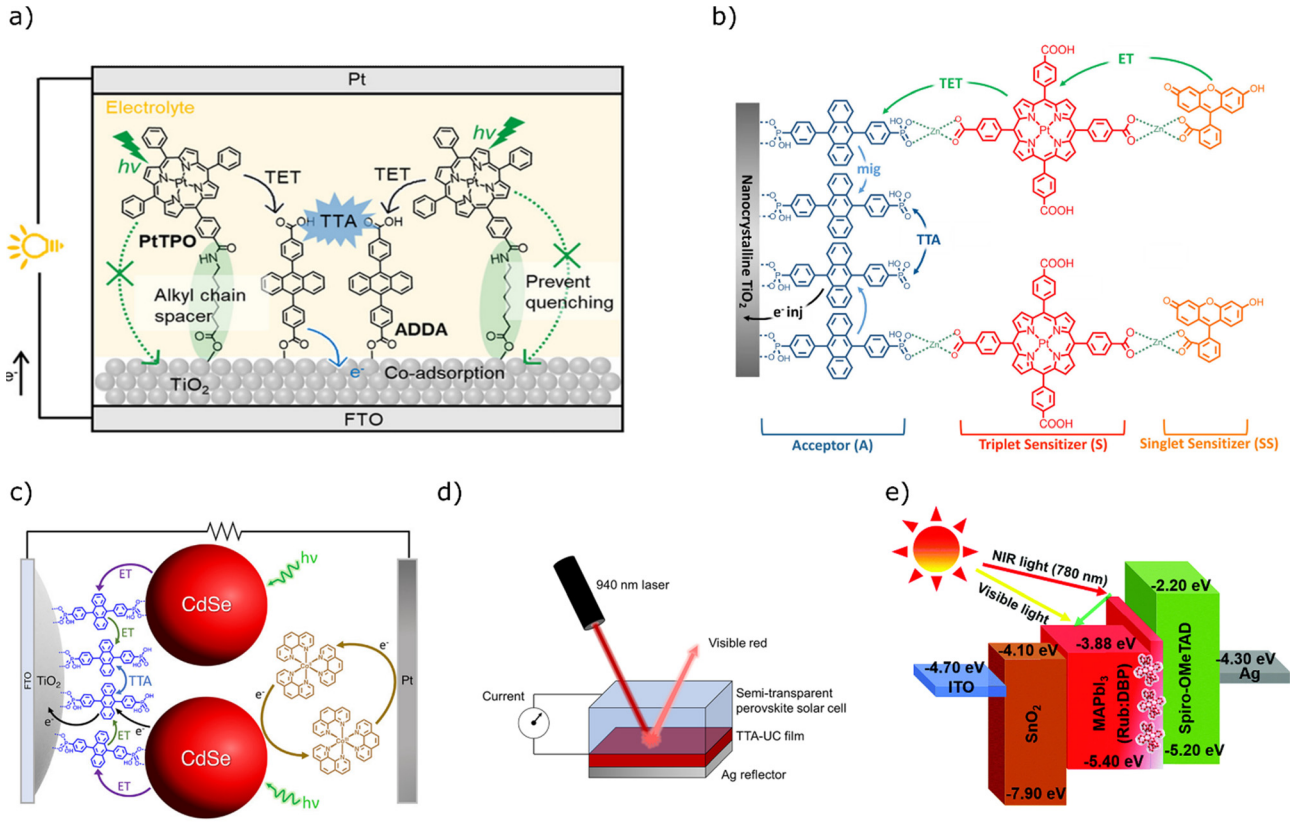

Fig. 16 (a)–(d) Structures of the PV devices discussed in this review, all devices except for (c) were tested under 1 sun conditions. This figure has been adapted with permission from references (a) ref. 158, copyright 2019 American Chemical Society; (b) ref. 365, copyright 2019 American Chemical Society; (c) ref. 366, copyright 2020 American Chemical Society; (d) ref. 370, copyright 2020 Wiley-VCH GmbH; and (e) ref. 371, copyright 2021 Royal Society of Chemistry.

sensitiser–annihilator bilayer. A record J_{SC} for a TTA-UC solar cell was reported (0.315 mA cm^{-2}). According to the definition above however, the ΔJ_{uc} should be the increase offered only by upconversion and not by direct dye sensitisation of the solar cell. This value was not directly reported. CdSe NCs were later used by the same group in the fabrication of TiO_2 solar cells with upconversion assisted efficiencies.[366] CdSe NCs were coated with a DPA derivative before being implanted between the TiO_2 and Pt electrodes together with an electron mediator (Fig. 16c). The cells showed, however, lower J_{sc} values (29 μA cm^{-2}) than their previously reported systems. Unfortunately, there are several drawbacks regarding the use of CdSe NCs in solar cells. Below unity energy transfer yields from the NC to the DPA were observed, along with slow electron regeneration, and competitive excited state quenching by the redox mediator. These are all challenges that need addressing.

We will now turn our attention to some recent examples of perovskite based PVs, which have been explored in upconversion applications.[367–369] Kimizuka *et al.* applied a known singlet to triplet sensitiser (5) as an add-on technology to increase the number of photons absorbed (Fig. 16d).[370] The sensitiser was immobilised in a PVA matrix, along with rubrene as an annihilator, and DPB as a singlet sink. The PVA film was applied below the solar cell material and a 938 nm laser was used as an excitation source. Measuring the current density with and without the PVA layer achieved a $\Delta J_{uc} \sim 0.1$ mA cm^{-2}, however, this value was only achieved at an excitation density of 4 W cm^{-2}, around 40 times higher than the entire energy of the solar spectrum. Chen *et al.* used perovskite and rubrene:DPB mixed layers, which were spin coated into the device creating a charge transfer complex through coulombic interactions.[371] The perovskite was described as the sensitiser, the rubrene as the annihilator and the DPB as the emitter (Fig. 16e). Increased power conversion efficiency and a high ΔJ_{sc} were measured. The conclusions of this work have, however, been subject to some criticism from others within the field.[372] Earlier work demonstrated the complex nature, and non-optimised procedure of using perovskite as a sensitiser, and rubrene as an annihilator in the TTA-UC process.[172,367–369] The efficiency gains are likely to be valid, but due to improvements made to the continuity and crystallinity of the perovskite surface. It is unlikely that in the material proposed by Chen *et al.*, TTA-UC is the main mechanism of efficiency improvement, although we note the authors explanation that it is possible for these mechanisms to operate synergistically.[373]

Singlet fission in solar cells

There are numerous ways of incorporating SF materials with solar cells. A common approach is to incorporate the SF

Open Access Article. Published on 02 November 2022. Downloaded on 10/16/2025 7:02:22 PM.
This article is licensed under a Creative Commons Attribution 3.0 Unported Licence.

materials as part of the active material in the solar cell, for example as one of the dyes in a dye sensitised solar cell (DSSC),[34,292] or organic photovoltaic (OPV).[51] Perhaps the most intuitive way to incorporate SF with solar cells is to directly couple the SF material on top of a solar cell material. Here the triplet states could either transfer to the SC through triplet energy transfer or dissociate into free charges at the SC/SF interface. This approach was first proposed by Dexter over 40 years ago,[271] but it has turned out to be extremely challenging to achieve efficient sensitisation of the SC in this way.[43,271,374] A more recent approach that has been proposed, but not yet implemented in photovoltaics, is to convert the SF process into a photon multiplication process. Photon multiplication requires the dark triplet states generated by SF to be converted into emissive states, so that two low energy photons can be emitted for every high energy photon absorbed.[72,273] In the next few paragraphs we will discuss the progress in applying SF to photovoltaic devices and the future prospect of the various approaches. We will start with devices where SF materials are part of the active material (DSSC, Organic PV, Inorganic PVs) and continue with devices where the SF material instead is coupled to the solar cell.

DSSC

As the prospect of using SF in solar cells re-emerged as a possible and practical way to improve the efficiency of solar cells in the early 2000's, Michl and co-workers pursued the idea of applying SF to DSSCs. To effectively achieve the theoretical efficiency gain of around 45%, a SF dye with E_{T_1} of 0.9–1.1 eV and E_{S_1} of 1.8–2.2 eV would have to be combined with a conventional dye with E_{S_1} of 0.9–1.1 eV.[292] Michl, Johnson and co-workers initially used a 1,3-diphenylisobenzofuran derivative that could anchor to the TiO_2 electrode of an DSSC.[375] The main challenge with this approach is that electron injection from the singlet state out-competes SF in these surface bound chromophores.[112,375–377] To overcome this issue, a surface passivation strategy has been pursued, where a thin insulating layer of ZrO_2 or AlO_2 is deposited to slow down electron injection allowing SF to occur (Fig. 17).[112,375–377] Kunzmann *et al.* used a pentacene dimer where SF occurred intra-molecularly, and electron injection up to 130% was reported.[378] By using a dimer structure the chromophore coupling can be directly designed compared to surface bound monomer structures where the non-ideal coupling compared to solid-state crystals has led to a slowing of the SF process.[377] Another advantage with a dimer approach is that SF would not be directly influenced by adding in a conventional low bandgap dye. Banerjee *et al.* recently demonstrated an alternative approach to adding a low bandgap dye to a surface anchored SF dye by metal–ion assisted self-assembly.[376]

To achieve highly efficient SF sensitised DSSC the focus should lie in finding a suitable SF dye, one that is efficient in dimer form, has a suitable triplet energy relative to the conventional TiO_2 electrodes and is stable enough for long-term illumination. As new SF materials are developed, these conditions can hopefully be met, as the DSSC structure, already

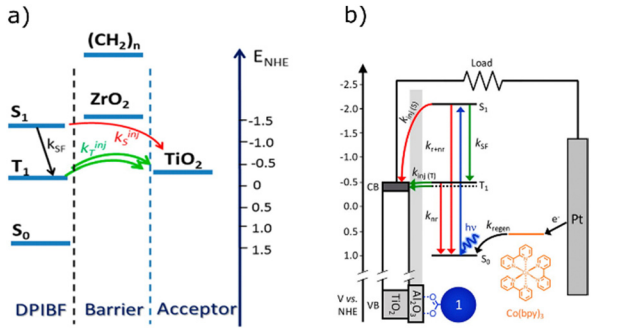

Fig. 17 Energy level alignment and device configuration of the two 1,3-diphenylisobenzofuran (DPIBF, 1) DSSCs studied by (a) Schrauben *et al.* and (b) Banerjee *et al.* 1,3-diphenylisobenzofuran functions as the SF sensitizer and an insulating layer of ZrO_2 or Al_2O_3 is required to minimize direct electron transfer from S_1 to the TiO_2. (a) Reprinted from ref. 375, with permission from the American Chemical Society. Copyright 2015. (b) Reprinted from ref. 376 with permission from the American Chemical Society. Copyright 2018.

relying on dye incorporation, is particularly suitable for SF sensitisation.

Organic PVs

Another PV type that already uses molecular dyes is organic photovoltaics (OPVs). It is perhaps not surprising that the first examples of solar cells with EQEs and IQEs exceeding 100% were reported in OPVs containing SF dyes.[283,379–381] Careful molecular engineering is required, to obtain the correct morphology and minimise charge recombination and triplet-charge annihilation, whilst maintaining an optimal interface and energetics for electron transfer.[382–389] In all cases to date, even though SF is operational, the benefit in these OPV is minimal on overall performance compared to an optimised OPV without SF.[390,391] One reason for this poor enhancement is related to the morphology of the device. For efficient SF to occur, bilayer OPVs must be used,[42,283,379,381,386,388,389,392] which sets strict limits to device thickness. This is due to the short triplet diffusion lengths,[393] and hence total photon absorption.[380] In traditional OPVs, bulk heterojunctions are more common, but these structures have proved less efficient for SF materials.[386,388] However, in some instances SF can be compatible in mixed blends if the SF chromophores aggregate appropriately, as observed by Jadhav *et al.* for tetracene in a C60 copper-phthalocyanine (CuPc) blend.[394]

Many of the above-mentioned proof-of-principle SF-OPVs also have another significant short coming, to obtain any gain from SF a low energy absorber is also needed in the device. This has been addressed by Jadhav *et al.*[394] and Tritsch *et al.*[389] where CuPc has been incorporated as a low bandgap chromophore (Fig. 18).

An alternative to adding in a low bandgap chromophore to the OPV device is to use the SF OPV as a top cell in a voltage matched parallel connected tandem cell, with a low bandgap bottom cell (Fig. 19).[395,396] This approach has been successfully used to demonstrate an overall EQE exceeding 100%. An additional

Open Access Article. Published on 02 November 2022. Downloaded on 10/16/2025 7:02:22 PM.
This article is licensed under a Creative Commons Attribution 3.0 Unported Licence.

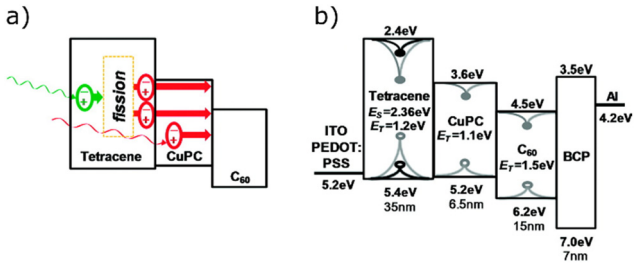

Fig. 18 (a) Schematic illustration of a tetracene/CuPc/C_{60} OPV where the CuPc low bandgap donor and C_{60} acceptor constitute the traditional OPV and tetracene functions as an additional singlet fission sensitizer for high energy photons. (b) energy alignment of the materials in the device in (a). Reprinted from ref. 394, with permission from American Chemical Society. Copyright 2011.

benefit of a voltage matched, rather than current matched series connected tandem cell is their better spectral stability, and smaller sensitivity to diffuse rather than direct lighting (Fig. 19).[395,396]

Challenges remain in bringing SF OPVs to real life practical PV applications. One must obtain a suitable morphology for SF, charge separation and electron/hole migration in one device. Furthermore, the device must constitute a SF molecule, a low bandgap chromophore and an acceptor molecule. Collating everything into a single device is one of the major hurdles in this field. Conventional OPVs struggle with morphology optimisation as is and blending in another dye that also has stringent requirements on morphology results in a difficult puzzle to solve. Moreover, moving away from acene based SF chromophores would be required for photostable SF chromophores that can be used in devices. However, parallel connected voltage matched tandem cells by the use of SF top cells is an interesting and highly promising implementation of SF warranting further efforts to achieving efficient SF sensitised OPVs.

Inorganic PVs

SF chromophores have also been combined with inorganic PV materials. For example, Ehrler *et al.* combined pentacene with PbS NCs and PbSe NC/amorphous silicon in functioning devices.[397,398] Even though the IQE did not exceed 100%, they concluded that triplet excitons could be dissociated into free charges at the organic/inorganic interface.[397,398] They later improved the device performance by using a solution processable pentacene derivative (TIPS-Pc), together with PbS NCs. This system was able to achieve a 170% IQE and 4.8% overall device efficiency.[399]

The potential for SF to sensitise perovskite solar cells has been investigated recently. Even though no devices were prepared, the demonstration of ultrafast charge injection from the triplet pair state or SF generated triplet states to perovskite films is a promising first step.[400,401] In these two studies TIPS-Pc was used as the SF material, and a $MAPbI_3$ perovskite film was used as the device relevant electron acceptor.[400,401] These studies call for evaluating SF systems in full devices. However, as discussed above (Fig. 1), the most SF relevant devices are those with low bandgap (<1.4 eV) material. Hence the future direction of SF sensitised inorganic PVs should build on this advantage compared to organic PVs, and exploit the many low bandgap materials available, such as PbS/PbSe NCs and NIR perovskite materials.

Directly coupled singlet fission solar cell devices

A drawback to the SF active material PVs described above, is that a completely new device has to be designed, optimised and fabricated. By adding a SF material to an already optimised and efficient solar cell, part of the wheel does not have to be re-invented. Ideally, SF could be combined with a c-Si cell, as c-Si is the dominating PV technology today and has a suitable bandgap for SF enhancement (Fig. 1d). However, adding a layer of SF material to a c-Si cell, as proposed by Dexter almost half a century ago, has not resulted in any significant gains.[43,374] In 2018 MacQueen *et al.* evaporated 100 nm tetracene on top of a hydrogen passivated n-doped c-Si bottom cell. PEDOT:PSS was used as a hole transporting layer on top of the tetracene. This design was chosen to achieve triplet harvesting from tetracene, either through exciton dissociation or triplet energy transfer at the tetracene-silicon interface (Fig. 20). The Si substrate remained well passivated, but the tetracene acted to shadow the device and slightly lower the overall current.[43]

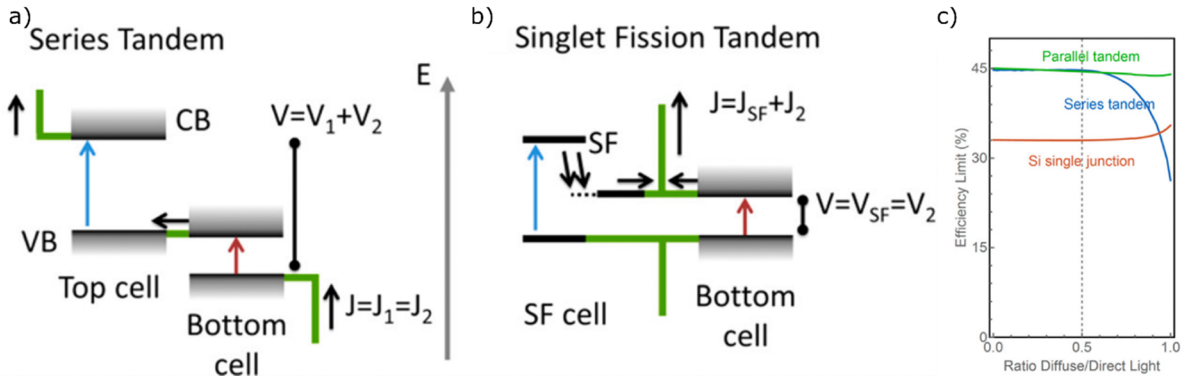

Fig. 19 (a) Conventional series connected tandem which requires current matching to operate efficiently. (b) A singlet fission-based voltage matched tandem connected in parallel. (c) theoretical maximum efficiency of a Si single junction device, a parallel and series connected tandem as a function of the ratio between diffuse and direct lighting. Reprinted from ref. 396, with permission from American Chemical Society, Copyright 2020.

Open Access Article. Published on 02 November 2022. Downloaded on 10/16/2025 7:02:22 PM.
This article is licensed under a Creative Commons Attribution 3.0 Unported Licence.

They concluded that the SF material did not improve the device performance, likely due to a potential mismatch between the tetracene triplet ionisation energy and the Si conduction band edge (Fig. 20a). The triplet yield was not measured directly, but modelling suggested about 8% exciton to photocurrent generation from tetracene.[43] It has been reported previously that Si can have a quenching effect of tetracene singlet emission with negligible triplet injection, and that an insulating interlayer can alleviate the quenching.[402,403] Importantly, an insulating layer on the c-Si surface is often employed in solar cells already to passivate the Si surface. Moreover, one might envision that a properly designed interlayer might even participate and facilitate energy transfer from a SF material. Einzinger *et al.* used an 8 Å layer of hafnium oxynitride on Si to enable efficient triplet injection into the semiconductor.[374] The insulating layer allowed for an overall 133% exciton transfer from tetracene to Si, with 56% being singlet transfer and 76% triplet transfer. However, the overall power conversion efficiency was recorded as 5.1%, significantly lower than conventional c-Si PVs. The poor efficiency was limited by carrier collection from the front surface of the cell, as the device structure employed was a interdigitated back contacted cell, (Fig. 20c).[374] Future directions will require understanding and optimisation of the surface passivation required for efficient solar cell performance, while maintaining efficient triplet and/or charge injection from the SF material. Daiber *et al.* recently introduced an optical screening method to test triplet quenching at the organic–silicon interface, to quickly evaluate the effect of different surface treatments.[404] Another significant hurdle for these types of SF devices is the small absorption afforded by the 30–100 nm thin SF layer deposited on the solar cell surface.[43,374] This is limited by the triplet diffusion length of the SF material to ensure efficient triplet migration to the interface.[405–407]

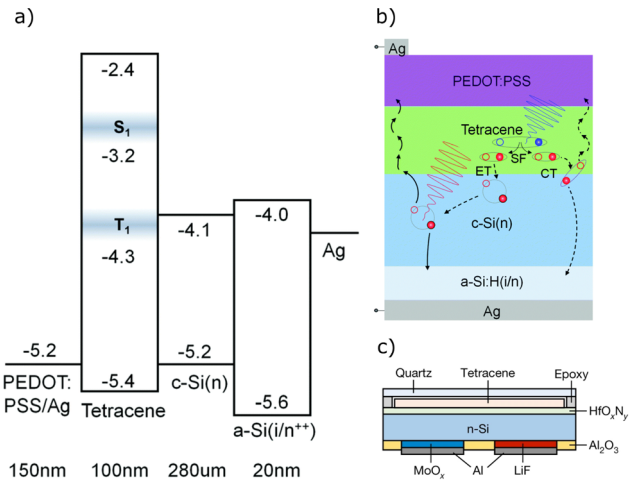

Fig. 20 (a) Band alignment of tetracene in a c-Si PV device. (b) Schematic illustration of the device and the processes SF, triplet energy transfer and charge transfer in the device studied by MacQueen *et al.* (a) and (b) Reprinted from ref. 36 with permission from Royal Society of Chemistry. (c) Device structure of the tetracene sensitized c-Si interdigitated back contacted solar cell used by Einzinger *et al.* Reprinted with permission from ref. 374. Copyright Nature Springer 2019.

Any developed SF material must be photostable over years, while also meeting the energetic requirements for SF and charge/triplet injection to the solar cell. If these challenges can be overcome there are a significant gains to expect for silicon PVs.[404] Depending on if the triplet transfer occurs through charge transfer or Dexter transfer, Daiber *et al.* estimated that the efficiency limit of a SF-silicon solar cell could reach 34.6% and 32.9%, respectively.[404] An additional advantage of using SF, or any other type of multi exciton generation process, with c-Si PVs is that the operating temperature of the device is decreased as thermalisation is minimised.[408] The decreased operating temperature in turn leads to a longer device lifetime.[408]

Singlet fission based photon multiplication

Ideally, a SF material could be added to an optimised solar cell as is, without the need to modify the underlying device. However, this ambition has turned out to be challenging, as discussed above. By converting the SF process into a photon multiplication process (PM), *i.e.* a high energy photon is split into two low energy photons, a solar cell could be optimised for what it does best, absorbing photons to generate current, and the SF material could be optically coupled to the device (Fig. 21a). This approach would overcome the requirements of direct and close contact between the solar cell and SF material, as charge or electron transfer would be exchanged for photon emission and re-absorption.[273,409] A photon multiplier could enhance c-Si cells above 30% efficiency under real-world conditions (Fig. 21d–f).

The question is then, how to convert the SF process into a photon multiplication process? There are in principle two strategies: the SF process could be engineered to generate two singlet excited states instead of triplet states.[410,411] Alternatively, the two generated triplets could be transferred to an emissive material not sensitive to the spin of the exciton, such as semiconducting nanocrystals (NCs).[289,412] The former approach has not gained much interest and there remains many uncertainties about how viable this approach is.[410] The latter approach has recently been demonstrated practically in solution,[286] and in films.[285] The overall process (Fig. 21b and c) occurs as follows: in a solution or film with high density of SF materials, a high energy photon is first absorbed by the SF material to initiate SF. The two formed triplet states are eventually transferred to a NC of appropriate energy, *via* a surface anchored triplet mediator ligand. The NC then relaxes radiatively emitting a low energy photon. With this approach Allardice *et al.* demonstrated how the emission of PbS NCs could be enhanced 1.25 times when exciting the SF material in solution.[286] With close to quantitative triplet transfer to the NC the emission enhancement could also be used to calculate the actual free triplet yield in the SF material according to eqn (11).[286,287,289]

$$\eta_T = \left(\left(\frac{\Phi_{PM}}{\Phi_{NC}}\right) - \left(\frac{Abs_{NC}^{Ex}}{Abs_{Tot}^{Ex}}\right)\right)\left(\frac{Abs_{SF}^{Ex}}{Abs_{Tot}^{Ex}}\right)^{-1} \quad (11)$$

Open Access Article. Published on 02 November 2022. Downloaded on 10/16/2025 7:02:22 PM.
This article is licensed under a Creative Commons Attribution 3.0 Unported Licence.

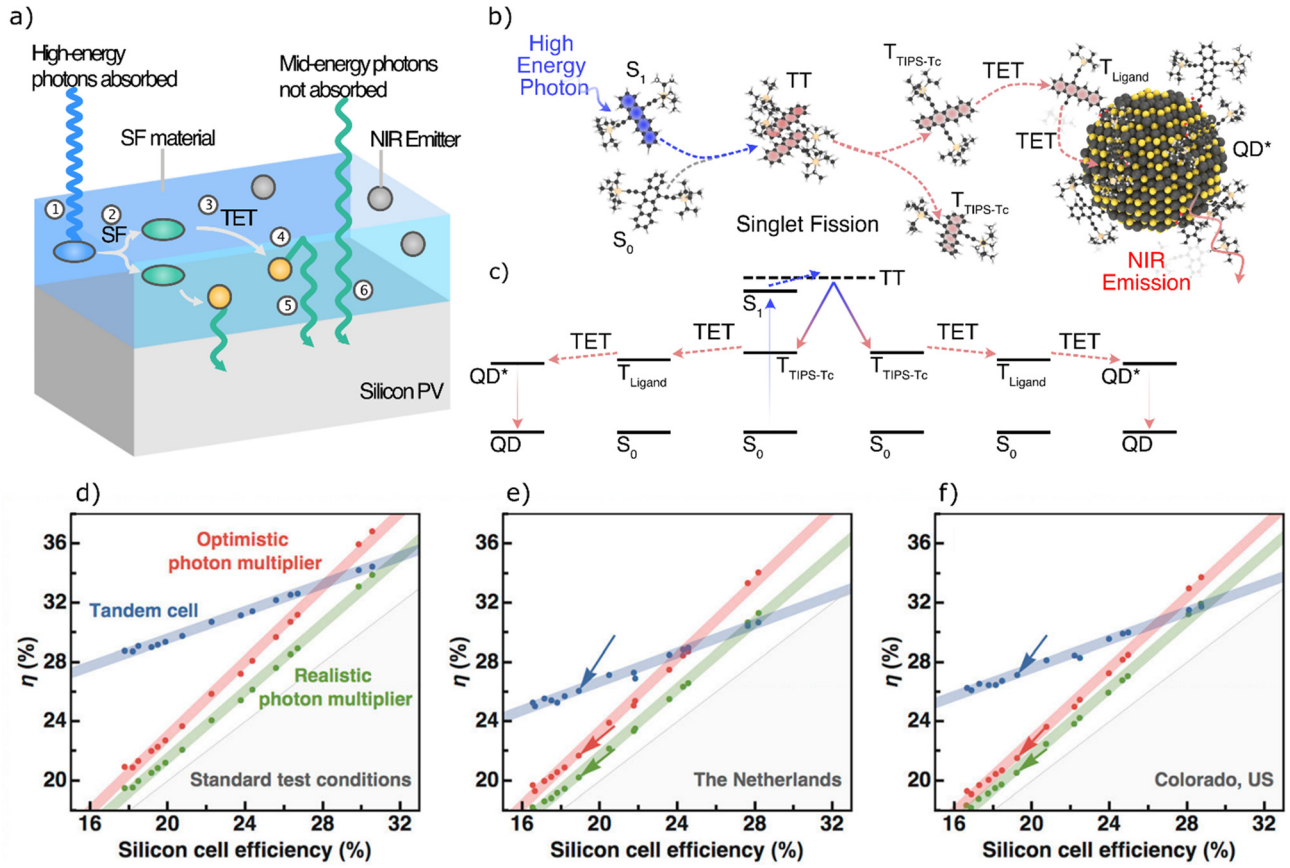

Fig. 21 (a) Schematic of a photon multiplier material coupled to a silicon PV. The SF material first absorbs a high energy photon and undergoes SF to generate two triplet states. These non-emissive triplet states are transferred *via* triplet energy transfer (TET) to a NIR emitter, for example a semiconducting NC (QD). The NIR emitters emits two low energy photons for every high energy photon absorbed. The low energy photons are subsequently absorbed by the PV device. Adapted from ref. 133 with permission from AIP publishing. (b) and (c) Detailed illustration of the photon multiplier process with a PbS NC NIR emitter and TIPS-tetracene carboxylic acid mediator ligands. A high energy photon is absorbed by the SF material TIPS-tetracene. After triplet generation from SF the two triplets migrate and transfer to NCs *via* a mediator ligand. The NCs then relaxes radiatively emitting NIR photons. Reprinted from ref. 288, with permission from American Chemical Society. Copyright 2020. (d–f) Estimated PV efficiencies using a photon multiplier approach or tandem device applied to silicon cells of different base efficiencies for standard test conditions (d), sun light and temperature conditions in Netherlands (e) and Colorado (f). Reprinted from ref. 409, with permission from the American Chemical Society, Copyright 2018.

where Φ_{PM} is the quantum yield of emission when exciting the SF material, Φ_{NC} is the intrinsic quantum yield of emission of the NC, Abs_{Tot}^{Ex} is the total absorbance at the excitation wavelength and is the sum of the absorption of the SF material (Abs_{SF}^{Ex}) and the NC (Abs_{NC}^{Ex}). It was also highlighted that for efficient triplet transfer, a triplet mediator ligand on the NC surface is required, hence the overall process is effectively the reverse of NC sensitised TTA-UC (Fig. 21b and c).[136]

In thin films, as the SF yield is usually higher than in solution, Allardice *et al.* later showed a 190% exciton multiplication factor using TIPS-tetracene films with PbS NCs emitters and TIPS-tetracene carboxylic acid mediator ligands. The overall photon multiplication was limited by the low emission quantum yield of the PbS NCs.[285] However, one key demonstration was that the photon multiplier approach was compatible with thick films of the SF material TIPS-tetracene. Thick films allowed >95% of the incoming high energy light to be absorbed by the SF material while minimal NC absorption across the spectra was maintained.[285]

Gray *et al.* worked out the energetic requirement for efficient triplet transfer to ligated NCs. They concluded that SF materials with triplet energies around 1.4 eV would be required for NCs with emission relevant for c-Si.[287] This triplet energy is slightly higher than most common SF chromophores, hence warranting further research to develop new SF materials.

In 2018 Nagata *et al.* used a SF-PM approach in OLEDs to improve the light emission efficiency.[413] Instead of NCs as the low energy emitter they used an erbium(III) complex to harvest the triplets generated in rubrene, resulting in a 100.8% exciton generation efficiency.[413] The Er emission at 1530 nm is too low in energy to be combined with c-Si, but other lanthanide ions could be considered with more suitable emission wavelengths.[414]

The photon multiplication approach is relatively new and has not been applied to PVs yet. Two key challenges remain: firstly, finding a combination of materials (SF chromophores and NCs) that can operate at energies relevant for c-Si.

Open Access Article. Published on 02 November 2022. Downloaded on 10/16/2025 7:02:22 PM. This article is licensed under a Creative Commons Attribution 3.0 Unported Licence.

Secondly, developing NCs (or other emitters) with emission quantum yields exceeding 80–90% that can still efficiently accept triplets. Ultimately, a combination of materials that can be mixed and processed into a suitable film morphology that allows high yields of triplet generation, triplet transfer and NC emission will be required.

Challenges & opportunities in TTA-UC and SF application to PVs

Radiative transfer of photons to PVs

In most TTA-UC systems, and in SF-PM, the end product is photons. In many aspects this is a unique advantage of TTA-UC and SF-PM compared to other approaches to improve solar cells such as multi junction cells, which are hampered by the need to current match the individual PV materials. It reduces the complexity and, at least theoretically, decouples the device and photon conversion material, allowing for the separate optimisation of each part. It also might allow for incorporating these materials with already existing devices in the future, greatly enhancing the potential impact. However, for the generated photons to benefit a solar cell they have to be transferred to the device. There are numerous ways one can imagine this to be done with varying degrees of complexity and associated cost.

First, the simplest and probably the most desirable approach is to add the TTA-UC or SF-PM layer underneath or on top of the PV device, respectively. With a realistic refractive index of the photon conversion material of 1.7 theoretical modelling suggest that only 10% of the emitted light in a SF-PM is lost due to emission leaving the layer away from the solar cell.[409] Most of the light is in fact directed to the solar cell directly or through total internal reflection.[409] Since SF and TTA materials are very similar it is reasonable to believe that similar high coupling efficiencies can be reached for a TTA-UC layer.

Most TTA-UC PV devices in literature have used the simple back layer approach,[370,415] even when employing liquid TTA-UC systems.[350,351,357,359,360,416] For TTA-UC this requires the PV to have transparent back electrodes (for the relevant low energy photons). This might require a change in device structure for some types of PVs, accompanied with a decreased efficiency.[339] Hence, any gain from TTA-UC must outperform any losses due to change in device structure. Furthermore, to maximise the photon flux into the TTA-UC material, the layer is often capped by a reflecting back surface.[350,351,359,370,416] A TTA-UC back layer might compete with the implementation of bifacial PV modules.[339] It has been argued that these bifacial modules can conservatively estimate a 10% efficiency gain, compared to a monofacial module, any TTA-UC layer must be able to compete with this gain to be implemented. However, bifacial modules is a technique mostly relevant for high efficiency Si devices used in solar farms. As discussed in Fig. 1, Si devices have less to gain from TTA-UC and hence a competitive comparison between TTA-UC and bifacial modules is not the most relevant. Instead, considering that bifacial modules are not possible for building mounted or building integrated PVs, and that these types of PVs are proposed to benefit from next generation PV materials such as the higher bandgap perovskites, OPVs and DSSC, we believe that TTA-UC can still play an important role in improving these systems.

Another possibility is to develop luminescent solar concentrators (LSC) that incorporate TTA-UC and/or SF-PM and use these with relevant PV devices. A LSC is a device that absorbs sunlight in luminescent chromophores dispersed in a polymer or glass layer.[417] Both direct and diffuse sunlight is concentrated at the edges by re-emission from the chromophores followed by total internal reflection, effectively waveguiding the light to the edges.[417] Hence the PV device is attached to the edges of the LSC. In LSCs, light is lost by emission that escapes the emissive layer. Typically ~25% of the absorbed photons are lost in this way.[417] Furthermore, for LSCs to effectively concentrate light, there has to be a free energy loss to compensate for the loss in entropy associated with the light concentration.[418] This free energy loss is usually achieved by a Stokes shift between the absorbed and re-emitted photons. Hence, some energy will be lost as heat with the LSC approach. However, it was recently shown that for SF-PM LSCs this loss requirement is relaxed, and at low intensities a SF-PM based LSC might outperform standard LSCs.[418] How the fundamental limits of a LSC change for a TTA-UC based LSC has not yet been discussed, but would be a useful way to evaluate the potential of this approach. Ha *et al.* experimentally demonstrated a TTA-UC LSC coupled to a DSSC.[419] Although, the reported efficiency has been questioned.[420] Still, much is left to explore for the LSC approach. For example, in some LSC designs, the light concentration could also be used to ensure that the TTA-UC system operates above its I_{th}.[339]

Regardless of the approach to couple TTA-UC and SF-PM to a device, the emissive material would require a high QY to minimise losses. This is particularly important as in a thick film or LSC, substantial amounts of reabsorption can occur. The simplicity of the layer approach makes it particularly attractive for incorporating photon conversion materials with devices. Proof-of-principle devices for TTA-UC and theoretical modelling of SF-PM materials indicate that optical coupling these materials to PVs is feasible, and the bottle neck is now associated with inefficient systems or materials limitations.

Stability and cost considerations

Both TTA-UC and SF materials research has been heavily reliant on acene materials. Efforts have been made to develop more stable SF materials. However, the photo instability of TTA-UC and SF materials is a common challenge that remains.

Considering that commercial solar cell modules have degradation rates of approximately 0.5% per year,[421] and lifetimes exceeding 25 years, it would be interesting to consider the maximum degradation rate of the photon conversion material that still allows for economic viability. For example, it was recently estimated for perovskite-silicon tandem solar cell with an PCE of 28% would still be economically viable if the perovskite material degraded at a rate of 2% per year.[422] A possible advantage with some of the organic photon conversion

Open Access Article. Published on 02 November 2022. Downloaded on 10/16/2025 7:02:22 PM.
This article is licensed under a Creative Commons Attribution 3.0 Unported Licence.

materials is that the degradation product is mostly transparent to visible light, hence not affecting the intrinsic PV device performance. This might mean that a higher degree of degradation is acceptable.[408]

Besides degradation, materials toxicity and scarcity should be considered. Recent work by Wickerts *et al.* highlighted that photon upconversion materials using NC sensitisers need to achieve a 0.05–2 percentage points increase of module efficiency per applied gram of NC for it to be preferable over installing more PVs, from a climate perspective.

Finally, for TTA-UC and SF to become practically relevant they must provide efficiency gains that overcome any additional cost of adding the photon conversion material to the PV module. Richards *et al.* concluded that it was unlikely that an NIR upconversion material (TTA-UC or rare earth based) would be economically viable to improve the commercially dominant c-Si PV modules.[339] Even with the most optimistic estimates, like sensitiser absorption in the 1400–1650 nm region and 50% UC yield, the low cost and high efficiency of current c-Si modules makes it unfeasible.[339] However, as shown in Fig. 1, c-Si is not the most optimal PV material to benefit from photon upconversion. Efforts should instead focus on complementing next generation solar cells with higher band gaps, like OPVs and perovskite devices. Moreover, other applications, such as solar driven photocatalysis, could be more economically relevant.[339]

A cost and life cycle analysis of SF coupled PVs would be highly relevant. Especially as several approaches towards incorporating SF materials with PVs are approaching practical feasibility. A number of theoretical papers indicate that SF enhanced solar cells have many properties that can compete with silicon based tandem devices.[396,408,409] Considering that tandem devices are on the verge of commercialisation there is much hope that SF will also be feasible in the near future.

Concluding remarks and future requirements in solving fundamental TTA and SF limitations

TTA-UC and SF have been growing in prevalence within the scientific literature, but have remained largely separated and discussed without a clear connection. This is unfortunate owing to the intertwined nature of the photophysical processes in both techniques. We have discussed herein how SF and TTA-UC systems have been thoroughly investigated, understood, and some level of optimisation has occurred. However, we also note there is a long away to go before TTA-UC and SF can be practically used in devices. We provide an analysis of the future challenges and prospects with regards to utilisation of TTA-UC and SF in photovoltaic technology.

Specifically, we started this review with an introduction to the major existing challenges in SF and TTA. It was clear that challenges common to both techniques include, but are not limited to poor triplet diffusion in solid state, reversibility of TTA and SF, and poor matching of the energy levels to PV materials. It should be noted that both the TTA and SF processes are very efficient under optimised conditions, such as in solution. The challenge then is to retain these high efficiencies when applying them to photovoltaic relevant conditions. In tandem we must improve the transfer of energy to the PV through improved energy/electron/photon transfer pathways. No challenge within photon conversion for PV applications is completely solved. The most direct path forward might be to look over the shoulder of other research areas.

Increasing relevance of solar energy capture

Solar capture with focus towards defined PV bandgaps (Fig. 1) must remain a vital research area.[67,184] Here, the selection of PV must be carefully considered. For TTA-UC, the PV materials with large bandgaps would benefit most. These include GaAs, InP, GaInP, CdTe, Organic and ABX_3. Many of these are expensive technologies with little commercial viability, although promising research continues into perovskite, organic and CdTe PVs and efforts of combining TTA-UC with these devices would therefore be most relevant. The rapidly moving research field of thermally activated delayed fluorescence could serve as a source of inspiration when designing new low-loss sensitisers. QD sensitizers is another promising direction in this regard, where there still remain fundamental questions to address in terms of mediating efficient triplet transfer. Conversely, SF may be applied to low bandgap PV materials, such as c-Si and CIGS, for maximal benefit. Given the huge number of commercial c-Si systems in place around the world, it would seem as though these are the natural target. From a material perspective, the increased understanding of excited state aromaticity could provide a pathway towards new molecular motifs for SF.[336,423]

Improving triplet exciton diffusion

Especially in the solid-state this is crucial. The number of studies targeting triplet diffusion could increase in the field of TTA-UC. Here, the field of SF is considerably ahead, and many lessons has been learned that could be implemented in TTA-UC systems. An alternative approach to self-assembled systems are framework materials such as MOFs, where there is a scope of engineering long distance conjugation and thus diffusion.[249]

Material stability and abundancy

Both are important factors for commercial implementation. The material stability in photon conversion remains under-reported in the literature, and it would seem beneficial to see a rise in reporting of this data. Furthermore, scarce transition metals must be replaced in triplet sensitisers. Here, CT mediated ISC can play a role, and inspiration can further be taken from the research of photodynamic therapy, which have similar requirements on sensitisers.

Ultimately, both SF and TTA-UC have potential to become practical technologies for PV applications. While the efficiency enhancements observed in TTA-UC and SF PV devices currently remain below commercially relevant values, a pathway exists to increase efficiency gains and improve cost viability. Currently,

 This journal is © The Royal Society of Chemistry 2022

Open Access Article. Published on 02 November 2022. Downloaded on 10/16/2025 7:02:22 PM.
This article is licensed under a Creative Commons Attribution 3.0 Unported Licence.

there is a lack of efficient and stable materials and solid-state morphology tuning is complicated. However, the mechanisms are understood much better today, and therefore the future is bright for photon conversion.

Conflicts of interest

There are no conflicts to declare.

Acknowledgements

KB gratefully acknowledge financial support from the Knut and Alice Wallenberg Foundation (KAW 2017.0192). VG acknowledges funding from the Swedish research council, Vetenskapsrådet 2018-00238 and 2021-03744.

Notes and references

1 A. International, ASTM G173 - 03(2020), (accessed 27 May 2021).
2 EIA, What is the heat content of U.S. coal? https://www.eia.gov/tools/faqs/faq.php?id=72&t=2, (accessed 04 November 2021).
3 S. R. Kurtz, A. M. Leilaeioun, R. R. King, I. M. Peters, M. J. Heben, W. K. Metzger and N. M. Haegel, *MRS Bull.*, 2020, **45**, 159–164.
4 S. Department, U.S.-China Joint Statement Addressing the Climate Crisis, https://www.state.gov/u-s-china-joint-statement-addressing-the-climate-crisis/, (accessed 20 May 2021, 2021).
5 Lancet, *The Lancet*, 2019, **393**, 1911.
6 A. Jäger-Waldau, I. Kougias, N. Taylor and C. Thiel, *Renewable Sustainable Energy Rev.*, 2020, **126**, 109836.
7 I. E. Agency, *Snapshot 2021*, 2021.
8 IRENA, *Renewable Power Generation Costs in 2019*, IRENA, 2020.
9 A. Jäger-Waldau, *PV Status Report 2019*, Publications Office of the European Union, 2020.
10 H. Gholami and H. Nils Røstvik, *Energies*, 2021, **14**, 2531.
11 W. Shockley and H. J. Queisser, *J. Appl. Phys.*, 1961, **32**, 510–519.
12 S. Rühle, *Solar Energy*, 2016, **130**, 139–147.
13 L. Hirst and N. Ekins-Daukes, *Quantifying intrinsic loss mechanisms in solar cells: Why is power efficiency fundamentally limited?* SPIE, 2010.
14 C. H. Henry, *J. Appl. Phys.*, 1980, **51**, 4494–4500.
15 L. C. Hirst and N. J. Ekins-Daukes, *Prog. Photovolt. Res. Appl.*, 2011, **19**, 286–293.
16 O. Dupré, R. Vaillon and M. A. Green, *Solar Energy*, 2016, **140**, 73–82.
17 A. Wang and Y. Xuan, *Energy*, 2018, **144**, 490–500.
18 P. Baruch and J. E. Parrott, *J. Phys. D: Appl. Phys.*, 1990, **23**, 739–743.
19 J. F. Geisz, M. A. Steiner, N. Jain, K. L. Schulte, R. M. France, W. E. McMahon, E. E. Perl and D. J. Friedman, *IEEE J. Photovoltaics*, 2018, **8**, 626–632.
20 A. D. Vos, *J. Phys. D: Appl. Phys.*, 1980, **13**, 839–846.
21 S. Sundaram, D. Benson and T. K. Mallick, in *Solar Photovoltaic Technology Production*, ed. S. Sundaram, D. Benson and T. K. Mallick, Academic Press, 2016, pp. 7–22, DOI: 10.1016/B978-0-12-802953-4.00002-0.
22 X. Li, Q. Xu, L. Yan, C. Ren, B. Shi, P. Wang, S. Mazumdar, G. Hou, Y. Zhao and X. Zhang, *Nanophotonics*, 2021, **10**, 2001–2022.
23 M. Safdar, A. Ghazy, M. Lastusaari and M. Karppinen, *J. Mater. Chem. C*, 2020, **8**, 6946–6965.
24 B. Zhou, L. Yan, J. Huang, X. Liu, L. Tao and Q. Zhang, *Nat. Photonics*, 2020, **14**, 760–766.
25 T. N. Singh-Rachford and F. N. Castellano, *Coord. Chem. Rev.*, 2010, **254**, 2560–2573.
26 B. Mehrdel, A. Nikbakht, A. A. Aziz, M. S. Jameel, M. A. Dheyab and P. M. Khaniabadi, *Nanotechnology*, 2021, **33**, 082001.
27 A. Nadort, J. Zhao and E. M. Goldys, *Nanoscale*, 2016, **8**, 13099–13130.
28 D. Kang, E. Jeon, S. Kim and J. Lee, *BioChip J.*, 2020, **14**, 124–135.
29 S. Wen, J. Zhou, K. Zheng, A. Bednarkiewicz, X. Liu and D. Jin, *Nat. Commun.*, 2018, **9**, 2415.
30 M. V. DaCosta, S. Doughan, Y. Han and U. J. Krull, *Anal. Chim. Acta*, 2014, **832**, 1–33.
31 M. Li, R. Begum, J. Fu, Q. Xu, T. M. Koh, S. A. Veldhuis, M. Grätzel, N. Mathews, S. Mhaisalkar and T. C. Sum, *Nat. Commun.*, 2018, **9**, 4197.
32 H. Goodwin, T. C. Jellicoe, N. J. L. K. Davis and M. L. Böhm, *Nanophotonics*, 2018, **7**, 111–126.
33 D. Zhou, D. Liu, G. Pan, X. Chen, D. Li, W. Xu, X. Bai and H. Song, *Adv. Mater.*, 2017, **29**, 1704149.
34 M. B. Smith and J. Michl, *Chem. Rev.*, 2010, **110**, 6891–6936.
35 R. Datt, S. Bishnoi, D. Hughes, P. Mahajan, A. Singh, R. Gupta, S. Arya, V. Gupta and W. C. Tsoi, *Solar RRL*, 2022, **6**, 2200266.
36 R. T. Wegh, H. Donker, K. D. Oskam and A. Meijerink, *Science*, 1999, **283**, 663–666.
37 W. G. J. H. M. V. Sark, A. Meijerink and R. E. I. Schropp, in *Third Generation Photovoltaics*, ed. F. Vasilis, IntechOpen, Rijeka, 2012, Ch. 1, DOI: 10.5772/39213.
38 K. J. Karki, F. Ma, K. Zheng, K. Zidek, A. Mousa, M. A. Abdellah, M. E. Messing, L. R. Wallenberg, A. Yartsev and T. Pullerits, *Sci. Rep.*, 2013, **3**, 2287.
39 M. C. Beard, J. M. Luther, O. E. Semonin and A. J. Nozik, *Acc. Chem. Res.*, 2013, **46**, 1252–1260.
40 H. Goodwin, T. C. Jellicoe, N. J. L. K. Davis and M. L. Böhm, *Nanophotonics*, 2018, **7**, 111–126.
41 R. Casillas, I. Papadopoulos, T. Ullrich, D. Thiel, A. Kunzmann and D. M. Guldi, *Energy Environ. Sci.*, 2020, **13**, 2741–2804.
42 P. D. Reusswig, D. N. Congreve, N. J. Thompson and M. A. Baldo, *Appl. Phys. Lett.*, 2012, **101**, 113304.

Open Access Article. Published on 02 November 2022. Downloaded on 10/16/2025 7:02:22 PM.
This article is licensed under a Creative Commons Attribution 3.0 Unported Licence.

43 R. W. MacQueen, M. Liebhaber, J. Niederhausen, M. Mews, C. Gersmann, S. Jäckle, K. Jäger, M. J. Y. Tayebjee, T. W. Schmidt, B. Rech and K. Lips, *Mater. Horiz.*, 2018, **5**, 1065–1075.
44 M. Green, E. Dunlop, J. Hohl-Ebinger, M. Yoshita, N. Kopidakis and X. Hao, *Prog. Photovolt. Res. Appl.*, 2021, **29**, 3–15.
45 B. M. Kayes, H. Nie, R. Twist, S. G. Spruytte, F. Reinhardt, I. C. Kizilyalli and G. S. Higashi, *2011 37th IEEE Photovoltaic Specialists Conference*, 2011, 000004–000008.
46 T. Trupke, A. Shalav, B. S. Richards, P. Würfel and M. A. Green, *Sol. Energy Mater. Sol. Cells*, 2006, **90**, 3327–3338.
47 T. Trupke, M. A. Green and P. Würfel, *J. Appl. Phys.*, 2002, **92**, 4117–4122.
48 J. Ramanujam, A. Verma, B. González-Díaz, R. Guerrero-Lemus, C. del Cañizo, E. García-Tabarés, I. Rey-Stolle, F. Granek, L. Korte, M. Tucci, J. Rath, U. P. Singh, T. Todorov, O. Gunawan, S. Rubio, J. L. Plaza, E. Diéguez, B. Hoffmann, S. Christiansen and G. E. Cirlin, *Prog. Mater. Sci.*, 2016, **82**, 294–404.
49 H. J. Snaith, *Nat. Mater.*, 2018, **17**, 372–376.
50 V. M. Fthenakis, *Renewable Sustainable Energy Rev.*, 2004, **8**, 303–334.
51 J. Lee, P. Jadhav, P. D. Reusswig, S. R. Yost, N. J. Thompson, D. N. Congreve, E. Hontz, T. Van Voorhis and M. A. Baldo, *Acc. Chem. Res.*, 2013, **46**, 1300–1311.
52 M. J. Y. Tayebjee, D. R. McCamey and T. W. Schmidt, *J. Phys. Chem. Lett.*, 2015, **6**, 2367–2378.
53 J. Y. T. Murad, R. Akshay and W. S. Timothy, *J. Photonics Energy*, 2018, **8**, 1–9.
54 R. C. Johnson and R. E. Merrifield, *Phys. Rev. B: Condens. Matter Mater. Phys.*, 1970, **1**, 896–902.
55 M. W. B. Wilson, A. Rao, J. Clark, R. S. S. Kumar, D. Brida, G. Cerullo and R. H. Friend, *J. Am. Chem. Soc.*, 2011, **133**, 11830–11833.
56 A. B. Pun, A. Asadpoordarvish, E. Kumarasamy, M. J. Y. Tayebjee, D. Niesner, D. R. McCamey, S. N. Sanders, L. M. Campos and M. Y. Sfeir, *Nat. Chem.*, 2019, **11**, 821–828.
57 G. D. Scholes, *J. Phys. Chem. A*, 2015, **119**, 12699–12705.
58 P. M. Zimmerman, Z. Zhang and C. B. Musgrave, *Nat. Chem.*, 2010, **2**, 648–652.
59 A. J. Musser and J. Clark, *Annu. Rev. Phys. Chem.*, 2019, **70**, 323–351.
60 R. D. Pensack, E. E. Ostroumov, A. J. Tilley, S. Mazza, C. Grieco, K. J. Thorley, J. B. Asbury, D. S. Seferos, J. E. Anthony and G. D. Scholes, *J. Phys. Chem. Lett.*, 2016, **7**, 2370–2375.
61 K. Miyata, F. S. Conrad-Burton, F. L. Geyer and X. Y. Zhu, *Chem. Rev.*, 2019, **119**, 4261–4292.
62 H. Kim and P. M. Zimmerman, *Phys. Chem. Chem. Phys.*, 2018, **20**, 30083–30094.
63 S. N. Sanders, A. B. Pun, K. R. Parenti, E. Kumarasamy, L. M. Yablon, M. Y. Sfeir and L. M. Campos, *Chem*, 2019, **5**, 1988–2005.
64 W. Heisenberg, *Zeitschrift für Physik*, 1926, **38**, 411–426.
65 S. L. Bayliss, L. R. Weiss, A. Rao, R. H. Friend, A. D. Chepelianskii and N. C. Greenham, *Phys. Rev. B*, 2016, **94**, 045204.
66 T. F. Schulze and T. W. Schmidt, *Energy Environ. Sci.*, 2015, **8**, 103–125.
67 V. Gray, D. Dzebo, M. Abrahamsson, B. Albinsson and K. Moth-Poulsen, *Phys. Chem. Chem. Phys.*, 2014, **16**, 10345–10352.
68 V. Gray, K. Moth-Poulsen, B. Albinsson and M. Abrahamsson, *Coord. Chem. Rev.*, 2018, **362**, 54–71.
69 D. G. Bossanyi, Y. Sasaki, S. Wang, D. Chekulaev, N. Kimizuka, N. Yanai and J. Clark, *JACS Au*, 2021, **1**, 2188–2201.
70 C. Ye, V. Gray, K. Kushwaha, S. Kumar Singh, P. Erhart and K. Börjesson, *Phys. Chem. Chem. Phys.*, 2020, **22**, 1715–1720.
71 C. Ye, V. Gray, J. Mårtensson and K. Börjesson, *J. Am. Chem. Soc.*, 2019, **141**, 9578–9584.
72 D. Casanova, *Chem. Rev.*, 2018, **118**, 7164–7207.
73 W.-L. Chan, M. Ligges and X. Y. Zhu, *Nat. Chem.*, 2012, **4**, 840–845.
74 M. B. Smith and J. Michl, *Annu. Rev. Phys. Chem.*, 2013, **64**, 361–386.
75 J. C. Johnson, A. J. Nozik and J. Michl, *Acc. Chem. Res.*, 2013, **46**, 1290–1299.
76 J. J. Burdett and C. J. Bardeen, *Acc. Chem. Res.*, 2013, **46**, 1312–1320.
77 W.-L. Chan, T. C. Berkelbach, M. R. Provorse, N. R. Monahan, J. R. Tritsch, M. S. Hybertsen, D. R. Reichman, J. Gao and X. Y. Zhu, *Acc. Chem. Res.*, 2013, **46**, 1321–1329.
78 P. M. Zimmerman, C. B. Musgrave and M. Head-Gordon, *Acc. Chem. Res.*, 2013, **46**, 1339–1347.
79 D. Beljonne, H. Yamagata, J. L. Brédas, F. C. Spano and Y. Olivier, *Phys. Rev. Lett.*, 2013, **110**, 226402.
80 G. B. Piland, J. J. Burdett, R. J. Dillon and C. J. Bardeen, *J. Phys. Chem. Lett.*, 2014, **5**, 2312–2319.
81 S. R. Yost, J. Lee, M. W. B. Wilson, T. Wu, D. P. McMahon, R. R. Parkhurst, N. J. Thompson, D. N. Congreve, A. Rao, K. Johnson, M. Y. Sfeir, M. G. Bawendi, T. M. Swager, R. H. Friend, M. A. Baldo and T. Van Voorhis, *Nat. Chem.*, 2014, **6**, 492–497.
82 N. Monahan and X. Y. Zhu, *Annu. Rev. Phys. Chem.*, 2015, **66**, 601–618.
83 E. A. Margulies, C. E. Miller, Y. Wu, L. Ma, G. C. Schatz, R. M. Young and M. R. Wasielewski, *Nat. Chem.*, 2016, **8**, 1120–1125.
84 N. R. Monahan, D. Sun, H. Tamura, K. W. Williams, B. Xu, Y. Zhong, B. Kumar, C. Nuckolls, A. R. Harutyunyan, G. Chen, H.-L. Dai, D. Beljonne, Y. Rao and X. Y. Zhu, *Nat. Chem.*, 2017, **9**, 341–346.
85 R. W. A. Havenith, H. D. de Gier and R. Broer, *Mol. Phys.*, 2012, **110**, 2445–2454.
86 K. Aryanpour, A. Shukla and S. Mazumdar, *J. Phys. Chem. C*, 2015, **119**, 6966–6979.
87 T. C. Berkelbach, M. S. Hybertsen and D. R. Reichman, *J. Chem. Phys.*, 2014, **141**, 074705.
88 E. C. Greyson, J. Vura-Weis, J. Michl and M. A. Ratner, *J. Phys. Chem. B*, 2010, **114**, 14168–14177.

 This journal is © The Royal Society of Chemistry 2022

Open Access Article. Published on 02 November 2022. Downloaded on 10/16/2025 7:02:22 PM.
This article is licensed under a Creative Commons Attribution 3.0 Unported Licence.

89 P. M. Zimmerman, F. Bell, D. Casanova and M. Head-Gordon, *J. Am. Chem. Soc.*, 2011, **133**, 19944–19952.
90 T. Zeng, R. Hoffmann and N. Ananth, *J. Am. Chem. Soc.*, 2014, **136**, 5755–5764.
91 D. Casanova, *J. Chem. Theory Comput.*, 2014, **10**, 324–334.
92 T. C. Berkelbach, M. S. Hybertsen and D. R. Reichman, *J. Chem. Phys.*, 2013, **138**, 114103.
93 M. Chen, J. Y. Shin, R. M. Young and M. R. Wasielewski, *J. Chem. Phys.*, 2020, **153**, 094302.
94 B. S. Basel, J. Zirzlmeier, C. Hetzer, S. R. Reddy, B. T. Phelan, M. D. Krzyaniak, M. K. Volland, P. B. Coto, R. M. Young, T. Clark, M. Thoss, R. R. Tykwinski, M. R. Wasielewski and D. M. Guldi, *Chem*, 2018, **4**, 1092–1111.
95 R. M. Young and M. R. Wasielewski, *Acc. Chem. Res.*, 2020, **53**, 1957–1968.
96 Y. Hong, J. Kim, W. Kim, C. Kaufmann, H. Kim, F. Würthner and D. Kim, *J. Am. Chem. Soc.*, 2020, **142**, 7845–7857.
97 E. A. Margulies, J. L. Logsdon, C. E. Miller, L. Ma, E. Simonoff, R. M. Young, G. C. Schatz and M. R. Wasielewski, *J. Am. Chem. Soc.*, 2017, **139**, 663–671.
98 S. Lukman, K. Chen, J. M. Hodgkiss, D. H. P. Turban, N. D. M. Hine, S. Dong, J. Wu, N. C. Greenham and A. J. Musser, *Nat. Commun.*, 2016, **7**, 13622.
99 A. M. Alvertis, S. Lukman, T. J. H. Hele, E. G. Fuemmeler, J. Feng, J. Wu, N. C. Greenham, A. W. Chin and A. J. Musser, *J. Am. Chem. Soc.*, 2019, **141**, 17558–17570.
100 J. N. Schrauben, J. L. Ryerson, J. Michl and J. C. Johnson, *J. Am. Chem. Soc.*, 2014, **136**, 7363–7373.
101 S. W. Eaton, L. E. Shoer, S. D. Karlen, S. M. Dyar, E. A. Margulies, B. S. Veldkamp, C. Ramanan, D. A. Hartzler, S. Savikhin, T. J. Marks and M. R. Wasielewski, *J. Am. Chem. Soc.*, 2013, **135**, 14701–14712.
102 Y. J. Bae, G. Kang, C. D. Malliakas, J. N. Nelson, J. Zhou, R. M. Young, Y.-L. Wu, R. P. Van Duyne, G. C. Schatz and M. R. Wasielewski, *J. Am. Chem. Soc.*, 2018, **140**, 15140–15144.
103 E. A. Buchanan and J. Michl, *J. Am. Chem. Soc.*, 2017, **139**, 15572–15575.
104 P. E. Hartnett, E. A. Margulies, C. M. Mauck, S. A. Miller, Y. Wu, Y.-L. Wu, T. J. Marks and M. R. Wasielewski, *J. Phys. Chem. B*, 2016, **120**, 1357–1366.
105 T. Nagami, S. Ito, T. Kubo and M. Nakano, *ACS Omega*, 2017, **2**, 5095–5103.
106 A. Zaykov, P. Felkel, E. A. Buchanan, M. Jovanovic, R. W. A. Havenith, R. K. Kathir, R. Broer, Z. Havlas and J. Michl, *J. Am. Chem. Soc.*, 2019, **141**, 17729–17743.
107 D. Guzmán, I. Papadopoulos, G. Lavarda, P. R. Rami, R. R. Tykwinski, M. S. Rodríguez-Morgade, D. M. Guldi and T. Torres, *Angew. Chem., Int. Ed.*, 2021, **60**, 1474–1481.
108 G. He, E. Busby, K. Appavoo, Q. Wu, J. Xia, L. M. Campos and M. Y. Sfeir, *J. Chem. Phys.*, 2020, **153**, 244902.
109 C. M. Mauck, Y. J. Bae, M. Chen, N. Powers-Riggs, Y.-L. Wu and M. R. Wasielewski, *ChemPhotoChem*, 2018, **2**, 223–233.
110 R. Montero, V. Martínez-Martínez, A. Longarte, N. Epelde-Elezcano, E. Palao, I. Lamas, H. Manzano, A. R. Agarrabeitia, I. López Arbeloa, M. J. Ortiz and I. Garcia-Moreno, *J. Phys. Chem. Lett.*, 2018, **9**, 641–646.
111 I. Papadopoulos, M. J. Álvaro-Martins, D. Molina, P. M. McCosker, P. A. Keller, T. Clark, Á. Sastre-Santos and D. M. Guldi, *Adv. Energy Mater.*, 2020, **10**, 2001496.
112 E. Sundin, R. Ringström, F. Johansson, B. Küçüköz, A. Ekebergh, V. Gray, B. Albinsson, J. Mårtensson and M. Abrahamsson, *J. Phys. Chem. C*, 2020, **124**, 20794–20805.
113 L. Xue, X. Song, Y. Feng, S. Cheng, G. Lu and Y. Bu, *J. Am. Chem. Soc.*, 2020, **142**, 17469–17479.
114 T. W. Schmidt, *J. Chem. Phys.*, 2019, **151**, 054305.
115 A. A. Bakulin, S. E. Morgan, T. B. Kehoe, M. W. B. Wilson, A. W. Chin, D. Zigmantas, D. Egorova and A. Rao, *Nat. Chem.*, 2016, **8**, 16–23.
116 R. Tempelaar and D. R. Reichman, *J. Chem. Phys.*, 2017, **146**, 174703.
117 R. Tempelaar and D. R. Reichman, *J. Chem. Phys.*, 2017, **146**, 174704.
118 Y. Fujihashi, L. Chen, A. Ishizaki, J. Wang and Y. Zhao, *J. Chem. Phys.*, 2017, **146**, 044101.
119 H.-G. Duan, A. Jha, X. Li, V. Tiwari, H. Ye, K. Nayak Pabitra, X.-L. Zhu, Z. Li, J. Martinez Todd, M. Thorwart and R. J. D. Miller, *Sci. Adv.*, 2020, **6**, eabb0052.
120 A. J. Musser, M. Liebel, C. Schnedermann, T. Wende, T. B. Kehoe, A. Rao and P. Kukura, *Nat. Phys.*, 2015, **11**, 352–357.
121 H. L. Stern, A. Cheminal, S. R. Yost, K. Broch, S. L. Bayliss, K. Chen, M. Tabachnyk, K. Thorley, N. Greenham, J. M. Hodgkiss, J. Anthony, M. Head-Gordon, A. J. Musser, A. Rao and R. H. Friend, *Nat. Chem.*, 2017, **9**, 1205–1212.
122 T. S. Lee, Y. L. Lin, H. Kim, R. D. Pensack, B. P. Rand and G. D. Scholes, *J. Phys. Chem. Lett.*, 2018, **9**, 4087–4095.
123 S. Lukman, J. M. Richter, L. Yang, P. Hu, J. Wu, N. C. Greenham and A. J. Musser, *J. Am. Chem. Soc.*, 2017, **139**, 18376–18385.
124 C. K. Yong, A. J. Musser, S. L. Bayliss, S. Lukman, H. Tamura, O. Bubnova, R. K. Hallani, A. Meneau, R. Resel, M. Maruyama, S. Hotta, L. M. Herz, D. Beljonne, J. E. Anthony, J. Clark and H. Sirringhaus, *Nat. Commun.*, 2017, **8**, 15953.
125 A. B. Kolomeisky, X. Feng and A. I. Krylov, *J. Phys. Chem. C*, 2014, **118**, 5188–5195.
126 H. Nagashima, S. Kawaoka, S. Akimoto, T. Tachikawa, Y. Matsui, H. Ikeda and Y. Kobori, *J. Phys. Chem. Lett.*, 2018, **9**, 5855–5861.
127 N. V. Korovina, C. H. Chang and J. C. Johnson, *Nat. Chem.*, 2020, **12**, 391–398.
128 P. Irkhin and I. Biaggio, *Phys. Rev. Lett.*, 2011, **107**, 017402.
129 G. M. Akselrod, P. B. Deotare, N. J. Thompson, J. Lee, W. A. Tisdale, M. A. Baldo, V. M. Menon and V. Bulović, *Nat. Commun.*, 2014, **5**, 3646.
130 G. He, L. M. Yablon, K. R. Parenti, K. J. Fallon, L. M. Campos and M. Y. Sfeir, *J. Am. Chem. Soc.*, 2022, **144**, 3269–3278.
131 R. P. Groff, P. Avakian and R. E. Merrifield, *Phys. Rev. B: Condens. Matter Mater. Phys.*, 1970, **1**, 815–817.

Open Access Article. Published on 02 November 2022. Downloaded on 10/16/2025 7:02:22 PM.
This article is licensed under a Creative Commons Attribution 3.0 Unported Licence.

132 S. Lukman, A. J. Musser, K. Chen, S. Athanasopoulos, C. K. Yong, Z. Zeng, Q. Ye, C. Chi, J. M. Hodgkiss, J. Wu, R. H. Friend and N. C. Greenham, *Adv. Funct. Mater.*, 2015, **25**, 5452–5461.
133 X. Tang, R. Pan, X. Zhao, H. Zhu and Z. Xiong, *J. Phys. Chem. Lett.*, 2020, **11**, 2804–2811.
134 A. J. Carrod, A. Cravcenco, C. Ye and K. Börjesson, *J. Mater. Chem. C*, 2022, **10**, 4923–4928.
135 S. Hoseinkhani, R. Tubino, F. Meinardi and A. Monguzzi, *Phys. Chem. Chem. Phys.*, 2015, **17**, 4020–4024.
136 V. Gray, J. R. Allardice, Z. Zhang and A. Rao, *Chem. Phys. Rev.*, 2021, **2**, 031305.
137 A. J. Baldacchino, M. I. Collins, M. P. Nielsen, T. W. Schmidt, D. R. McCamey and M. J. Tayebjee, *arXiv*, 2022, preprint, arXiv:2202.01326.
138 O. Cvrčková and M. Ciganek, *Polycyclic Aromat. Compd.*, 2005, **25**, 141–156.
139 S. Dong, A. Ong and C. Chi, *J. Photochem. Photobiol., C*, 2019, **38**, 27–46.
140 A. K. Le, J. A. Bender, D. H. Arias, D. E. Cotton, J. C. Johnson and S. T. Roberts, *J. Am. Chem. Soc.*, 2018, **140**, 814–826.
141 P. J. Budden, L. R. Weiss, M. Müller, N. A. Panjwani, S. Dowland, J. R. Allardice, M. Ganschow, J. Freudenberg, J. Behrends, U. H. F. Bunz and R. H. Friend, *Nat. Commun.*, 2021, **12**, 1527.
142 P. Bharmoria, N. Yanai and N. Kimizuka, *Gels*, 2019, **5**, 18.
143 P. Bharmoria, S. Hisamitsu, H. Nagatomi, T. Ogawa, M.-A. Morikawa, N. Yanai and N. Kimizuka, *J. Am. Chem. Soc.*, 2018, **140**, 10848–10855.
144 D. Dzebo, K. Moth-Poulsen and B. Albinsson, *Photochem. Photobiol. Sci.*, 2017, **16**, 1327–1334.
145 Q. Liu, M. Xu, T. Yang, B. Tian, X. Zhang and F. Li, *ACS Appl. Mater. Interfaces*, 2018, **10**, 9883–9888.
146 A. D. Poletayev, J. Clark, M. W. B. Wilson, A. Rao, Y. Makino, S. Hotta and R. H. Friend, *Adv. Mater.*, 2014, **26**, 919–924.
147 D. Rai and R. J. Holmes, *J. Mater. Chem. C*, 2019, **7**, 5695–5701.
148 M. A. Baldo, C. Adachi and S. R. Forrest, *Phys. Rev. B: Condens. Matter Mater. Phys.*, 2000, **62**, 10967–10977.
149 M. Wakasa, T. Yago, Y. Sonoda and R. Katoh, *Commun. Chem.*, 2018, **1**, 9.
150 R. J. Hudson, D. M. Huang and T. W. Kee, *J. Phys. Chem. C*, 2020, **124**, 23541–23550.
151 V. K. Thorsmølle, R. D. Averitt, J. Demsar, D. L. Smith, S. Tretiak, R. L. Martin, X. Chi, B. K. Crone, A. P. Ramirez and A. J. Taylor, *Phys. Rev. Lett.*, 2009, **102**, 017401.
152 C. A. Parker and C. G. Hatchard, *Proc. Chem. Soc.*, 1962, 386–387, DOI: 10.1039/PS9620000373.
153 A. Monguzzi, J. Mezyk, F. Scotognella, R. Tubino and F. Meinardi, *Phys. Rev. B: Condens. Matter Mater. Phys.*, 2008, **78**, 195112.
154 R. R. Islangulov, J. Lott, C. Weder and F. N. Castellano, *J. Am. Chem. Soc.*, 2007, **129**, 12652–12653.
155 S. Baluschev, V. Yakutkin, T. Miteva, Y. Avlasevich, S. Chernov, S. Aleshchenkov, G. Nelles, A. Cheprakov, A. Yasuda, K. Müllen and G. Wegner, *Angew. Chem., Int. Ed.*, 2007, **46**, 7693–7696.
156 R. H. Clarke and R. M. Hochstrasser, *J. Mol. Spectrosc.*, 1969, **32**, 309–319.
157 S. Chen, F. Chen, P. Han, C. Ye, S. Huang, L. Xu, X. Wang and Y. Song, *RSC Adv.*, 2019, **9**, 36410–36415.
158 T. Morifuji, Y. Takekuma and M. Nagata, *ACS Omega*, 2019, **4**, 11271–11275.
159 Y. Kageshima, S. Tateyama, F. Kishimoto, K. Teshima, K. Domen and H. Nishikiori, *Phys. Chem. Chem. Phys.*, 2021, **23**, 5673–5679.
160 K. Chen, M. Hussain, S. S. Razi, Y. Hou, E. A. Yildiz, J. Zhao, H. G. Yaglioglu and M. D. Donato, *Inorg. Chem.*, 2020, **59**, 14731–14745.
161 C. E. Elgar, H. Y. Otaif, X. Zhang, J. Zhao, P. N. Horton, S. J. Coles, J. M. Beames and S. J. A. Pope, *Chem. – Eur. J.*, 2021, **27**, 3427–3439.
162 P. Xia, E. K. Raulerson, D. Coleman, C. S. Gerke, L. Mangolini, M. L. Tang and S. T. Roberts, *Nat. Chem.*, 2020, **12**, 137–144.
163 Z. A. VanOrman, C. R. Conti, G. F. Strouse and L. Nienhaus, *Chem. Mater.*, 2021, **33**, 452–458.
164 R. P. Groff, R. E. Merrifield, A. Suna and P. Avakian, *Phys. Rev. Lett.*, 1972, **29**, 429–431.
165 K. Chen, Y. Dong, X. Zhao, M. Imran, G. Tang, J. Zhao and Q. Liu, *Front. Chem.*, 2019, **7**, 821.
166 Z. Wang and J. Zhao, *Org. Lett.*, 2017, **19**, 4492–4495.
167 N. Kiseleva, M. A. Filatov, J. C. Fischer, M. Kaiser, M. Jakoby, D. Busko, I. A. Howard, B. S. Richards and A. Turshatov, *Phys. Chem. Chem. Phys.*, 2022, **24**, 3568–3578.
168 S. E. Braslavsky, *Pure Appl. Chem.*, 2007, **79**, 293–465.
169 Y. Zhou, F. N. Castellano, T. W. Schmidt and K. Hanson, *ACS Energy Lett.*, 2020, **5**, 2322–2326.
170 A. M. Brouwer, *Pure Appl. Chem.*, 2011, **83**, 2213–2228.
171 U. Resch-Genger and K. Rurack, *Pure Appl. Chem.*, 2013, **85**, 2005–2013.
172 Y. Y. Cheng, B. Fückel, T. Khoury, R. G. C. R. Clady, M. J. Y. Tayebjee, N. J. Ekins-Daukes, M. J. Crossley and T. W. Schmidt, *J. Phys. Chem. Lett.*, 2010, **1**, 1795–1799.
173 A. Haefele, J. Blumhoff, R. S. Khnayzer and F. N. Castellano, *J. Phys. Chem. Lett.*, 2012, **3**, 299–303.
174 F. Edhborg, A. Olesund and B. Albinsson, *Photochem. Photobiol. Sci.*, 2022, **21**, 1143–1158.
175 K. K.-W. Lo, in *Photophysics of Organometallics*, ed. A. J. Lees, Springer Berlin Heidelberg, Berlin, Heidelberg, 2010, pp. 73–114, DOI: 10.1007/3418_2009_3.
176 A. J. Carrod, F. Graglia, L. Male, C. Le Duff, P. Simpson, M. Elsherif, Z. Ahmed, H. Butt, G.-X. Xu, K. Kam-Wing Lo, P. Bertoncello and Z. Pikramenou, *Chem. – Eur. J.*, 2022, **28**, e202103541.
177 A. F. Rausch, H. H. H. Homeier and H. Yersin, in *Photophysics of Organometallics*, ed. A. J. Lees, Springer Berlin Heidelberg, Berlin, Heidelberg, 2010, pp. 193–235, DOI: 10.1007/3418_2009_6.
178 A. Harriman, *J. Chem. Soc., Faraday Trans. 2*, 1981, **77**, 1281–1291.

 This journal is © The Royal Society of Chemistry 2022

Open Access Article. Published on 02 November 2022. Downloaded on 10/16/2025 7:02:22 PM.
This article is licensed under a Creative Commons Attribution 3.0 Unported Licence.

179 E. l G. Azenha, A. C. Serra, M. Pineiro, M. M. Pereira, J. Seixas de Melo, L. G. Arnaut, S. J. Formosinho and A. M. d A. Rocha Gonsalves, *Chem. Phys.*, 2002, **280**, 177–190.
180 R. C. Evans and P. Douglas, *ACS Appl. Mater. Interfaces*, 2009, **1**, 1023–1030.
181 A. Gorski, M. Kijak, E. Zenkevich, V. Knyukshto, A. Starukhin, A. Semeikin, T. Lyubimova, T. Roliński and J. Waluk, *J. Phys. Chem. A*, 2020, **124**, 8144–8158.
182 T. N. Singh-Rachford and F. N. Castellano, *J. Phys. Chem. Lett.*, 2010, **1**, 195–200.
183 T. N. Singh-Rachford, A. Nayak, M. L. Muro-Small, S. Goeb, M. J. Therien and F. N. Castellano, *J. Am. Chem. Soc.*, 2010, **132**, 14203–14211.
184 F. Deng, J. R. Sommer, M. Myahkostupov, K. S. Schanze and F. N. Castellano, *Chem. Commun.*, 2013, **49**, 7406–7408.
185 J. R. Sommer, A. H. Shelton, A. Parthasarathy, I. Ghiviriga, J. R. Reynolds and K. S. Schanze, *Chem. Mater.*, 2011, **23**, 5296–5304.
186 J. K. Gallaher, K. M. Wright, L. Frazer, R. W. MacQueen, M. J. Crossley, F. N. Castellano and T. W. Schmidt, *Energy Environ. Sci.*, 2021, **14**, 5541–5551.
187 J. B. Bilger, C. Kerzig, C. B. Larsen and O. S. Wenger, *J. Am. Chem. Soc.*, 2021, **143**, 1651–1663.
188 M. Yang, S. Sheykhi, Y. Zhang, C. Milsmann and F. N. Castellano, *Chem. Sci.*, 2021, **12**, 9069–9077.
189 K. Hasan, A. K. Bansal, I. D. W. Samuel, C. Roldán-Carmona, H. J. Bolink and E. Zysman-Colman, *Sci. Rep.*, 2015, **5**, 12325.
190 A. F. Henwood and E. Zysman-Colman, *Chem. Commun.*, 2017, **53**, 807–826.
191 S. Amemori, Y. Sasaki, N. Yanai and N. Kimizuka, *J. Am. Chem. Soc.*, 2016, **138**, 8702–8705.
192 Y. Sasaki, S. Amemori, H. Kouno, N. Yanai and N. Kimizuka, *J. Mater. Chem. C*, 2017, **5**, 5063–5067.
193 R. Haruki, Y. Sasaki, K. Masutani, N. Yanai and N. Kimizuka, *Chem. Commun.*, 2020, **56**, 7017–7020.
194 Y. Wei, M. Zheng, L. Chen, X. Zhou and S. Liu, *Dalton Trans.*, 2019, **48**, 11763–11771.
195 M. Wu, D. N. Congreve, M. W. B. Wilson, J. Jean, N. Geva, M. Welborn, T. Van Voorhis, V. Bulović, M. G. Bawendi and M. A. Baldo, *Nat. Photonics*, 2016, **10**, 31–34.
196 Z. Huang, D. E. Simpson, M. Mahboub, X. Li and M. L. Tang, *Chem. Sci.*, 2016, **7**, 4101–4104.
197 M. Mahboub, Z. Huang and M. L. Tang, *Nano Lett.*, 2016, **16**, 7169–7175.
198 Z. Huang, Z. Xu, M. Mahboub, X. Li, J. W. Taylor, W. H. Harman, T. Lian and M. L. Tang, *Angew. Chem., Int. Ed.*, 2017, **56**, 16583–16587.
199 Z. Xu, Z. Huang, C. Li, T. Huang, F. A. Evangelista, M. L. Tang and T. Lian, *ACS Appl. Mater. Interfaces*, 2020, **12**, 36558–36567.
200 S. T. Hossain and S. K. Mukherjee, *J. Hazard. Mater.*, 2013, **260**, 1073–1082.
201 M. Ayoubi, P. Naserzadeh, M. T. Hashemi, M. Reza Rostami, E. Tamjid, M. M. Tavakoli and A. Simchi, *Sci. Rep.*, 2017, **7**, 12896.
202 L. Huang, E. Kakadiaris, T. Vaneckova, K. Huang, M. Vaculovicova and G. Han, *Biomaterials*, 2019, **201**, 77–86.
203 R. Lai, Y. Sang, Y. Zhao and K. Wu, *J. Am. Chem. Soc.*, 2020, **142**, 19825–19829.
204 R. J. Ellingson, J. L. Blackburn, P. Yu, G. Rumbles, O. I. Mićić and A. J. Nozik, *J. Phys. Chem. B*, 2002, **106**, 7758–7765.
205 E. M. Gholizadeh, S. K. K. Prasad, Z. L. Teh, T. Ishwara, S. Norman, A. J. Petty, J. H. Cole, S. Cheong, R. D. Tilley, J. E. Anthony, S. Huang and T. W. Schmidt, *Nat. Photonics*, 2020, **14**, 585–590.
206 B. Fückel, D. A. Roberts, Y. Y. Cheng, R. G. C. R. Clady, R. B. Piper, N. J. Ekins-Daukes, M. J. Crossley and T. W. Schmidt, *J. Phys. Chem. Lett.*, 2011, **2**, 966–971.
207 N. Nishimura, J. R. Allardice, J. Xiao, Q. Gu, V. Gray and A. Rao, *Chem. Sci.*, 2019, **10**, 4750–4760.
208 N. Tripathi, M. Ando, T. Akai and K. Kamada, *ACS Appl. Nano Mater.*, 2021, **4**, 9680–9688.
209 N. Tripathi, M. Ando, T. Akai and K. Kamada, *J. Mater. Chem. C*, 2022, **10**, 4563–4567.
210 D. G. Bossanyi, M. Matthiesen, S. Wang, J. A. Smith, R. C. Kilbride, J. D. Shipp, D. Chekulaev, E. Holland, J. E. Anthony, J. Zaumseil, A. J. Musser and J. Clark, *Nat. Chem.*, 2021, **13**, 163–171.
211 G. Mayonado, K. T. Vogt, J. D. B. Van Schenck, L. Zhu, G. Fregoso, J. Anthony, O. Ostroverkhova and M. W. Graham, *J. Phys. Chem. C*, 2022, **126**, 4433–4445.
212 Z. Xu, Z. Huang, T. Jin, T. Lian and M. L. Tang, *Acc. Chem. Res.*, 2021, **54**, 70–80.
213 B. Pfund, D. M. Steffen, M. R. Schreier, M.-S. Bertrams, C. Ye, K. Börjesson, O. S. Wenger and C. Kerzig, *J. Am. Chem. Soc.*, 2020, **142**, 10468–10476.
214 A. Ronchi and A. Monguzzi, *J. Appl. Phys.*, 2021, **129**, 050901.
215 D. Dzebo, K. Börjesson, V. Gray, K. Moth-Poulsen and B. Albinsson, *J. Phys. Chem. C*, 2016, **120**, 23397–23406.
216 C. E. McCusker and F. N. Castellano, *Top. Curr. Chem.*, 2016, **374**, 19.
217 S. Raišys, S. Juršėnas, Y. C. Simon, C. Weder and K. Kazlauskas, *Chem. Sci.*, 2018, **9**, 6796–6802.
218 C. Healy, L. Hermanspahn and P. E. Kruger, *Coord. Chem. Rev.*, 2021, **432**, 213756.
219 X. Liu, J. Fei, P. Zhu and J. Li, *Chem. – Asian J.*, 2016, **11**, 2700–2704.
220 K. Sripathy, R. W. MacQueen, J. R. Peterson, Y. Y. Cheng, M. Dvořák, D. R. McCamey, N. D. Treat, N. Stingelin and T. W. Schmidt, *J. Mater. Chem. C*, 2015, **3**, 616–622.
221 R. Vadrucci, C. Weder and Y. C. Simon, *Mater. Horiz.*, 2015, **2**, 120–124.
222 C. Ye, J. Ma, S. Chen, J. Ge, W. Yang, Q. Zheng, X. Wang, Z. Liang and Y. Zhou, *J. Phys. Chem. C*, 2017, **121**, 20158–20164.
223 P. Duan, D. Asthana, T. Nakashima, T. Kawai, N. Yanai and N. Kimizuka, *Faraday Discuss.*, 2017, **196**, 305–316.
224 P. Duan, N. Yanai, H. Nagatomi and N. Kimizuka, *J. Am. Chem. Soc.*, 2015, **137**, 1887–1894.

Open Access Article. Published on 02 November 2022. Downloaded on 10/16/2025 7:02:22 PM.
This article is licensed under a Creative Commons Attribution 3.0 Unported Licence.

225 D. F. Barbosa de Mattos, A. Dreos, M. D. Johnstone, A. Runemark, C. Sauvée, V. Gray, K. Moth-Poulsen, H. Sundén and M. Abrahamsson, *J. Chem. Phys.*, 2020, **153**, 214705.
226 S. N. Sanders, T. H. Schloemer, M. K. Gangishetty, D. Anderson, M. Seitz, A. O. Gallegos, R. C. Stokes and D. N. Congreve, *Nature*, 2022, **604**, 474–478.
227 A. M. Oddo, T. Mani and C. V. Kumar, *ACS Appl. Mater. Interfaces*, 2020, **12**, 39293–39303.
228 P. Bharmoria, S. Hisamitsu, Y. Sasaki, T. S. Kang, M.-A. Morikawa, B. Joarder, K. Moth-Poulsen, H. Bildirir, A. Mårtensson, N. Yanai and N. Kimizuka, *J. Mater. Chem. C*, 2021, **9**, 11655–11661.
229 F. Saenz, A. Ronchi, M. Mauri, R. Vadrucci, F. Meinardi, A. Monguzzi and C. Weder, *Adv. Funct. Mater.*, 2021, **31**, 2004495.
230 T. N. Singh-Rachford, J. Lott, C. Weder and F. N. Castellano, *J. Am. Chem. Soc.*, 2009, **131**, 12007–12014.
231 A. Turshatov, D. Busko, N. Kiseleva, S. L. Grage, I. A. Howard and B. S. Richards, *ACS Appl. Mater. Interfaces*, 2017, **9**, 8280–8286.
232 A. Monguzzi, M. Mauri, A. Bianchi, M. K. Dibbanti, R. Simonutti and F. Meinardi, *J. Phys. Chem. C*, 2016, **120**, 2609–2614.
233 M. J. Bennison, A. R. Collins, B. Zhang and R. C. Evans, *Macromolecules*, 2021, **54**, 5287–5303.
234 R. Vadrucci, A. Monguzzi, F. Saenz, B. D. Wilts, Y. C. Simon and C. Weder, *Adv. Mater.*, 2017, **29**, 1702992.
235 A. L. Hagstrom, H.-L. Lee, M.-S. Lee, H.-S. Choe, J. Jung, B.-G. Park, W.-S. Han, J.-S. Ko, J.-H. Kim and J.-H. Kim, *ACS Appl. Mater. Interfaces*, 2018, **10**, 8985–8992.
236 A. Monguzzi, A. Oertel, D. Braga, A. Riedinger, D. K. Kim, P. N. Knüsel, A. Bianchi, M. Mauri, R. Simonutti, D. J. Norris and F. Meinardi, *ACS Appl. Mater. Interfaces*, 2017, **9**, 40180–40186.
237 A. Monguzzi, F. Bianchi, A. Bianchi, M. Mauri, R. Simonutti, R. Ruffo, R. Tubino and F. Meinardi, *Adv. Energy Mater.*, 2013, **3**, 680–686.
238 D. Choi, S. K. Nam, K. Kim and J. H. Moon, *Angew. Chem., Int. Ed.*, 2019, **58**, 6891–6895.
239 S. R. Pristash, K. L. Corp, E. J. Rabe and C. W. Schlenker, *ACS Appl. Energy Mater.*, 2020, **3**, 19–28.
240 Q. Wang and D. Astruc, *Chem. Rev.*, 2020, **120**, 1438–1511.
241 C. Ye, S. Chen, J. Liao, Y. S. Zhang, X. Wang and Y. Song, *J. Phys. Chem. C*, 2020, **124**, 18482–18489.
242 I. Roy, S. Goswami, R. M. Young, I. Schlesinger, M. R. Mian, A. E. Enciso, X. Zhang, J. E. Hornick, O. K. Farha, M. R. Wasielewski, J. T. Hupp and J. F. Stoddart, *J. Am. Chem. Soc.*, 2021, **143**, 5053–5059.
243 F. Meinardi, M. Ballabio, N. Yanai, N. Kimizuka, A. Bianchi, M. Mauri, R. Simonutti, A. Ronchi, M. Campione and A. Monguzzi, *Nano Lett.*, 2019, **19**, 2169–2177.
244 S. Gharaati, C. Wang, C. Förster, F. Weigert, U. Resch-Genger and K. Heinze, *Chem. – Eur. J.*, 2020, **26**, 1003–1007.
245 P. Mahato, A. Monguzzi, N. Yanai, T. Yamada and N. Kimizuka, *Nat. Mater.*, 2015, **14**, 924–930.
246 B. Joarder, A. Mallick, Y. Sasaki, M. Kinoshita, R. Haruki, Y. Kawashima, N. Yanai and N. Kimizuka, *ChemNanoMat*, 2020, **6**, 916–919.
247 Y. Yang, S. Mallick, F. Izquierdo-Ruiz, C. Schäfer, X. Xing, M. Rahm and K. Börjesson, *Small*, 2021, **17**, 2103152.
248 M. Ratsch, C. Ye, Y. Yang, A. Zhang, A. M. Evans and K. Börjesson, *J. Am. Chem. Soc.*, 2020, **142**, 6548–6553.
249 D.-G. Ha, R. Wan, C. A. Kim, T.-A. Lin, L. Yang, T. Van Voorhis, M. A. Baldo and M. Dincă, *Nat. Mater.*, 2022, **21**, 1275–1281.
250 M. Hosoyamada, N. Yanai, T. Ogawa and N. Kimizuka, *Chem. – Eur. J.*, 2016, **22**, 2060–2067.
251 V. Gray, K. Börjesson, D. Dzebo, M. Abrahamsson, B. Albinsson and K. Moth-Poulsen, *J. Phys. Chem. C*, 2016, **120**, 19018–19026.
252 S. Raišys, K. Kazlauskas, S. Juršėnas and Y. C. Simon, *ACS Appl. Mater. Interfaces*, 2016, **8**, 15732–15740.
253 E. Radiunas, M. Dapkevičius, S. Raišys, S. Juršėnas, A. Jozeliūnaitė, T. Javorskis, U. Šinkevičiūtė, E. Orentas and K. Kazlauskas, *Phys. Chem. Chem. Phys.*, 2020, **22**, 7392–7403.
254 S. Wieghold, A. S. Bieber, Z. A. VanOrman, A. Rodriguez and L. Nienhaus, *J. Phys. Chem. C*, 2020, **124**, 18132–18140.
255 D. G. Bossanyi, Y. Sasaki, S. Wang, D. Chekulaev, N. Kimizuka, N. Yanai and J. Clark, *J. Mater. Chem. C*, 2022, **10**, 4684–4696.
256 K. M. Felter, M. C. Fravventura, E. Koster, R. D. Abellon, T. J. Savenije and F. C. Grozema, *ACS Energy Lett.*, 2020, **5**, 124–129.
257 T.-A. Lin, C. F. Perkinson and M. A. Baldo, *Adv. Mater.*, 2020, **32**, 1908175.
258 S. Izawa and M. Hiramoto, *Nat. Photonics*, 2021, **15**, 895–900.
259 S. Izawa, M. Morimoto, S. Naka and M. Hiramoto, *Adv. Opt. Mater.*, 2022, **10**, 2101710.
260 S. Izawa, N. Shintaku, M. Kikuchi and M. Hiramoto, *Appl. Phys. Lett.*, 2019, **115**, 153301.
261 Z. Zhang, J. Yuan, Q. Wei and Y. Zou, *Front. Chem.*, 2018, **6**, 414.
262 M. Wu, T.-A. Lin, J. O. Tiepelt, V. Bulović and M. A. Baldo, *Nano Lett.*, 2021, **21**, 1011–1016.
263 M. Wu, J. Jean, V. Bulović and M. A. Baldo, *Appl. Phys. Lett.*, 2017, **110**, 211101.
264 M. Hertzog, M. Wang, J. Mony and K. Börjesson, *Chem. Soc. Rev.*, 2019, **48**, 937–961.
265 C. Ye, S. Mallick, M. Hertzog, M. Kowalewski and K. Börjesson, *J. Am. Chem. Soc.*, 2021, **143**, 7501–7508.
266 M. Hertzog, B. Munkhbat, D. Baranov, T. Shegai and K. Börjesson, *Nano Lett.*, 2021, **21**, 1320–1326.
267 J. Lather, P. Bhatt, A. Thomas, T. W. Ebbesen and J. George, *Angew. Chem., Int. Ed.*, 2019, **58**, 10635–10638.
268 K. Nagarajan, A. Thomas and T. W. Ebbesen, *J. Am. Chem. Soc.*, 2021, **143**, 16877–16889.
269 S. Singh, W. J. Jones, W. Siebrand, B. P. Stoicheff and W. G. Schneider, *J. Chem. Phys.*, 1965, **42**, 330–342.

 This journal is © The Royal Society of Chemistry 2022

Open Access Article. Published on 02 November 2022. Downloaded on 10/16/2025 7:02:22 PM.
This article is licensed under a Creative Commons Attribution 3.0 Unported Licence.

270 C. E. Swenberg and W. T. Stacy, *Chem. Phys. Lett.*, 1968, **2**, 327–328.
271 D. L. Dexter, *J. Lumin.*, 1979, **18–19**, 779–784.
272 J. J. Burdett, G. B. Piland and C. J. Bardeen, *Chem. Phys. Lett.*, 2013, **585**, 1–10.
273 A. Rao and R. H. Friend, *Nat. Rev. Mater.*, 2017, **2**, 17063.
274 C. Hetzer, D. M. Guldi and R. R. Tykwinski, *Chem. – Eur. J.*, 2018, **24**, 8245–8257.
275 T. Ullrich, D. Munz and D. M. Guldi, *Chem. Soc. Rev.*, 2021, **50**, 3485–3518.
276 S. N. Sanders, E. Kumarasamy, A. B. Pun, M. T. Trinh, B. Choi, J. Xia, E. J. Taffet, J. Z. Low, J. R. Miller, X. Roy, X. Y. Zhu, M. L. Steigerwald, M. Y. Sfeir and L. M. Campos, *J. Am. Chem. Soc.*, 2015, **137**, 8965–8972.
277 J. C. Johnson, A. J. Nozik and J. Michl, *J. Am. Chem. Soc.*, 2010, **132**, 16302–16303.
278 S. Masoomi-Godarzi, C. R. Hall, B. Zhang, M. A. Gregory, J. M. White, W. W. H. Wong, K. P. Ghiggino, T. A. Smith and D. J. Jones, *J. Phys. Chem. C*, 2020, **124**, 11574–11585.
279 T. Sakuma, H. Sakai, Y. Araki, T. Mori, T. Wada, N. V. Tkachenko and T. Hasobe, *J. Phys. Chem. A*, 2016, **120**, 1867–1875.
280 H. L. Stern, A. J. Musser, S. Gelinas, P. Parkinson, L. M. Herz, M. J. Bruzek, J. Anthony, R. H. Friend and B. J. Walker, *Proc. Natl. Acad. Sci. U. S. A.*, 2015, **112**, 7656.
281 B. J. Walker, A. J. Musser, D. Beljonne and R. H. Friend, *Nat. Chem.*, 2013, **5**, 1019–1024.
282 Y. Jue Bae, M. D. Krzyaniak, M. B. Majewski, M. Desroches, J.-F. Morin, Y.-L. Wu and M. R. Wasielewski, *ChemPlusChem*, 2019, **84**, 1432–1438.
283 N. Congreve Daniel, J. Lee, J. Thompson Nicholas, E. Hontz, R. Yost Shane, D. Reusswig Philip, E. Bahlke Matthias, S. Reineke, T. Van Voorhis and A. Baldo Marc, *Science*, 2013, **340**, 334–337.
284 J. Lee, P. Jadhav and M. A. Baldo, *Appl. Phys. Lett.*, 2009, **95**, 033301.
285 J. Allardice, V. Gray, S. Dowland, D. T. Toolan, M. P. Weir, J. Xiao, Z. Zhang, J. F. Winkel, A. J. Petty II and J. Anthony, *arXiv*, 2020, preprint, arXiv:2009.05764.
286 J. R. Allardice, A. Thampi, S. Dowland, J. Xiao, V. Gray, Z. Zhang, P. Budden, A. J. Petty, N. J. L. K. Davis, N. C. Greenham, J. E. Anthony and A. Rao, *J. Am. Chem. Soc.*, 2019, **141**, 12907–12915.
287 V. Gray, J. R. Allardice, Z. Zhang, S. Dowland, J. Xiao, A. J. Petty, J. E. Anthony, N. C. Greenham and A. Rao, *ACS Nano*, 2020, **14**, 4224–4234.
288 V. Gray, Z. Zhang, S. Dowland, J. R. Allardice, A. M. Alvertis, J. Xiao, N. C. Greenham, J. E. Anthony and A. Rao, *J. Phys. Chem. Lett.*, 2020, **11**, 7239–7244.
289 N. J. Thompson, M. W. B. Wilson, D. N. Congreve, P. R. Brown, J. M. Scherer, T. S. Bischof, M. Wu, N. Geva, M. Welborn, T. V. Voorhis, V. Bulović, M. G. Bawendi and M. A. Baldo, *Nat. Mater.*, 2014, **13**, 1039–1043.
290 K. J. Fallon, P. Budden, E. Salvadori, A. M. Ganose, C. N. Savory, L. Eyre, S. Dowland, Q. Ai, S. Goodlett, C. Risko, D. O. Scanlon, C. W. M. Kay, A. Rao, R. H. Friend, A. J. Musser and H. Bronstein, *J. Am. Chem. Soc.*, 2019, **141**, 13867–13876.
291 W. Zeng, O. El Bakouri, D. W. Szczepanik, H. Bronstein and H. Ottosson, *Chem. Sci.*, 2021, **12**, 6159–6171.
292 I. Paci, J. C. Johnson, X. Chen, G. Rana, D. Popović, D. E. David, A. J. Nozik, M. A. Ratner and J. Michl, *J. Am. Chem. Soc.*, 2006, **128**, 16546–16553.
293 S. Ito, T. Minami and M. Nakano, *J. Phys. Chem. C*, 2012, **116**, 19729–19736.
294 T. Minami and M. Nakano, *J. Phys. Chem. Lett.*, 2012, **3**, 145–150.
295 T. Nagami, K. Okada, H. Miyamoto, W. Yoshida, T. Tonami and M. Nakano, *J. Phys. Chem. C*, 2020, **124**, 11800–11809.
296 M. Nakano, *The Chemical Record*, 2017, **17**, 27–62.
297 A. Akdag, Z. Havlas and J. Michl, *J. Am. Chem. Soc.*, 2012, **134**, 14624–14631.
298 J. Wen, Z. Havlas and J. Michl, *J. Am. Chem. Soc.*, 2015, **137**, 165–172.
299 S. V. Bhosale, M. Al Kobaisi, R. W. Jadhav, P. P. Morajkar, L. A. Jones and S. George, *Chem. Soc. Rev.*, 2021, **50**, 9845–9998.
300 A. Nowak-Król, K. Shoyama, M. Stolte and F. Würthner, *Chem. Commun.*, 2018, **54**, 13763–13772.
301 C. Yan, S. Barlow, Z. Wang, H. Yan, A. K. Y. Jen, S. R. Marder and X. Zhan, *Nat. Rev. Mater.*, 2018, **3**, 18003.
302 X. Zhan, A. Facchetti, S. Barlow, T. J. Marks, M. A. Ratner, M. R. Wasielewski and S. R. Marder, *Adv. Mater.*, 2011, **23**, 268–284.
303 G. Zhang, J. Zhao, P. C. Y. Chow, K. Jiang, J. Zhang, Z. Zhu, J. Zhang, F. Huang and H. Yan, *Chem. Rev.*, 2018, **118**, 3447–3507.
304 Y. V. Aulin, K. M. Felter, D. D. Günbas, R. K. Dubey, W. F. Jager and F. C. Grozema, *ChemPlusChem*, 2018, **83**, 230–238.
305 F. S. Conrad-Burton, T. Liu, F. Geyer, R. Costantini, A. P. Schlaus, M. S. Spencer, J. Wang, R. H. Sánchez, B. Zhang, Q. Xu, M. L. Steigerwald, S. Xiao, H. Li, C. P. Nuckolls and X. Zhu, *J. Am. Chem. Soc.*, 2019, **141**, 13143–13147.
306 S. W. Eaton, S. A. Miller, E. A. Margulies, L. E. Shoer, R. D. Schaller and M. R. Wasielewski, *J. Phys. Chem. A*, 2015, **119**, 4151–4161.
307 M. H. Farag and A. I. Krylov, *J. Phys. Chem. C*, 2018, **122**, 25753–25763.
308 A. K. Le, J. A. Bender and S. T. Roberts, *J. Phys. Chem. Lett.*, 2016, **7**, 4922–4928.
309 L. Ma, K. J. Tan, H. Jiang, C. Kloc, M.-E. Michel-Beyerle and G. G. Gurzadyan, *J. Phys. Chem. A*, 2014, **118**, 838–843.
310 K. Nagarajan, A. R. Mallia, V. S. Reddy and M. Hariharan, *J. Phys. Chem. C*, 2016, **120**, 8443–8450.
311 C. M. Mauck, K. E. Brown, N. E. Horwitz and M. R. Wasielewski, *J. Phys. Chem. A*, 2015, **119**, 5587–5596.
312 C. Schierl, A. Niazov-Elkan, L. J. W. Shimon, Y. Feldman, B. Rybtchinski and D. M. Guldi, *Nanoscale*, 2018, **10**, 20147–20154.
313 M. Chen, Y. J. Bae, C. M. Mauck, A. Mandal, R. M. Young and M. R. Wasielewski, *J. Am. Chem. Soc.*, 2018, **140**, 9184–9192.

Open Access Article. Published on 02 November 2022. Downloaded on 10/16/2025 7:02:22 PM.
This article is licensed under a Creative Commons Attribution 3.0 Unported Licence.

314 W. Ni, G. G. Gurzadyan, J. Zhao, Y. Che, X. Li and L. Sun, *J. Phys. Chem. Lett.*, 2019, **10**, 2428–2433.
315 A. B. Pun, L. M. Campos and D. N. Congreve, *J. Am. Chem. Soc.*, 2019, **141**, 3777–3781.
316 M. Chakali, H. Mandal, M. Venkatesan, B. Dyaga, V. J. Rao and P. R. Bangal, *J. Photochem. Photobiol., A*, 2021, **406**, 113017.
317 A. M. Levine, C. Schierl, B. S. Basel, M. Ahmed, B. A. Camargo, D. M. Guldi and A. B. Braunschweig, *J. Phys. Chem. C*, 2019, **123**, 1587–1595.
318 S. Masoomi-Godarzi, M. Liu, Y. Tachibana, V. D. Mitchell, L. Goerigk, K. P. Ghiggino, T. A. Smith and D. J. Jones, *Adv. Energy Mater.*, 2019, **9**, 1901069.
319 C. M. Mauck, P. E. Hartnett, E. A. Margulies, L. Ma, C. E. Miller, G. C. Schatz, T. J. Marks and M. R. Wasielewski, *J. Am. Chem. Soc.*, 2016, **138**, 11749–11761.
320 C. M. Mauck, P. E. Hartnett, Y.-L. Wu, C. E. Miller, T. J. Marks and M. R. Wasielewski, *Chem. Mater.*, 2017, **29**, 6810–6817.
321 E. G. Fuemmeler, S. N. Sanders, A. B. Pun, E. Kumarasamy, T. Zeng, K. Miyata, M. L. Steigerwald, X. Y. Zhu, M. Y. Sfeir, L. M. Campos and N. Ananth, *ACS Cent. Sci.*, 2016, **2**, 316–324.
322 E. Kumarasamy, S. N. Sanders, M. J. Y. Tayebjee, A. Asadpoordarvish, T. J. H. Hele, E. G. Fuemmeler, A. B. Pun, L. M. Yablon, J. Z. Low, D. W. Paley, J. C. Dean, B. Choi, G. D. Scholes, M. L. Steigerwald, N. Ananth, D. R. McCamey, M. Y. Sfeir and L. M. Campos, *J. Am. Chem. Soc.*, 2017, **139**, 12488–12494.
323 A. M. Müller, Y. S. Avlasevich, W. W. Schoeller, K. Müllen and C. J. Bardeen, *J. Am. Chem. Soc.*, 2007, **129**, 14240–14250.
324 K. R. Parenti, G. He, S. N. Sanders, A. B. Pun, E. Kumarasamy, M. Y. Sfeir and L. M. Campos, *J. Phys. Chem. A*, 2020, **124**, 9392–9399.
325 S. N. Sanders, E. Kumarasamy, A. B. Pun, K. Appavoo, M. L. Steigerwald, L. M. Campos and M. Y. Sfeir, *J. Am. Chem. Soc.*, 2016, **138**, 7289–7297.
326 S. N. Sanders, E. Kumarasamy, A. B. Pun, M. L. Steigerwald, M. Y. Sfeir and L. M. Campos, *Angew. Chem., Int. Ed.*, 2016, **55**, 3373–3377.
327 M. J. Y. Tayebjee, S. N. Sanders, E. Kumarasamy, L. M. Campos, M. Y. Sfeir and D. R. McCamey, *Nat. Phys.*, 2017, **13**, 182–188.
328 M. T. Trinh, A. Pinkard, B. Pun Andrew, N. Sanders Samuel, E. Kumarasamy, Y. Sfeir Matthew, M. Campos Luis, X. Roy and X. Y. Zhu, *Sci. Adv.*, 2017, **3**, e1700241.
329 J. D. Cook, T. J. Carey, D. H. Arias, J. C. Johnson and N. H. Damrauer, *J. Phys. Chem. A*, 2017, **121**, 9229–9242.
330 S. Nakamura, H. Sakai, H. Nagashima, Y. Kobori, N. V. Tkachenko and T. Hasobe, *ACS Energy Lett.*, 2019, **4**, 26–31.
331 Z. Wang, H. Liu, X. Xie, C. Zhang, R. Wang, L. Chen, Y. Xu, H. Ma, W. Fang, Y. Yao, H. Sang, X. Wang, X. Li and M. Xiao, *Nat. Chem.*, 2021, **13**, 559–567.
332 L. M. Yablon, S. N. Sanders, H. Li, K. R. Parenti, E. Kumarasamy, K. J. Fallon, M. J. A. Hore, A. Cacciuto, M. Y. Sfeir and L. M. Campos, *J. Am. Chem. Soc.*, 2019, **141**, 9564–9569.
333 A. J. Musser, M. Al-Hashimi, M. Maiuri, D. Brida, M. Heeney, G. Cerullo, R. H. Friend and J. Clark, *J. Am. Chem. Soc.*, 2013, **135**, 12747–12754.
334 E. Busby, J. Xia, Q. Wu, J. Z. Low, R. Song, J. R. Miller, X. Y. Zhu, L. M. Campos and M. Y. Sfeir, *Nat. Mater.*, 2015, **14**, 426–433.
335 J. Hu, K. Xu, L. Shen, Q. Wu, G. He, J.-Y. Wang, J. Pei, J. Xia and M. Y. Sfeir, *Nat. Commun.*, 2018, **9**, 2999.
336 O. El Bakouri, J. R. Smith and H. Ottosson, *J. Am. Chem. Soc.*, 2020, **142**, 5602–5617.
337 L. Wang, L. Lin, J. Yang, Y. Wu, H. Wang, J. Zhu, J. Yao and H. Fu, *J. Am. Chem. Soc.*, 2020, **142**, 10235–10239.
338 D. Padula, Ö. H. Omar, T. Nematiaram and A. Troisi, *Energy Environ. Sci.*, 2019, **12**, 2412–2416.
339 B. S. Richards, D. Hudry, D. Busko, A. Turshatov and I. A. Howard, *Chem. Rev.*, 2021, **121**, 9165–9195.
340 M. Barawi, F. Fresno, R. Pérez-Ruiz and V. A. de la Peña O'Shea, *ACS Appl. Energy Mater.*, 2019, **2**, 207–211.
341 H.-i Kim, S. Weon, H. Kang, A. L. Hagstrom, O. S. Kwon, Y.-S. Lee, W. Choi and J.-H. Kim, *Environ. Sci. Technol.*, 2016, **50**, 11184–11192.
342 T. Yu, Y. Liu, Y. Zeng, J. Chen, G. Yang and Y. Li, *Chem. – Eur. J.*, 2019, **25**, 16270–16276.
343 S. M. Borisov, C. Larndorfer and I. Klimant, *Adv. Funct. Mater.*, 2012, **22**, 4360–4368.
344 N. A. Kukhta, T. Matulaitis, D. Volyniuk, K. Ivaniuk, P. Turyk, P. Stakhira, J. V. Grazulevicius and A. P. Monkman, *J. Phys. Chem. Lett.*, 2017, **8**, 6199–6205.
345 D. Y. Kondakov, *Philos. Trans. R. Soc., A*, 2015, **373**, 20140321.
346 J. Yao, S. Xiao, S. Zhang, Q. Sun, Y. Dai, X. Qiao, D. Yang, J. Chen and D. Ma, *J. Mater. Chem. C*, 2020, **8**, 8077–8084.
347 L. Xing, Z.-L. Zhu, J. He, Z. Qiu, Z. Yang, D. Lin, W.-C. Chen, Q. Yang, S. Ji, Y. Huo and C.-S. Lee, *Chem. Eng. J.*, 2020, **421**, 127748.
348 T. Dilbeck, S. P. Hill and K. Hanson, *J. Mater. Chem. A*, 2017, **5**, 11652–11660.
349 C. Li, C. Koenigsmann, F. Deng, A. Hagstrom, C. A. Schmuttenmaer and J.-H. Kim, *ACS Photonics*, 2016, **3**, 784–790.
350 Y. Y. Cheng, A. Nattestad, T. F. Schulze, R. W. MacQueen, B. Fückel, K. Lips, G. G. Wallace, T. Khoury, M. J. Crossley and T. W. Schmidt, *Chem. Sci.*, 2016, **7**, 559–568.
351 A. Nattestad, Y. Y. Cheng, R. W. MacQueen, T. F. Schulze, F. W. Thompson, A. J. Mozer, B. Fückel, T. Khoury, M. J. Crossley, K. Lips, G. G. Wallace and T. W. Schmidt, *J. Phys. Chem. Lett.*, 2013, **4**, 2073–2078.
352 J. de Wild, A. Meijerink, J. K. Rath, W. G. J. H. M. van Sark and R. E. I. Schropp, *Energy Environ. Sci.*, 2011, **4**, 4835–4848.
353 A. Monguzzi, D. Braga, M. Gandini, V. C. Holmberg, D. K. Kim, A. Sahu, D. J. Norris and F. Meinardi, *Nano Lett.*, 2014, **14**, 6644–6650.
354 T. Dilbeck and K. Hanson, *J. Phys. Chem. Lett.*, 2018, **9**, 5810–5821.

 This journal is © The Royal Society of Chemistry 2022

Open Access Article. Published on 02 November 2022. Downloaded on 10/16/2025 7:02:22 PM.
This article is licensed under a Creative Commons Attribution 3.0 Unported Licence.

355 A. J. Robb, E. S. Knorr, N. Watson and K. Hanson, *J. Photochem. Photobiol., A*, 2020, **390**, 112291.
356 Y. L. Lin, M. Koch, A. N. Brigeman, D. M. E. Freeman, L. Zhao, H. Bronstein, N. C. Giebink, G. D. Scholes and B. P. Rand, *Energy Environ. Sci.*, 2017, **10**, 1465–1475.
357 Y. Y. Cheng, B. Fückel, R. W. MacQueen, T. Khoury, R. G. C. R. Clady, T. F. Schulze, N. J. Ekins-Daukes, M. J. Crossley, B. Stannowski, K. Lips and T. W. Schmidt, *Energy Environ. Sci.*, 2012, **5**, 6953–6959.
358 W. M. Rowan, F. S. Tim, K. Tony, C. Yuen Yap, S. Bernd, L. Klaus, J. C. Maxwel and S. Timothy, 2013.
359 T. F. Schulze, Y. Y. Cheng, B. Fückel, R. W. MacQueen, A. Danos, N. J. L. K. Davis, M. J. Y. Tayebjee, T. Khoury, R. G. C. R. Clady, N. J. Ekins-Daukes, M. J. Crossley, B. Stannowski, K. Lips and T. W. Schmidt, *Aust. J. Chem.*, 2012, **65**, 480–485.
360 T. F. Schulze, J. Czolk, Y.-Y. Cheng, B. Fückel, R. W. MacQueen, T. Khoury, M. J. Crossley, B. Stannowski, K. Lips, U. Lemmer, A. Colsmann and T. W. Schmidt, *J. Phys. Chem. C*, 2012, **116**, 22794–22801.
361 C. Simpson, T. M. Clarke, R. W. MacQueen, Y. Y. Cheng, A. J. Trevitt, A. J. Mozer, P. Wagner, T. W. Schmidt and A. Nattestad, *Phys. Chem. Chem. Phys.*, 2015, **17**, 24826–24830.
362 F. S. Tim, C. Yuen Yap, H. K. Tony, C. Maxwell, S. Bernd, L. Klaus and W. S. Timothy, *J. Photonics Energy*, 2013, **3**, 1–14.
363 J. Alves, J. Feng, L. Nienhaus and T. W. Schmidt, *J. Mater. Chem. C*, 2022, **10**, 7783–7798.
364 L. Frazer, J. K. Gallaher and T. W. Schmidt, *ACS Energy Lett.*, 2017, **2**, 1346–1354.
365 Y. Zhou, C. Ruchlin, A. J. Robb and K. Hanson, *ACS Energy Lett.*, 2019, **4**, 1458–1463.
366 D. Beery, J. P. Wheeler, A. Arcidiacono and K. Hanson, *ACS Appl. Energy Mater.*, 2020, **3**, 29–37.
367 S. Wieghold, A. S. Bieber, J. Lackner, K. Nienhaus, G. U. Nienhaus and L. Nienhaus, *ChemPhotoChem*, 2020, **4**, 704–712.
368 S. Wieghold, A. S. Bieber, Z. A. VanOrman, L. Daley, M. Leger, J.-P. Correa-Baena and L. Nienhaus, *Matter*, 2019, **1**, 705–719.
369 L. Nienhaus, J.-P. Correa-Baena, S. Wieghold, M. Einzinger, T.-A. Lin, K. E. Shulenberger, N. D. Klein, M. Wu, V. Bulović, T. Buonassisi, M. A. Baldo and M. G. Bawendi, *ACS Energy Lett.*, 2019, **4**, 888–895.
370 M. Kinoshita, Y. Sasaki, S. Amemori, N. Harada, Z. Hu, Z. Liu, L. K. Ono, Y. Qi, N. Yanai and N. Kimizuka, *ChemPhotoChem*, 2020, **4**, 5271–5278.
371 W. Sheng, J. Yang, X. Li, G. Liu, Z. Lin, J. Long, S. Xiao, L. Tan and Y. Chen, *Energy Environ. Sci.*, 2021, **14**, 3532–3541.
372 L. Nienhaus and T. W. Schmidt, *Energy Environ. Sci.*, 2021, **14**, 6050–6052.
373 W. Sheng, J. Yang, X. Li, S. Xiao, L. Tan and Y. Chen, *Energy Environ. Sci.*, 2021, **14**, 6053–6054.
374 M. Einzinger, T. Wu, J. F. Kompalla, H. L. Smith, C. F. Perkinson, L. Nienhaus, S. Wieghold, D. N. Congreve, A. Kahn, M. G. Bawendi and M. A. Baldo, *Nature*, 2019, **571**, 90–94.
375 J. N. Schrauben, Y. Zhao, C. Mercado, P. I. Dron, J. L. Ryerson, J. Michl, K. Zhu and J. C. Johnson, *ACS Appl. Mater. Interfaces*, 2015, **7**, 2286–2293.
376 T. Banerjee, S. P. Hill, M. A. Hermosilla-Palacios, B. D. Piercy, J. Haney, B. Casale, A. E. DePrince, M. D. Losego, V. D. Kleiman and K. Hanson, *J. Phys. Chem. C*, 2018, **122**, 28478–28490.
377 N. A. Pace, D. H. Arias, D. B. Granger, S. Christensen, J. E. Anthony and J. C. Johnson, *Chem. Sci.*, 2018, **9**, 3004–3013.
378 A. Kunzmann, M. Gruber, R. Casillas, J. Zirzlmeier, M. Stanzel, W. Peukert, R. R. Tykwinski and D. M. Guldi, *Angew. Chem., Int. Ed.*, 2018, **57**, 10742–10747.
379 M. Tabachnyk, B. Ehrler, S. Bayliss, R. H. Friend and N. C. Greenham, *Appl. Phys. Lett.*, 2013, **103**, 153302.
380 N. J. Thompson, D. N. Congreve, D. Goldberg, V. M. Menon and M. A. Baldo, *Appl. Phys. Lett.*, 2013, **103**, 263302.
381 T. C. Wu, N. J. Thompson, D. N. Congreve, E. Hontz, S. R. Yost, T. Van Voorhis and M. A. Baldo, *Appl. Phys. Lett.*, 2014, **104**, 193901.
382 A. V. Akimov and O. V. Prezhdo, *J. Am. Chem. Soc.*, 2014, **136**, 1599–1608.
383 W.-L. Chan, J. R. Tritsch and X. Y. Zhu, *J. Am. Chem. Soc.*, 2012, **134**, 18295–18302.
384 P. J. Jadhav, P. R. Brown, N. Thompson, B. Wunsch, A. Mohanty, S. R. Yost, E. Hontz, T. Van Voorhis, M. G. Bawendi, V. Bulović and M. A. Baldo, *Adv. Mater.*, 2012, **24**, 6169–6174.
385 S. Kawata, Y.-J. Pu, A. Saito, Y. Kurashige, T. Beppu, H. Katagiri, M. Hada and J. Kido, *Adv. Mater.*, 2016, **28**, 1585–1590.
386 Y. L. Lin, M. A. Fusella, O. V. Kozlov, X. Lin, A. Kahn, M. S. Pshenichnikov and B. P. Rand, *Adv. Funct. Mater.*, 2016, **26**, 6489–6494.
387 A. N. Stuart, P. C. Tapping, E. Schrefl, D. M. Huang and T. W. Kee, *J. Phys. Chem. C*, 2019, **123**, 5813–5825.
388 N. J. Thompson, E. Hontz, D. N. Congreve, M. E. Bahlke, S. Reineke, T. Van Voorhis and M. A. Baldo, *Adv. Mater.*, 2014, **26**, 1366–1371.
389 J. R. Tritsch, W.-L. Chan, X. Wu, N. R. Monahan and X. Y. Zhu, *Nat. Commun.*, 2013, **4**, 2679.
390 G. Bernardo, T. Lopes, D. G. Lidzey and A. Mendes, *Adv. Energy Mater.*, 2021, **11**, 2100342.
391 A. Wadsworth, M. Moser, A. Marks, M. S. Little, N. Gasparini, C. J. Brabec, D. Baran and I. McCulloch, *Chem. Soc. Rev.*, 2019, **48**, 1596–1625.
392 W.-L. Chan, M. Ligges, A. Jailaubekov, L. Kaake, L. Miaja-Avila and X. Y. Zhu, *Science*, 2011, **334**, 1541–1545.
393 T. Zhang, D. Rai and R. J. Holmes, *J. Phys. Chem. Lett.*, 2021, **12**, 966–972.
394 P. J. Jadhav, A. Mohanty, J. Sussman, J. Lee and M. A. Baldo, *Nano Lett.*, 2011, **11**, 1495–1498.
395 J. M. Lee, M. H. Futscher, L. M. Pazos-Outón and B. Ehrler, *Prog. Photovolt. Res. Appl.*, 2017, **25**, 936–941.

Open Access Article. Published on 02 November 2022. Downloaded on 10/16/2025 7:02:22 PM.
This article is licensed under a Creative Commons Attribution 3.0 Unported Licence.

396 L. M. Pazos-Outón, J. M. Lee, M. H. Futscher, A. Kirch, M. Tabachnyk, R. H. Friend and B. Ehrler, *ACS Energy Lett.*, 2017, **2**, 476–480.
397 B. Ehrler, K. P. Musselman, M. L. Böhm, R. H. Friend and N. C. Greenham, *Appl. Phys. Lett.*, 2012, **101**, 153507.
398 B. Ehrler, M. W. B. Wilson, A. Rao, R. H. Friend and N. C. Greenham, *Nano Lett.*, 2012, **12**, 1053–1057.
399 L. Yang, M. Tabachnyk, S. L. Bayliss, M. L. Böhm, K. Broch, N. C. Greenham, R. H. Friend and B. Ehrler, *Nano Lett.*, 2015, **15**, 354–358.
400 D. Guo, L. Ma, Z. Zhou, D. Lin, C. Wang, X. Zhao, F. Zhang, J. Zhang and Z. Nie, *J. Mater. Chem. A*, 2020, **8**, 5572–5579.
401 S. Lee, D. Hwang, S. I. Jung and D. Kim, *J. Phys. Chem. Lett.*, 2017, **8**, 884–888.
402 T. Hayashi, T. G. Castner and R. W. Boyd, *Chem. Phys. Lett.*, 1983, **94**, 461–466.
403 G. B. Piland, J. J. Burdett, T.-Y. Hung, P.-H. Chen, C.-F. Lin, T.-L. Chiu, J.-H. Lee and C. J. Bardeen, *Chem. Phys. Lett.*, 2014, **601**, 33–38.
404 B. Daiber, S. P. Pujari, S. Verboom, S. L. Luxembourg, S. W. Tabernig, M. H. Futscher, J. Lee, H. Zuilhof and B. Ehrler, *J. Chem. Phys.*, 2020, **152**, 114201.
405 Y. Wan, Z. Guo, T. Zhu, S. Yan, J. Johnson and L. Huang, *Nat. Chem.*, 2015, **7**, 785–792.
406 Y. Wan, G. P. Wiederrecht, R. D. Schaller, J. C. Johnson and L. Huang, *J. Phys. Chem. Lett.*, 2018, **9**, 6731–6738.
407 T. Zhu and L. Huang, *J. Phys. Chem. Lett.*, 2018, **9**, 6502–6510.
408 Y. Jiang, M. P. Nielsen, A. J. Baldacchino, M. A. Green, D. R. McCamey, M. J. Y. Tayebjee, T. W. Schmidt and N. J. Ekins-Daukes, *Prog. Photovolt. Res. Appl.*, 2021, **29**, 899–906.
409 M. H. Futscher, A. Rao and B. Ehrler, *ACS Energy Lett.*, 2018, **3**, 2587–2592.
410 D. Casanova, *J. Chem. Theory Comput.*, 2015, **11**, 2642–2650.
411 G. Klein and R. Voltz, *Int. J. Radiat. Phys. Chem.*, 1975, **7**, 155–174.
412 M. Tabachnyk, B. Ehrler, S. Gélinas, M. L. Böhm, B. J. Walker, K. P. Musselman, N. C. Greenham, R. H. Friend and A. Rao, *Nat. Mater.*, 2014, **13**, 1033–1038.
413 R. Nagata, H. Nakanotani, W. J. Potscavage Jr and C. Adachi, *Adv. Mater.*, 2018, **30**, 1801484.
414 T. J. Milstein, D. M. Kroupa and D. R. Gamelin, *Nano Lett.*, 2018, **18**, 3792–3799.
415 K. Kim, S. K. Nam and J. H. Moon, *ACS Appl. Energy Mater.*, 2020, **3**, 5277–5284.
416 J.-E. Bernice Mae Yu, W. Haibin, E. E. Achilles, K. Takaya, S. Hiroshi, A. Nazmul and O. Yoshitaka, *J. Photonics Energy*, 2020, **10**, 1–20.
417 J. Roncali, *Adv. Energy Mater.*, 2020, **10**, 2001907.
418 T. K. Baikie, A. Ashoka, A. Rao and N. C. Greenham, *arXiv*, 2022, preprint, arXiv:2203.06736.
419 S.-J. Ha, J.-H. Kang, D. H. Choi, S. K. Nam, E. Reichmanis and J. H. Moon, *ACS Photonics*, 2018, **5**, 3621–3627.
420 C. Yang and R. R. Lunt, *ACS Photonics*, 2021, **8**, 678–681.
421 D. C. Jordan and S. R. Kurtz, *Prog. Photovolt. Res. Appl.*, 2013, **21**, 12–29.
422 J. Qian, M. Ernst, N. Wu and A. Blakers, *Sustainable Energy Fuels*, 2019, **3**, 1439–1447.
423 W. Zeng, D. W. Szczepanik and H. Bronstein, *J. Phys. Org. Chem.*, 2022, e4441.

 This journal is © The Royal Society of Chemistry 2022